



VCU

Virginia Commonwealth University
VCU Scholars Compass

Theses and Dissertations

Graduate School

2018

STAT3 in the Regulation of Brown Adipocyte Differentiation

Marc Cantwell

Virginia Commonwealth University

Follow this and additional works at: <https://scholarscompass.vcu.edu/etd>

Part of the Developmental Biology Commons

© The Author

Downloaded from

<https://scholarscompass.vcu.edu/etd/5507>

This Dissertation is brought to you for free and open access by the Graduate School at VCU Scholars Compass. It has been accepted for inclusion in Theses and Dissertations by an authorized administrator of VCU Scholars Compass. For more information, please contact libcompass@vcu.edu.

© Marc Taylor Cantwell
All Rights Reserved

STAT3 in the Regulation of Brown Adipocyte Differentiation

A dissertation submitted in partial fulfillment of the requirements for the degree of Doctor of Philosophy at Virginia Commonwealth University

by

Marc Taylor Cantwell
B.S. Virginia Commonwealth University, 2008

Director: ANDREW C. LARNER
PROFESSOR, DEPARTMENT OF BIOCHEMISTRY

Virginia Commonwealth University
Richmond, Virginia
March 2018

Acknowledgements

First and foremost, I want to thank my family: my mother Estelle, my father John, and my sister Kristin. I would not be where I am today without your influences. You have provided me the opportunities and guidance necessary to get me to this point in my life. Without you none of this would have been possible.

Second, I want to thank my mentor, Andrew Larner. It was a tough five years of work, with many failures along the way, but you were confident that I would emerge successfully from those failures. I will always try to learn from my failures and keep growing as a physician and a scientist.

I also want to thank my past mentors Sarah Rutan and Deborah Lannigan. You opened your labs to me and took responsibility to guide me at the beginning of my science career. I appreciate the opportunities you gave me to get my foot into the door in science.

Thanks also to my committee members Joyce Lloyd, Daniel Conrad, Clive Baumgarten, and Tomasz Kordula. Your guidance and advising helped steer this project. You are all committed to mentoring and creating the next generation of scientists, and I respect that passion. I hope to emulate it when it is my turn to guide the new generation.

Thank you to Jared Farrer, Joseph Lownik, Michael Waters, and Sheela Damle for their help advising and collaborating with me on areas of their expertise, which I utilized in generating the data.

I want to thank the current and former members of the Larner Laboratory, with special mention to Jeremy Meir. Jeremy- your counsel over the years in lab was crucial for me to keep going even when I wanted to stop. You were a sounding board; you helped me see the forest when I was wrapped up all in the leaves.

I want to thank the MD/PhD program and Gordon Archer for accepting me into the program. I hope I have been and will continue to be what you were hoping for in a student.

Finally, I want to thank my close friends from the MD/PhD program: Mackenzie Lind, Spencer Harris, and Sheela Damle. Your support out of class and out of lab helped carry me to this point.

Table of Contents

Acknowledgements	ii
List of Tables	v
List of Figures	vi
List of Abbreviations	viii
Abstract	1
Chapter 1: Introduction	3
1.1 Epidemiology, Etiology, and Associated Comorbidities of Obesity	5
1.2 BAT Function and Human Relevance	11
1.3 Genes Involved in Adipogenesis and Browning.....	25
1.4 The JAK/STAT Pathway and its Known Roles in Adipogenesis.....	30
1.5 The Wnt Pathway and its Role in Suppressing Adipogenesis	38
1.6 Dissertation Rationale and Objectives	42
Chapter 2: Materials and Methods	43
2.1 Generation of Mice	43
2.2 Mouse Genotyping.....	43
2.3 Isolation of Primary Brown Preadipocytes	44
2.4 Induction of Differentiation	45
2.5 Temporal Knockout Studies	45
2.6 <i>In-Vitro</i> Treatments.....	46
2.7 siRNA Transfection	46
2.8 SDS-PAGE and Immunoblotting.....	47
2.9 RNA Extraction and Real-Time PCR	48
2.10 Oil-Red O Staining	48
2.11 Proliferation Studies.....	49
2.12 Chromatin Immunoprecipitation Assays.....	49
2.13 Mitochondrial Isolation.....	50
2.14 Apoptosis Assays	51
2.15 <i>In-vivo</i> Beiging Studies.....	51
2.16 Statistical Analysis.....	52
Chapter 3: Results	59
3.1 STAT3 is Phosphorylated During the Induction Period	59
3.2 Inhibition of STAT3 Blocks Differentiation of Brown Adipocytes	61
3.3 Inhibition of STAT3 During the Induction Period Only Blocks Differentiation.....	63
3.4 Generation of a Floxed-STAT3, Tamoxifen Inducible Cre Leads to Efficient Total Knockout.....	65
3.5 Deletion of STAT3 Does Not Affect Proliferation of Preadipocytes in the Growth Phase	67

3.6 STAT3 KO Preadipocytes Have Reduced Proliferation After Induction	70
3.7 Deletion of STAT3 Leads to Significant Reduction in Differentiation and Brown Specific Genes.....	72
3.8 Tamoxifen is not Responsible for the Defects in Differentiation	77
3.9 PPAR γ is Less Stable in the STAT3 KO	79
3.10 Deletion of STAT3 after the Induction Phase does not alter UCP1 levels.....	82
3.11 pan-JAK Inhibition Suggests that the JAK/STAT Pathway has a Biphasic Response to Differentiation.....	84
3.12 STAT3 KO Cells Have Increased Apoptosis in the Early Terminal Differentiation Phase	86
3.13 Inhibition of Wnt Ligand Secretion During Induction Rescues the Adipogenic and Thermogenic Program in STAT3 KO Preadipocytes	89
3.14 STAT3 KO Cells have Reduced Histone H3K27 Acetylation at the UCP1 Promoter and Enhancer Regions and can be Rescued with IWP2	93
3.15 Wnt Inhibition is needed only during the Induction Period, showing temporal correlation with STAT3	95
3.16 β -Catenin Levels are not Down Regulated in the STAT3 KO	97
3.17 STAT3 KO adipocytes have increased Wnt/ β -Catenin signaling during the induction phase	100
3.18 Wnt Ligands 3a, 1, and 10b are elevated in STAT3 KO adipocytes during the induction phase	102
3.19 The Canonical β -Catenin Pathway is responsible for suppression of differentiation in STAT3 KO Brown Preadipocytes	104
3.20 Knockdown of β -Catenin Before Induction Fully Rescues UCP1 Levels.....	115
3.21 Beige Cells also Require STAT3 Prior to Induction and can be Partially Rescued with Wnt Inhibition.....	117
3.22 Pilot <i>In-Vivo</i> Beiging Study Shows Equal Induction of UCP1 in the STAT3 WT and KO animals	119
3.23 Primary Tyk2 KO cells Differentiate Normally	121
3.24 Tyk2 KO animals Appear to Beige Normally under β 3 Agonist Stimulation.....	123
3.25 Immortalization of STAT3 Preadipocytes Appears to Remove the Requirement for STAT3 in Differentiation.....	125
3.26 Mitochondrial STAT3 Levels Decrease During the Induction Period and Remained Depressed Throughout the Terminal Differentiation Phase	127
Chapter 4: Discussion	129
References.....	137
VITA	151

List of Tables

Table 1.1- Summary of WAT and BAT Characteristics.....	14
Table 2.1- Genotyping Primers.....	54
Table 2.2- Plating Volumes for Primary Cells.....	55
Table 2.3- Antibodies for Immunoblotting.....	56
Table 2.4- Primers for Real-Time qPCR	57
Table 2.5- Primers for Chromatin Immunoprecipitation	58

List of Figures

Figure 1.1- Basic Neural Regulation of Appetite	10
Figure 1.2- Histology of BAT and WAT	13
Figure 1.3- The Electron Transport Chain	18
Figure 1.4- Immunofluorescence staining of human fat tissue biopsies.....	24
Figure 1.5- Schematic representation of the major genes involved in general- and brown-adipogenesis.....	29
Figure 1.6- Schematic of the JAK family of tyrosine kinases	32
Figure 1.7- Schematic of STAT3	33
Figure 1.8- Schematic of the canonical JAK/STAT pathway.....	34
Figure 1.9- The canonical Wnt/β-catenin pathway	41
Figure 2.1- <i>In-Vitro</i> time course	53
Figure 3.1- STAT3 levels during <i>in-vitro</i> differentiation	60
Figure 3.2- Inhibition of STAT3 suppresses expression of terminal adipogenic markers	62
Figure 3.3- Inhibition of STAT3 during the induction phase reduces UCP1 expression	64
Figure 3.5- No difference in proliferation to confluence between WT and KO preadipocytes....	69
Figure 3.6- STAT3 KO brown adipocytes have reduced proliferation after induction	71
Figure 3.7- KO of STAT3 significantly reduces expression of UCP1	73
Figure 3.8- Expression of brown fat markers are more affected by knockout of STAT3 than general fat markers.....	74
Figure 3.9- Knockout of STAT3 significantly reduces lipid accumulation.....	76
Figure 3.10- Tamoxifen treatment has no affect on brown preadipocytes ability to differentiate	78
Figure 3.11- PPAR γ has increased turnover in the STAT3 KO preadipocytes	81
Figure 3.12- Deletion of STAT3 after the induction phase has no effect on UCP1 protein levels	83
Figure 3.13- Inhibition of JAK shows a biphasic response	85
Figure 3.14- STAT3 KO have increased apoptosis during the early terminal differentiation phase	88
Figure 3.15- Inhibition of PORCN rescues STAT3 KO brown adipocytes	92
Figure 3.16- STAT3 KO cells have reduced H3K27Ac levels that can be rescued with IWP2... ...	94
Figure 3.17- IWP2 can only rescue STAT3 KO preadipocyte differentiation when applied during the induction period	96
Figure 3.18 -β-Catenin is not down regulated in the STAT3 KO.....	99
Figure 3.19- Wnt/β-catenin signaling is elevated during induction phase in STAT3 KO.....	101
Figure 3.20- Canonical Wnt/β-catenin ligands are up regulated during the induction phase in STAT3 KO adipocytes.....	103
Figure 3.21- β-catenin pathway inhibitors rescue STAT3 KO brown adipocytes.....	108
Figure 3.22- RT-qPCR analysis of Wnt inhibitors	109
Figure 3.23- Treatment with Wnt inhibitors reduces Annexin V staining in the KO brown adipocytes	110
Figure 3.24- Wnt inhibition fails to rescue proliferation defect in STAT3 KO	111
Figure 3.25- Canonical Wnt inhibitors block β-catenin signaling	112
Figure 3.26- XAV939, a second β-catenin inhibitor, rescues STAT3 KO while a GSK3 β inhibitor, CHIR99021, blocks differentiation in WT STAT3 brown adipocytes	114

Figure 3.27- Knockdown of β -catenin can fully rescue UCP1 in the STAT3 KO brown adipocyte	116
Figure 3.28 Beige cells also require STAT3 during the induction period, but Wnt inhibition is not as robust	118
Figure 3.29- Deletion of STAT3 in inguinal fat pad of 8 week old mice appears to not affect UCP1 induction with the β 3 agonist CL316,243	120
Figure 3.30- Primary Tyk2 KO brown adipocytes have equal UCP1 and CIDEA expression to the WT	122
Figure 3.31- Induction of UCP1 mRNA by CL316,243 in Tyk2 KO mice appear to be normal	124
Figure 3.32- UCP1 mRNA expression appears to be equal in SV40 immortalized WT and KO STAT3 brown adipocytes	126
Figure 3.33- STAT3 rapidly exits the mitochondria during brown adipocyte differentiation....	128
Figure 4.1- Model of STAT3 Suppressing β -Catenin in Brown Adipogenesis	136

List of Abbreviations

ADP	Adenosine Diphosphate
ANOVA	Analysis of Variance
APC	Adenomatous Polyposis Coli
ATP	Adenosine Triphosphate
BAT	Brown Adipose Tissue
BMI	Body Mass Index
CDC	Centers for Disease Control and Prevention
CEBP	CCAAT/Enhancer Binding Proteins
CIDEA	Cell death-inducing DFFA-like effector
Cre	Cre Recombinase
DNA	Deoxyribonucleic Acid
EBF2	Early B Cell Factor 2
ETC	Electron Transport Chain
FABP4/aP2	Fatty Acid Binding Protein 4
FADH2	Flavin Adenine Dinucleotide
FFA	Free Fatty Acids
Flox	Flanking LoxP
GAPDH	Glyceraldehyde-3-phosphate Dehydrogenase
GSK3 β	Glycogen Synthase Kinase 3 β
GWAS	Genome Wide Association Study
HFD	High Fat Diet
HSL	Hormone Sensitive Lipase
I.P.	Intraperitoneal
JAK	Janus Kinase
LRP5/6	Lipoprotein Receptor-Related Protein 5 and 6
MCE	Mitotic Clonal Expansion
MCR4	Melanocortin Receptor 4
MFI	Mean Fluorescent Intensity
NADH	Nicotinamide adenine dinucleotide
NHANES	National Health and Nutrition Examination Survey
PET	Positron-Emission Tomography
PGC1 α	Proliferator Activated Receptor Gamma Co-Activator 1 Alpha
PKA	Protein Kinase A
PORCN	Porcupine
PPAR	Peroxisome Proliferator Activated Receptor
PRDM16	PR Domain Containing 16
RT-qPCR	Reverse Transcriptase-quantitative Polymerase Chain Reaction
SD	Standard Deviation
SEM	Standard Error of the Mean
SH2	Src Homology Domain 2
SNP	Single Nucleotide Polymorphism
STAT	Signal Transducer and Activator of Transcription
SVF	Stromal Vascular Fraction
T2D	Type 2 Diabetes

TAGTriacylglycerides
TBPTATA Binding Protein
TDEETotal Daily Energy Expenditure
UCP1Uncoupling Protein 1
WATWhite Adipose Tissue

Abstract

STAT3 IN THE REGULATION OF BROWN ADIPOCYTE DIFFERENTIATION

Marc Cantwell, B.S.

A dissertation submitted in partial fulfillment of the requirements for the degree of Doctor of Philosophy at Virginia Commonwealth University

Virginia Commonwealth University, 2018

Advisor: Andrew C. Larner, M.D., Ph.D.
Professor, Department of Biochemistry and Molecular Biology

Thermogenic fat is a promising target for new therapies in diabetes and obesity.

Understanding how thermogenic fat develops is important to develop rational strategies to treat obesity. Previously, we have shown that Tyk2 and STAT3, part of the JAK-STAT pathway, are necessary for proper development of classical brown fat. Using primary preadipocytes isolated from newborn mice we demonstrate that STAT3 is required for differentiation and robust expression of Uncoupling Protein 1. We also confirm that STAT3 is necessary during the early induction stage of differentiation and is dispensable during the later terminal differentiation stage. Without STAT3, the brown preadipocytes have increased apoptosis early in the terminal differentiation phase. We also show that the block in differentiation is caused by an inability of STAT3 knockouts to down regulate β -catenin by the end of the induction phase. Application of Wnt/ β -catenin inhibitors or knockdown of β -catenin during the induction phase is sufficient to fully rescue differentiation of brown adipocytes from the Myf5+ lineage, including reduction in

apoptosis, restoration of histone acetylation in the UCP1 promoter and enhancer regions, and full restoration of the expression of brown fat genes. Finally, we show that in the beige lineage, STAT3 is also necessary during the induction phase and can be rescued by Wnt/β-catenin inhibitors, although the rescue is not as robust as it is in the Myf5+ lineage.

Chapter 1: Introduction

Obesity is a medical condition that occurs when an individual has increased adipose tissue mass compared to amounts that are considered normal based on the individuals age, height, and gender. The prevalence of obesity has increased in the past forty years in the United States: fully one-third of the adult population is obese (1). The major impact of obesity is due to the comorbidities that develop in parallel; there are currently more than thirty medical conditions that are associated with obesity (2). Consequently, obesity is associated with an increase in overall mortality. Obesity together with its comorbidities are estimated to cost the US population 190 billion dollars per year, or approximately two thousand dollars per year per person (3). Due to this burden on the American healthcare system as well as the increased morbidity and mortality associated with obesity, new therapies and treatments are needed to reverse the weight gain trends of the last forty years.

One approach that has attracted much attention over the past few years has been to increase the mass of a specialized type of adipose tissue called Brown Adipose Tissue (BAT). BAT is a thermogenic tissue; its purpose is to generate heat through the metabolism of lipids in order to maintain optimal body temperature (4). There are ample amounts of this tissue present in animals such as rodents; however, it used to be thought that in humans BAT is only present in newborn infants and regressed to undetectable levels in adulthood. That understanding has been overturned in the last decade by findings that adults do in fact possess significant depots of BAT (5). The presence of BAT in adults has ignited interest in understanding the mechanisms of

development of this tissue in order to translate this knowledge into clinical applications towards obesity treatment.

The purpose of this dissertation is to explore the role of a transcription factor called Signal Transducer and Activator of Transcription 3 (STAT3) in the regulation of the development of BAT. The following section gives an overview on the epidemiology, etiology, and associated comorbidities of obesity. Next, a review of BAT tissue function, how it may prevent or diminish obesity and related metabolic diseases gleaned from *in-vivo* studies in rodents, and the human relevance of this tissue. Afterwards, a brief background on the genes currently known to impact the development of adipose tissue, a process referred to as adipogenesis, will be given. The JAK/STAT pathway will be introduced afterwards, with emphasis on what is already known about this pathway's role in regulating adipogenesis. Finally, the Wnt signaling pathway and its role in suppressing adipogenesis will be introduced—this dissertation presents evidence that this pathway is negatively regulated by STAT3 during brown adipocyte development.

1.1 Epidemiology, Etiology, and Associated Comorbidities of Obesity

Epidemiology of Obesity. Obesity in adults is defined by the World Health Organization and the National Institutes of Health as having a body mass index (BMI) greater than 30kg/m² (6, 7). Surveys of obesity have been conducted in the United States for years—the most prominent survey is the National Health and Nutrition Examination Survey (NHANES), conducted by the U.S. Centers for Disease Control and Prevention (CDC) (8). NHANES utilizes a mobile examination center where physical assessments can be made using standardized protocols, rather than relying on self-reported data (9). The data from NHANES has shown that since the 1980s, the rates of obesity have been increasing in both men and women. In 1980, the prevalence of obesity in the U.S. population was approximately 10% for men and 15% for women, but by 2014, the prevalence was 35% among men and 40% among women (9, 10). Geographically, the rates of obesity are not evenly distributed across the United States: southern states like Mississippi have a higher prevalence of obesity compared to west coast and northeastern states (11). Worldwide, while there is variation from country to country, there has been an increasing trend from 29/30% (men/women) in 1980 to 37/38% in 2013 (12).

For children, the prevalence of obesity has also been increasing over time, which is a particularly grave problem as risks of developing comorbidities and reduced life expectancy are increased the longer an individual is obese (2). Obesity is defined in children in the US as being above the 95th percentile in the CDC BMI-for-age growth charts; for adolescents the prevalence of obesity increased from 10% in 1994 to 20% in 2014 (13). Worldwide, the prevalence in 2013 was 24% in developed countries and 13% in developing countries (12).

Etiology of Obesity. Fundamentally, obesity is caused by a mismatch between caloric intake and total daily energy expenditure (TDEE). When the daily caloric content of food

exceeds the TDEE, the excess calories are stored as fat. The adipose tissue expands, both through hypertrophy and hyperplasia (14). However, while thermodynamics is the fundamental cause for increase adipose tissue mass, how this mismatch is established is more complex and involves interactions between genes and the environment.

Genetic disorders that display a Mendelian pattern of inheritance are rare contributors to the etiology of obesity; however, they illuminate the control these genes have over regulation of appetite. These disorders can be classified as monogenic, where the primary finding is obesity, or syndromic, where obesity is one clinical finding among a constellation of findings (and generally includes some form of mental retardation) (2, 15). The most common monogenic disorders involve disturbances to the Leptin signaling pathway and the Melanocortin 4 receptor, while the most common syndromic disorder is Prader-Willi Syndrome (15).

Leptin is a hormone that is produced in adipose tissue and produces satiety when it binds to its cognate receptor on the POMC and NPY/AGRP neurons in the arcuate nucleus of the hypothalamus (**Figure 1.1**) (16). Loss of either leptin or the leptin receptor results in hyperphagia and, subsequently, obesity (17). Individuals that are leptin deficient can receive subcutaneous injection of leptin that results in dramatic reduction in appetite and weight (18). Mouse models of leptin deficiency (ob/ob) and leptin receptor deficiency (db/db) exist and are popular for studies of obesity and Type II Diabetes (T2D) (19).

Mutations in the Melanocortin 4 receptor (MCR4) are the most common form of monogenic obesity (20). MCR4 is involved in the same neural regulation of appetite pathway as leptin and leptin receptor (21). In fact, leptin signaling increases production of the pro-opiomelanocortin (POMC) gene (22). POMC is a prohormone that is converted into multiple products, the most relevant product here being α -Melanocyte Stimulating Hormone (α MSH).

α MSH is released by the POMC neuron and binds to the MC4R on the melanin-concentrating hormone (MCH) neuron, where it acts to decrease firing of this neuron. Administration of MCR4 agonists in rodents leads to a decrease in food intake (23).

Overall, monogenic and syndromic causes of obesity make up a small percentage of the obese cohort, therefore most genetic contributors to obesity are polygenic in origin, i.e., Single Nucleotide Polymorphisms (SNPs) that an individual possesses each contribute and interact with each other to modify an individual's risk of developing obesity. Genome Wide Association Studies (GWAS) have been conducted in an attempt to identify common polymorphisms that increase an individual's risk of developing obesity or associated comorbidities (i.e. T2D) (24). The most studied allele that increases risk of obesity and T2D is the fat mass and obesity-associated gene (FTO) (25). Individuals who are homozygous for the most common obesity-causing variant weigh 3kg more and had an elevated risk of developing obesity 1.67 fold above those not carrying the risk variant (26). In the last few years, the function of the FTO allele and how it may contribute to obesity has been discovered (see section I.II-Human Studies of BAT).

Common environmental contributors to obesity include an increase in the sedentary lifestyle, reduced physical activity including exercise, and increased availability of low cost, high caloric density foods (27). Numerous studies in adults and children have documented the increase risk that a sedentary lifestyle paired with a diet that is considered unhealthy (e.g. high in processed sugars) is positively correlated with obesity (28-31). Lastly, another potentially major environmental contributor to obesity risk is currently under intense study: the gut microbiome. Analyzing the microbiome of the gut has begun to show associations with obesity and metabolic disorders, but causality has yet to be established (32-34).

Associated Comorbidities. Diabetes is a disease where the plasma levels of glucose are elevated (hyperglycemia). The major hormone that regulates plasma glucose levels is insulin. Insulin promotes the uptake of glucose into tissues such as adipose and skeletal muscle tissue. Chronic elevation of plasma glucose levels leads to pathologies in the kidneys, eyes, peripheral nervous system, and the cardiovascular system (35). There are two major types of Diabetes: Type I and Type II. Type I is defined by the lack of insulin production and is an autoimmune disorder against the cells of the endocrine pancreas that produce insulin (the pancreatic β cells) (36). Type II diabetes is defined by a systemic reduction in insulin responsiveness (insulin insensitivity); the pancreas is still able to produce insulin in Type II diabetes, at least in the initial stages of the disease (37). Adipose tissue contributes to the regulation of plasma glucose levels via release of hormones that regulates insulin sensitivity in other tissues, while also increasing the uptake of glucose with the insulin-regulated GLUT4 glucose transporter (38, 39). However, in obese individuals, the adipose tissue releases elevated levels of free fatty acids and pro-inflammatory cytokines like tumor necrosis factor alpha ($TNF\alpha$), which act locally and systemically to reduce responsiveness to insulin (40-43). Therefore, obese individuals have a higher risk of developing diabetes than their lean counterparts.

Increased adiposity is correlated with increased risk of 13 types of cancers (44). While casual mechanisms are still unclear, it is likely that the combination of increased hormones and inflammatory cytokines coupled with a conducive microenvironment increases risk of tumor initiation and progression (45, 46).

Obesity increased the risk of developing hypertension and increases risks of stroke, atherosclerosis, and myocardial infarction (47). In women, obesity can exacerbate Polycystic

Ovarian Syndrome, a disorder that involves increased androgen production and insulin insensitivity (48). Additionally, obese women have a higher risk of ovulatory infertility (49, 50).

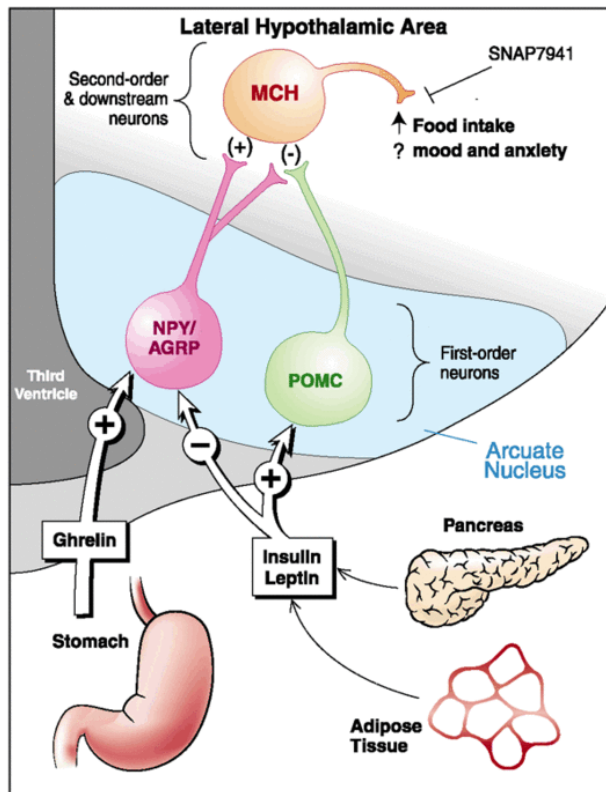


Figure 1.1- Basic Neural Regulation of Appetite

Leptin is a hormone produced by the adipose tissue and circulates to the arcuate nucleus of the hypothalamus where it binds to the leptin receptor on the POMC neuron, resulting in the increased probability of an action potential. The POMC neuron releases αMSH into the synaptic cleft between the POMC and MCH neuron. The MCH neuron contains the MC4R and binding of αMSH reduces the likelihood of the MCH firing an action potential. AGRP neuron produces the Agouti Related Protein, which is an antagonist of the MC4R. Adapted from (51), copyright license: 4282461312035.

1.2 BAT Function and Human Relevance

Comparison of BAT and WAT. There are two general types of adipose tissue present in humans: Brown Adipose Tissue and White Adipose Tissue (WAT). Each type of adipose tissue serves a specific purpose. BAT and WAT are so named because of the coloration of the tissue at the gross level. BAT is brown in coloration due to large amounts of mitochondria present in the adipocytes. The large numbers of mitochondria are necessary for BAT to serve its function (*vide infra*). In contrast, WAT contains relatively fewer mitochondria compared to BAT, and as a result is paler in color. Histologically, WAT and BAT can be easily discriminated based upon the lipid droplet morphology present in the cell (**Figure 1.2**). WAT contains a single large lipid droplet, while BAT contains multiple smaller lipid droplets (with the mitochondria interspersed between the smaller lipid droplets). Additionally, BAT is more highly innervated by the sympathetic nervous system and more vascularized than WAT. **Table 1.1** summarizes the basic characteristics of these two adipose tissues.

The anatomic locations of the two adipose tissues are also different. WAT is generally distributed across the body with large depots in the hypodermis of the skin and within the abdominal cavity. In contrast, BAT is more restricted in its locations; BAT is present in the human in supraclavicular, perirenal, and paravertebral depots. In the rodent, BAT is also present in axillary and interscapular depots.

WAT's major role is to store energy in the form of triacylglycerides (TAG) and to distribute the energy to the rest of the organism during periods of negative caloric balance. When fasting, lower levels of blood glucose stimulate epinephrine release from the adrenal glands. The epinephrine signals onto beta-adrenergic receptors on the adipocyte that result in activation of a lipase called Hormone Sensitive Lipase (HSL). HSL liberates free fatty acids (FFA) and glycerol

from the TAGs and secrete the FFAs into the blood for distribution to other tissues (mainly the liver and skeletal muscle), and secretes the glycerol to serve as a gluconeogenic substrate in the liver. Activation of HSL is opposed by insulin, which levels rise in response to higher blood glucose levels.

Additionally, WAT functions as an endocrine organ; the hormones they secrete are termed “adipokines”. Two major adipokines produced by WAT are Leptin and Adiponectin. Adiponectin serves to modulate glucose and fatty acid modulation; treatment with exogenous adiponectin has been found to reduce serum glucose levels and increase insulin sensitivity (52, 53). The levels of leptin in the serum are positively correlated to the total amount of adipose tissue in the organism, therefore, leptin signals to the hypothalamus the status of the fat reserves (17). Interestingly, leptin signals through a Type I cytokine receptor, and the downstream STAT that mediates this signaling is STAT3 (54). Deletion of STAT3 using a Nestin Cre, which targets both neuronal and glial cells, resulted in mice that were hyperphagic, obese, and diabetic, which is phenotypically similar to the ob/ob and db/db mice (55). Additionally, the mice were unable to maintain their core body temperature upon cold challenge. Histology revealed disorganized BAT that the authors believed was due to the reduced sympathetic output to the BAT.

In contrast, BAT does not store TAGs for distribution to other tissues during periods of starvation, rather, it is a thermoregulatory tissue; BAT metabolizes TAGs to produce heat in order to maintain optimal body temperature. BAT accomplishes its thermoregulatory function through an inner mitochondrial transmembrane protein called Uncoupling Protein 1 (UCP1).

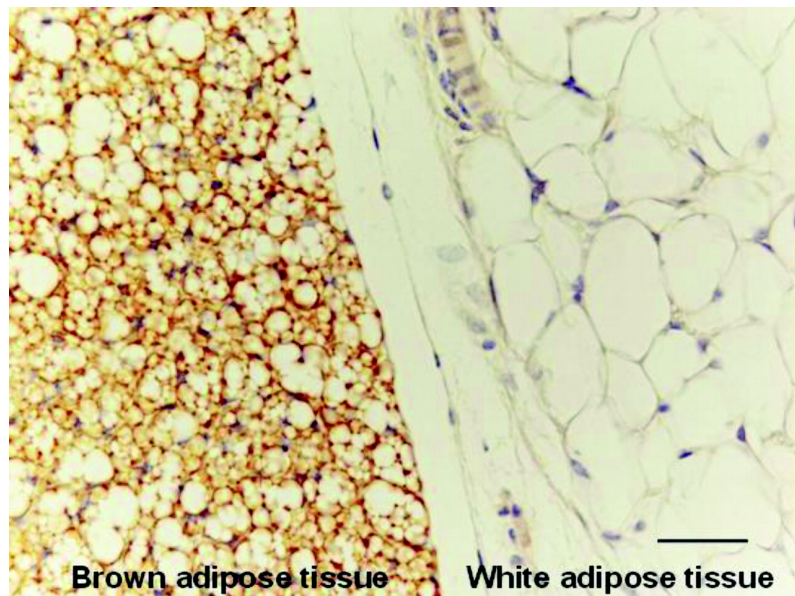


Figure 1.2- Histology of BAT and WAT

BAT and WAT can be discriminated by the lipid droplet morphology. BAT contains a centralized nucleus in addition to multiple small lipid droplets, which, when looked at through electron microscopy, are surrounded by large numbers of mitochondria (left). In contrast, WAT contains one single large lipid droplet with a nucleus relegated to the periphery of the cell (right). Additionally, the white adipocytes are larger in size compared to brown adipocytes. The brown coloration of the BAT is due to immunohistochemical staining for UCP1, the functional protein of BAT. Scale bar = 40 μ m. Adapted from (56), copyright license: 4277360251493.

Characteristics	WAT	BAT
Function	Energy Storage, Lipolysis and Secretion of FFAs/glycerol, Secretion of hormones such as Leptin and Adiponectin	Non-shivering Thermogenesis, Low Secretory Ability
Macroscopic Features	Locations: Subcutaneous, abdominal, retroperitoneal, perirenal, gonadal Color: White; yellow to off-white hue Adequate Vascularization (++) Sympathetic (++) Tissue Organization: Small lobules densely packed	Interscapular (rodents), paravertebral, axillary, and periadrenal Color: Brown; light pink to dark red Highly Vascularized (++++) Sympathetic (++++) Tissue Organization: lobular organization with gland-like structure
Microscopic Features	Cell Architecture: Unilocular lipid droplet occupying 90% of volume, variable size and shape (25-200µm) Nucleus: Peripherally located Mitochondria: Few High presence of other cell types (fibroblasts and immune cells)	Cell Architecture: Multilocular lipid droplets, polygonal and small (15-60µm) Nucleus: Centrally located Mitochondria: Abundant Low presence of other cell types
Molecular Markers	UCP1 (-), UCP2 (++) β3 adrenoreceptor (+) PGC1α (+) PRDM16 (-) CIDEA (-) Leptin (+++)	UCP1 (++++) β3 adrenoreceptor (+++) PGC1α (+++) PRDM16 (+++) CIDEA (+++) Leptin (+)

Table 1.1- Summary of WAT and BAT Characteristics

Modified from (57); Copyright License: 4278460310955

The Mitochondria Structure and Function. The mitochondrion is a membrane-bound organelle that is important in regulating metabolism and generating adenosine triphosphate (ATP). The mitochondrion contains two membranes: an inner and outer membrane. These membranes separate the internal components of the mitochondrion into two compartments: the intermembrane space, located between the inner and outer membrane, and the matrix. The inner mitochondrial membrane is uniquely structured to be highly impermeant to many small molecules, and as a result, many different types of solute carriers are needed to transport molecules across this membrane. The impermeance of the membrane is necessary for its function in generating ATP. Complexes of proteins, collectively called the Electron Transport Chain (ETC), form a series of oxidation/reduction (redox) reactions that take electrons from the substrates Nicotinamide adenine dinucleotide (NADH) and Flavin Adenine Dinucleotide (FADH₂), and ultimately pass the electrons to the terminal acceptor, molecular oxygen (**Figure 1.3**). These complexes couple the energy released in the redox reactions to pump hydrogen ions from the matrix into the intermembrane space against an electrochemical gradient. This hydrogen ion gradient is a form of potential energy and generates a membrane potential across the inner mitochondrial membrane. ATP Synthase, another integral membrane protein of the inner membrane, utilizes the electrochemical gradient in order to produce ATP. The Hydrogen ions flow down the electrochemical gradient through a pore in the ATP Synthase, and the energy released by the ions moving down this gradient is coupled to the formation of a phosphodiester bond between adenosine diphosphate (ADP) and inorganic phosphate.

The Uncoupling Protein 1. UCP1 is a member of the Uncoupling proteins family, which is a subfamily of the Solute Carrier family (SLC). There are five members of the Uncoupling protein family in mammals: UCP1, UCP2, UCP3, UCP4, and UCP5. Each member has a

different tissue distribution: UCP1 is restricted solely to BAT; UCP2 is more widespread, but with abundant expression in skeletal muscle; UCP4 and UCP5 are expressed in the nervous system (58).

All members of the family are localized to the inner mitochondrial membrane and function as a hydrogen ion transporter. In this regard they are similar to ATP synthase; however, the energy released by the flow of hydrogen ions down the electrochemical gradient is not coupled to ATP synthesis. As a result, the energy released is in the form of heat rather than chemical work. Therefore, the uncoupling proteins are so called because they “uncouple” respiration (the redox reactions of the ETC), from ATP synthesis. The increased permeability of the inner membrane to hydrogen ions results in the collapse of the mitochondrial membrane potential; this reduction in membrane potential can be utilized as a functional output of UCP1 function.

Under resting conditions, UCP1 has low conductance to hydrogen ions. Binding of long chain FFAs to UCP1 results in increased conductance (59). As a result, only when the cells are stimulated to increase lipolysis does UCP1 become maximally activated. This activation occurs when the organism senses its core body temperature decreasing; increased sympathetic output to BAT results in release of norepinephrine and subsequent binding to the β 3-adrenergic receptor (60). The β 3 adrenergic receptor is a G-protein coupled receptor (GPCR) that is associated with adenylyl cyclase, an enzyme that produces 3',5' cyclic adenosine monophosphate (cAMP). Upon stimulation of the β 3-adrenergic receptor cAMP levels rise in the cell, which leads to activation of a protein kinase called Protein Kinase A (PKA). PKA subsequently phosphorylates HSL and this leads to liberation of FFAs for use in binding and activating UCP1 as well as serving as

substrates for β -oxidation to maintain ATP levels. This regulation assures that UCP1 is properly activated when environmental conditions require thermogenesis to hypothermia.

While all members of the uncoupling family release the energy of the hydrogen ion gradient as heat, only UCP1 appears to function solely to generate heat for maintaining body temperature. While the primary function of the other UCPs are not as well characterized as UCP1, it appears they may primarily serve to reduce production of Reactive Oxygen Species (ROS) produced by the ETC, as well as play a role in regulating insulin secretion from the beta cells of the pancreas (58, 61, 62).

The factors that directly regulate UCP1 will be discussed in detail in section III of this chapter.

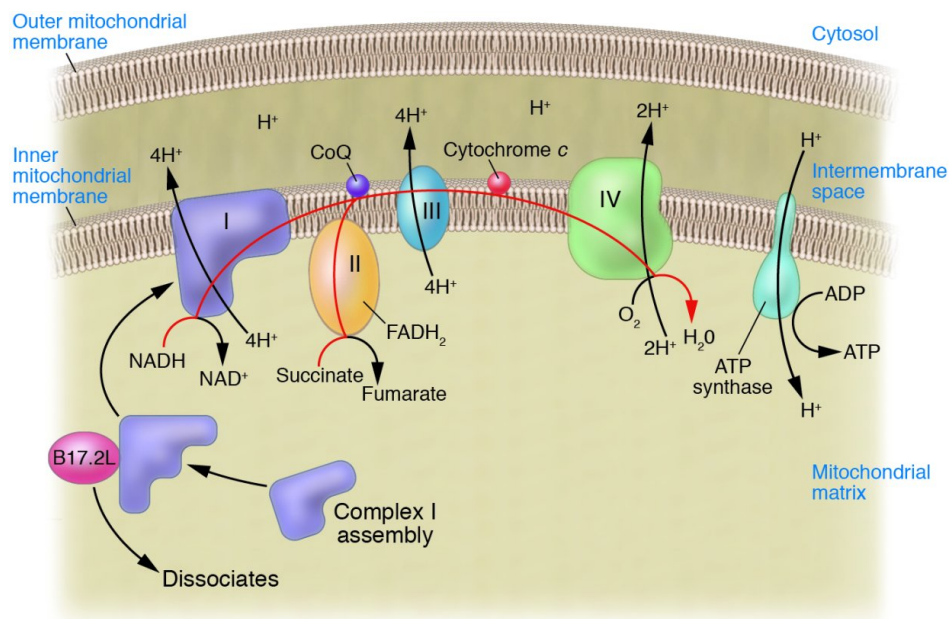


Figure 1.3- The Electron Transport Chain

NADH and FADH₂ are products of glycolysis and the citric acid cycle. They are carriers of electrons and are oxidized by Complex I (NADH) and Complex II (FADH₂). As the electrons are passed in a series of redox reactions to the terminal electron acceptor molecular oxygen, hydrogen ions are pumped from the matrix to the intermembrane space. This creates an electrochemical gradient that is harnessed to produce ATP by ATP Synthase. Adapted from (63), copyright license: 4277400364416.

BAT in the prevention of weight gain and Insulin Resistance. Whether the mass of BAT can actually affect whole-body energy balance and metabolic performance is an important question if this tissue should be realistically considered as part of future therapy in humans. Stanford et al. showed that increasing BAT in rodents through surgical transplantation can mitigate the effects of a western style high-fat diet (HFD) (64). In this study, male mice were assigned to 100mg BAT transplant, 100mg WAT transplant, or sham treatment. The mice receiving the BAT transplant were highly resistant to weight gain on a HFD. Additionally, the BAT implanted mice had improved glucose tolerance up to twelve weeks post-implantation, as well as more rapid glucose clearing. Interestingly, this enhanced glucose clearing was due to increased glucose uptake in many endogenous tissues, including visceral WAT and heart. This increased glucose uptake was due to increased circulating levels of fibroblast growth factor 21 (FGF21), and Interleukin-6 (IL-6) that was secreted by the transplanted tissue. FGF21 is a growth factor that has been shown to affect glucose levels and insulin sensitivity (65). IL-6 is important to mention here, as this cytokine signals through STAT3 (see section IV in this chapter). Indeed, if the transplanted BAT was IL6^{-/-}, the levels of circulating FGF21 decreased, indicating that paracrine action of IL-6 in BAT drives FGF21 expression and secretion. Further studies in mice utilizing BAT transplantation have shown that increasing BAT mass can partially revert obesity in Leptin receptor mice (Ob/Ob strain), reduce PCOS signs in rats, reduce atherosclerosis in a high cholesterol diet mouse model, and improve glucose tolerance independent of insulin in a Type I diabetic model (66-69).

Human Studies of BAT. While studies in rodent models of BAT on obesity and metabolic performance are promising, the relevance of BAT on affecting those metabolic parameters in humans is of intense interest. Adult humans possess significant stores of BAT, which can be visualized using ¹⁸F-fluorodeoxyglucose positron-emission tomography (¹⁸F-FDG PET) and computed tomography (70). Under thermoneutral conditions (defined as an ambient temperature that can sustain core body temperature under basal metabolic conditions, 22°C for humans), PET activity of BAT was negligible, but when the volunteers were submitted to cold exposure (16°C), PET activity increased in the supraclavicular and paraspinal regions. Interestingly, there is a negative correlation of BAT activity with BMI and body fat percentage. The supraclavicular, paraspinal, and periadrenal regions that are PET active under cold exposure are true BAT; biopsy of these locations reveals fat cells that have the histological hallmark of multilocular lipid droplets and positive staining for UCP1 (**Figure 1.4**). Interestingly, one study identified that there may be a sex difference in brown adipose tissue mass, with women potentially possessing more BAT than men (5).

The stores of BAT in humans may be of clinical consequence to obesity. Claussnitzer et al. reported a remarkable connection between obesity genetics and BAT development (5). They showed that the FTO allele, an allele that has been found to have a moderate association with adiposity and T2D, led to an increase in two developmental factors IRX3 and IRX5. These two factors repress the thermogenic program and promote differentiation into WAT instead. The authors knocked out IRX3 in adipose tissue in mice, which led to reduced body weight and increased energy expenditure that was not due to any increased physical activity. Knock out in human preadipocytes with the FTO allele restored the browning potential of the cells. Mutating the FTO allele to the non-risk variant also restored the ability of the preadipocytes to express the

thermogenic program. They further determined that the mutation in the FTO allele destroys a binding site for a repressor called ARID5B in an enhancer region for the IRX3 and IRX5 genes. This is some of the first evidence that altering the ability of preadipocytes to express the thermogenic program can have important consequences for the development of obesity and diabetes.

Now that there is evidence that BAT is present in humans and that aberrant development of BAT can lead to increased risk of obesity and diabetes, the next step is to determine if it is possible to manipulate the amount of BAT tissue in humans; if this is possible then it is a proof-of-principle that BAT can be a viable therapeutic target. Since BAT is a thermoregulatory tissue that is stimulated under conditions of suboptimal environmental temperature, the easiest- and safest- way to attempt to induce increases in BAT mass is to expose humans to mild cold stress environments. Lee et al. took five volunteers and subjected them to mild overnight cold stress (71). In this crossover study, the volunteers were housed overnight in a controlled environment where they were exposed to cyclical changes in temperature: either a mild cold stress of 19°C or warm conditions (27°C). They found that just sleeping in a cold environment for one month was enough to increase BAT mass by 42 percent. The participants were able to go about their lives normally during the day, but the time spent in the cold environment overnight was enough to induce the recruitment of additional BAT mass. Additionally, return to the warm environment for one month was enough to reduce the BAT mass that was accumulated prior. This was one of the first pieces of evidence that BAT mass is plastic in humans and that interventions can indeed alter the amount of tissue in a human.

Altering the temperature can certainly increase BAT in man, but it is not a therapeutic option to house patients overnight in a climate-controlled chamber. Thus, pharmacological

methods are needed. As stated above, BAT and BAT precursors carry a unique isoform of a beta-adrenergic receptor: the β 3- adrenergic receptor. Specific β 3 agonists exist, and treatment of cell cultures or administration to experimental animals *in vivo* can induce expression of the thermogenic program and UCP1 (72). Additionally, the β 3 receptor is restricted to mostly adipose tissue and bladder wall muscle (73). In the bladder, β 3 agonism results in relaxation of the bladder wall muscle (the detrusor muscle), and as a result, there is a β 3 agonist that is currently FDA approved drug for treatment of overactive bladder (74). Because this drug is already approved, testing for a new application in increasing BAT mass would be easier. Cypess et al. recruited healthy volunteers to take this β 3 agonist, trade name Mirabegron, to see if they could induce BAT mass/activity in a reversible manner (75). They observed that one 200mg dose was sufficient to increase BAT activity as measured by 18F-FDG PET, increased glucose uptake in the BAT, and led to an increase of the resting metabolic rate by 200 kcal. However, administration of this drug currently has some drawbacks. While Mirabegron is a specific β 3 agonist, the dose given to the participants led to considerable side effects of increased heart rate and blood pressure. More specific agonists that are less likely to affect the cardiovascular system are thus needed.

Two types of BAT: Myf5⁺ and Myf5⁻. In recent years the brown fat field has identified distinct developmental lineages of UCP1+ positive adipose tissue. Classically, studies in rodents have focused on the BAT found in the interscapular fat pad. This was termed “classical” brown fat. This lineage of BAT is termed Myf5⁺ brown fat, and these cells share an immediate precursor with skeletal muscle (76). However, in the rodent, another depot of UCP1+ brown adipocytes can be found in the subcutaneous fat pads in the inguinal region. These cells are not related to the Myf5 lineage and are thus called Myf5⁻/beige/brite cells (77). While both types of

cells express UCP1, each differ in molecular markers they express (78). Additionally, these two types of BAT have important functional differences. Myf5⁺ brown fat contains large amount of mitochondria and highly express UCP1 in the absence of stimulation, however, beige cells under resting conditions do not express the thermogenic program and have few mitochondria- only under sympathetic stimulation do the beige cells activate the thermogenic program and express UCP1 at similar levels to Myf5⁺ brown fat (77). This can be recapitulated *in-vitro*: Myf5⁺ preadipocytes will differentiate and express the thermogenic program after induction with no additional stimuli, while beige preadipocytes must be stimulated with either β-adrenergic agonists or PPARγ agonists (i.e. thiazolidinediones) after induction in order to express UCP1 (79, 80). In humans, clonal analysis has identified that the majority of the deposits that contain UCP1 are from a beige origin (77, 81). Therefore, while understanding the development of BAT using Myf5⁺ precursors is a valuable tool and can provide key insights into beige development, studies in beige cell development are more likely to have human relevance.

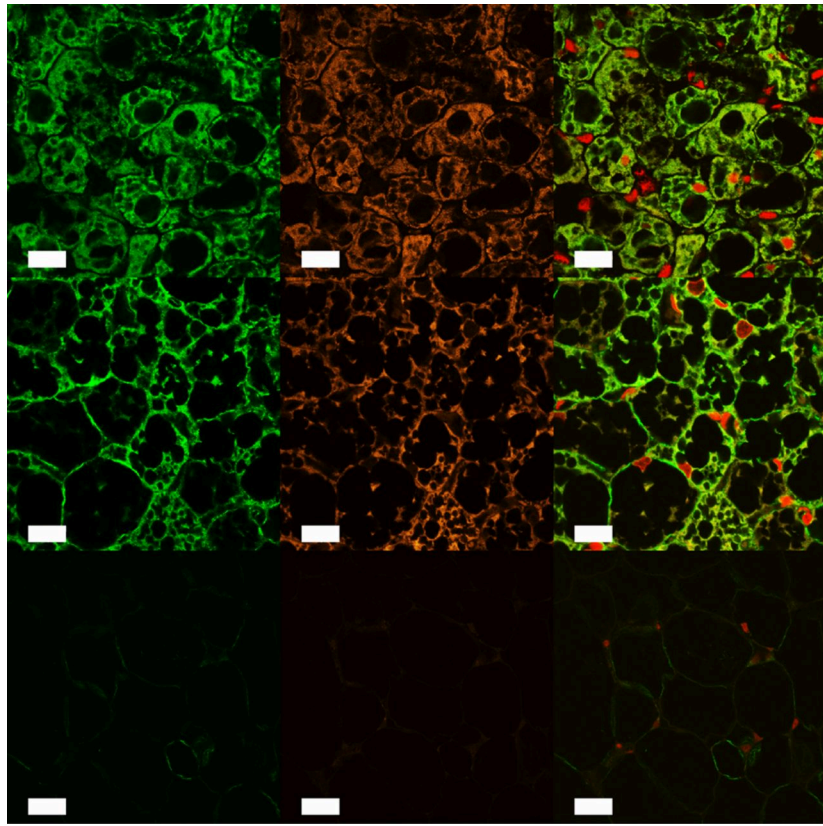


Figure 1.4- Immunofluorescence staining of human fat tissue biopsies

Human fat tissue was obtained at the supraclavicular (top row), periadrenal (middle row), or subcutaneous (bottom row) sites and were stained for UCP1 (green fluorescence, left column), and Cytochrome C Oxidase (marker of mitochondrial mass, red fluorescence, middle column). The rightmost column is a superimposed image. Both the supraclavicular and periadrenal sites contain UCP1⁺ fat tissue, while subcutaneous tissue is negative for UCP1 expression. Adapted from (82), copyright license: 4278520154370.

1.3 Genes Involved in Adipogenesis and Browning

Studies using cell lines of preadipocytes and transgenic animals have determined much of the core program of adipogenesis that is shared by all types of adipose tissue. Additionally, factors that specifically regulate the thermogenic program and UCP1 expression have been identified. Review of the identity and function of these genes as well as the temporal order in which these genes operate is provided here. A general schematic of the genetic program of brown adipogenesis is presented in **Figure 1.5**.

The CCAAT/Enhancer Binding Proteins (CEBP). The CEBP transcription factor family contains six members: CEBP α , CEBP β , CEBP δ , CEBP ϵ , and CEBP ζ . They are members of the basic-leucine zipper (bZIP) transcription factor family (83). Of the six members, CEBP α , CEBP β , and CEBP δ are important for adipogenesis *in-vitro* and *in-vivo*, and CEBP σ is directly regulated by STAT3 (84, 85). When the preadipocytes are stimulated to differentiate in culture, CEBP β and CEBP δ are one of the first genes to be induced; they reach peak expression within 4 hours of stimulation (86). *In-vitro*, CEBP β is sufficient for differentiation, while CEBP δ is dispensable (87). However, *in-vivo* loss of CEBP β or CEBP δ alone does not lead to a significant reduction in adipose mass, but the CEBP β /CEBP δ double knockout does result in significant loss of adipose mass, suggesting that *in-vivo* these two transcription factors are redundant (88). CEBP β and CEBP δ 's major targets are the next two transcription factors necessary for differentiation, CEBP α and Peroxisome Proliferator Activated Receptor Gamma (PPAR γ) (89, 90). CEBP β also cooperatively binds to PPAR γ to regulate genes involved in the terminal differentiation program. During the first 48 hours of differentiation *in-vitro*, the cells re-enter the cell cycle and proliferate during the phase called the “Mitotic Clonal Expansion” (MCE) (91). CEBP α is anti-proliferative and ends the MCE by increasing expression and stability of the cell

cycle inhibitor, p21 (92). Additionally, CEBP α regulates some of the common terminal markers of mature adipocytes like leptin, fatty acid binding protein 4 (FABP4/aP2), and GLUT4 (93, 94). *In-vivo*, CEBP α is absolutely necessary; knockout animals have reduced lipid droplet size and BAT has reduced UCP1 expression (95).

Peroxisome Proliferator Activated Receptor Gamma (PPAR γ). The PPAR family is a member of the nuclear receptor superfamily, and they function by heterodimerizing with the retinoid X receptor (RXR) and binding to peroxisome proliferator response elements (PPREs) in the promoters of target genes (96). PPAR γ is considered the “master regulator” of adipogenesis, because no other factor has been identified that can compensate for loss of PPAR γ (97). There are two isoforms of PPAR γ : PPAR γ 1 and PPAR γ 2 (98). PPAR γ 1 is more widely distributed across different tissues, but PPAR γ 2 is restricted to adipose tissue. PPAR γ 2 levels begin to increase around day 4 after stimulation to differentiate, and is regulated by CEBP α , while PPAR γ 1 is constitutively expressed throughout the entire differentiation time course (99). PPAR γ works cooperatively with CEBP α and CEBP β to regulate the genes expressed during the terminal differentiation phase of adipocytes (100). PPAR γ , along with its co-factor Peroxisome Proliferator Activated Receptor Gamma Co-Activator 1 Alpha (PGC1 α), directly regulate transcription of the UCP1 gene (101). Both PPAR γ 1 and PPAR γ 2 can induce the adipocyte program, however, PPAR γ 2 can induce adipogenesis under reduced ligand concentrations compared to PPAR γ 1 (102). *In-vitro*, PPAR γ 2 is sufficient to induce differentiation of fibroblasts into adipocytes, indicating that PPAR γ may also have a role in determining cell fate (103). The thiazolidinediones, a class of anti-diabetic drugs, are agonists for PPAR γ , and can be used in cell culture to increase expression of UCP1, especially in beige cells (77, 80).

Peroxisome Proliferator Activated Receptor Gamma Co-Activator 1 Alpha (PGC1 α).

PGC1 α regulates mitochondrial biogenesis and increases the cells ability to generate energy (104). PGC1 α accomplishes these by co-activating Nuclear Respiratory Factors 1 and 2 (NRF1 and NRF2), two transcriptions factors that regulate nuclear-encoded components of the ETC and mitochondrial transcription factor A (Tfam), which regulates mitochondrial DNA transcription and replication (105). It is expressed in tissues that have high rates of oxidative phosphorylation such as cardiac muscle, Type I (oxidative, slow-twitch) skeletal muscle, and BAT (106). PGC1 α increases UCP1 expression by augmenting the transcriptional abilities of PPAR γ and thyroid hormone receptor (104). PGC1 α also regulates the expression of cell death-inducing DFFA-like effector (CIDEA), a negative regulator of UCP1 function (106, 107).

PR Domain Containing 16 (PRDM16). PRDM16 was the first transcription factor identified that specifically controls the determination of BAT; when expressed in WAT progenitors, it is able to induce the thermogenic program, in part by upregulating PGC1 α (108, 109). Conversely, deleting PRDM16 in adipose tissue using and adiponectin promoter driven Cre leads to an inability of subcutaneous fat to beige and insulin resistance (110). In Myf5 $^+$ progenitor cells, expression of PRDM16 promotes the differentiation into BAT, while ablation of PRDM16 promotes differentiation into skeletal muscle (111). PRDM16 interacts with Med1, part of the mediator complex, and recruits the complex to enhancer regions of thermogenic genes (112, 113). Interestingly, BAT specific knockout of PRDM16 does not affect the embryonic development of BAT tissue, however, it is required for maintenance of the BAT phenotype as the mice age (114).

Early B-cell Factor 2 (EBF2). PPAR γ is present in both WAT and BAT and directly regulates UCP1 expression, yet in WAT UCP1 is undetectable. Therefore, it was postulated that

a factor exists in classical BAT and beige cells that allows selective recruitment of PPAR γ to thermogenic genes. The EBF binding motif was found near PPAR γ binding sites in BAT specific genes and subsequent ChIPseq experiments revealed that EBF2 binds to these motifs and recruits PPAR γ to these sites in part by interacting with the BAF chromatin remodeling complex to control access to the promoters (115, 116). Knockout of EBF2 either *in-vitro* or *in-vivo* resulted in loss of the thermogenic program with no effects on the general adipocyte program.

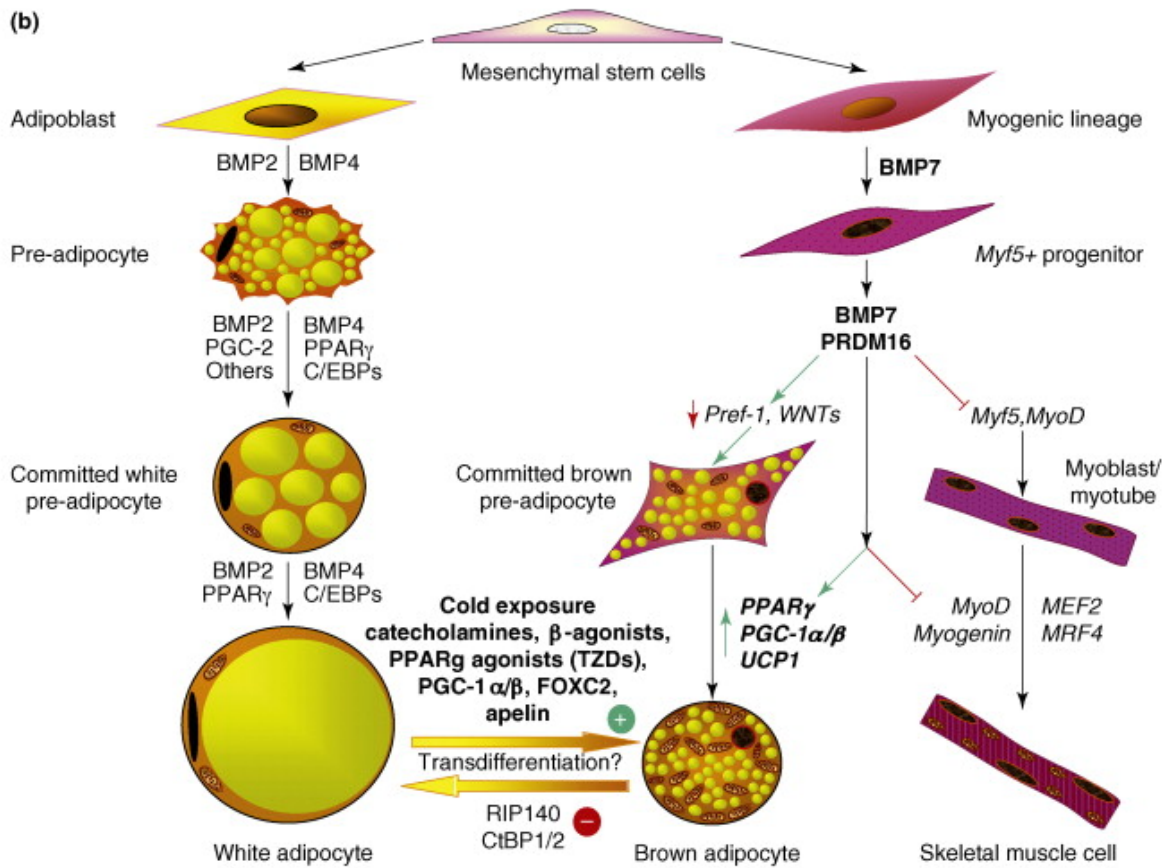


Figure 1.5- Schematic representation of the major genes involved in general- and brown-adipogenesis

Left Column: Myf5- adipocyte lineage (which includes beige cells). Right Column: Myf5+ lineage containing the classical brown fat cell. Adapted from (57), copyright license 4301971047874.

1.4 The JAK/STAT Pathway and its Known Roles in Adipogenesis

Introduction of the JAK/STAT Pathway. The Janus Kinase (JAK)-Signal Transducer and Activator of Transcription (STAT) pathway was initially identified in the 1990s as the mediator of interferon signaling (117). Subsequently, this pathway has been implicated in a variety of other processes such as development (especially in the hematopoietic system), cell growth, immune responses, and cancer (118).

The JAKs are a family of tyrosine kinases consisting of four members: JAK1, JAK2, JAK3, and Tyrosine Kinase 2 (Tyk2). These kinases have a FERM domain that is necessary for interaction with their cognate cytokine receptors and two tyrosine kinase domains, JH1 and JH2; however, JH2 is a pseudo kinase domain that lacks an ATP binding site, yet is necessary for full functionality of JAKs (**Figure 1.6**) (119). JAK1, JAK2, and Tyk2 are widely distributed across different tissues, whereas JAK3 is mostly restricted to the hematopoietic lineage (120).

There are seven known STATs in mammals: STAT1, STAT2, STAT3, STAT4, STAT5A, STAT5B, and STAT6 (121). The structures of the different STATs are mostly conserved, with some important differences that will not be addressed here. For STAT3, the structural schematic is found in **Figure 1.7**. STAT3 contains an N-terminal domain, which is used to form STAT3 tetramers, following by a coiled-coiled domain which is involved in protein-protein interactions with other transcription factors and regulators (122). The DNA binding domain contains residues that recognize specific DNA sequences found in the promoters of STAT3 regulated genes. The SH2 domain is involved in recognizing phosphotyrosine residues and is used to dock to the cytoplasmic tails of cytokine receptors, as well as dimerize with other STATs. C-terminal to the SH2 domain is a tyrosine residue that is phosphorylated by the JAKs (Y705). In STAT3, there exists two forms owing to differential splicing: STAT3 α and STAT3 β .

These isoforms differ in the possession of a C-terminal Transactivation Domain (TAD), which is present in the alpha form, but is absent in the beta form. The TAD contains a serine site that is phosphorylated by members of the MAPK and mTOR families (123, 124). The TAD enhances the transcriptional regulatory ability of STAT3 through its protein-protein interactions with other members of the transcriptional machinery such as CBP/p300 (125).

The JAKs associate with cytokine receptors, which are single transmembrane proteins with an extracellular ligand binding domain and an intracellular cytoplasmic tail that serves as a docking site for JAKs and STATs (126). Different cytokine receptors recruit different JAKs and STATs, allowing for increased complexity with a small set of components (127). Cytokine receptors are not active on their own, however, cytokines bind two cytokine receptors and bring them in close apposition. The JAKs associated with each cytokine receptor phosphorylate themselves, leading to maximal kinase activation, as well as phosphorylating the cytoplasmic tail of the receptor. These phosphotyrosine residues in the cytoplasmic tail serve as docking sites for the STATs. The STATs dock at the cytokine receptor through their SH2 domain, where they are subsequently tyrosine phosphorylated by the JAKs. The STATs dissociate from the receptor and then either homo- or hetero-dimerize through binding of the phosphotyrosine residue present in the other STAT through their SH2 domains. Once the STATs dimerize, they are able to transport to the nucleus and bind to conserved DNA binding sequences where they can exert their gene regulatory effects (128). A schematic of this classical pathway is shown in **Figure 1.8**.

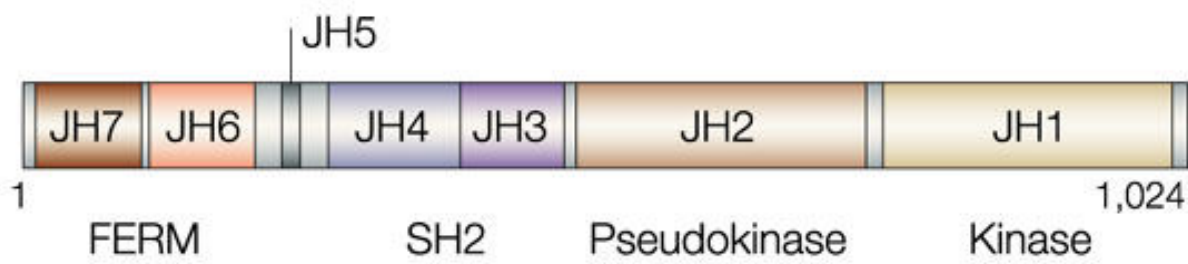


Figure 1.6- Schematic of the JAK family of tyrosine kinases

Adapted from (129), copyright license 4301961262534.

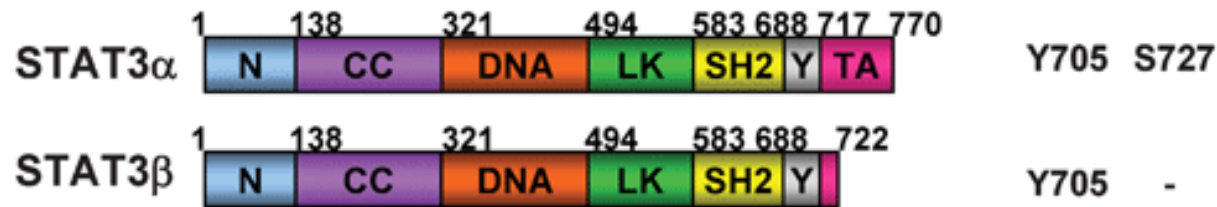
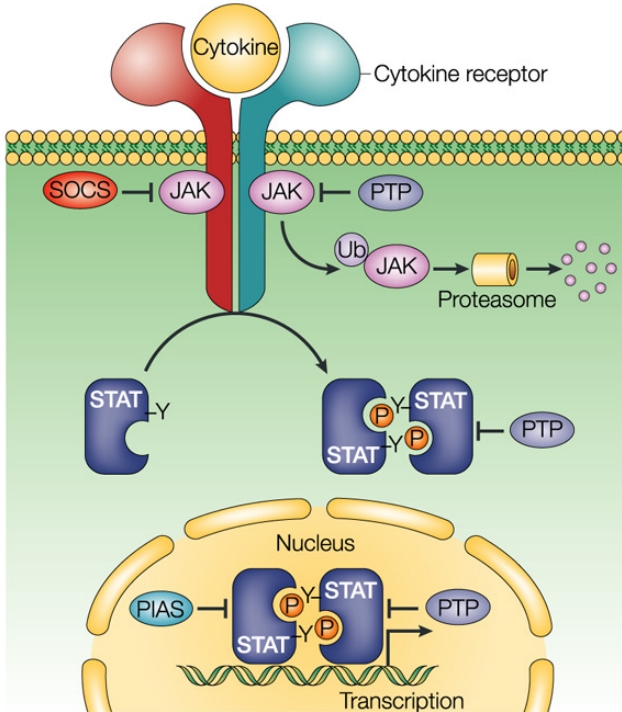


Figure 1.7- Schematic of STAT3

N= N-terminal Domain, CC= Coiled-Coiled Domain, DNA = DNA binding Domain, LK= Linker Domain, SH2= SH2 Domain, Y= JAK phosphorylated tyrosine residue, TA = Transactivation Domain. Adapted from (122), copyright license 4301951395247.



Nature Reviews | Immunology

Figure 1.8- Schematic of the canonical JAK/STAT pathway

Cytokine binding to cytokine receptors activate the associated JAKs, which tyrosine phosphorylate the cytoplasmic tail of the receptor, creating a docking site for STATs. STATs dock at the receptor and are phosphorylated by the JAKs. The STATs dimerize and translocate to the nucleus where they bind to DNA and affect transcription. The pathway is tightly regulated through the actions of other proteins, such as Suppressor of Cytokine Signaling (SOCS), protein tyrosine phosphatases (PTP) and Protein Inhibitor of Activated STAT (PIAS). Adapted from (130). Copyright license: 4318860682296.

STAT3 in Adipogenesis. The majority of studies to date looking into the role of STAT3 in adipogenesis have utilized the 3T3-L1 cell line, an immortalized mouse cell line that is committed to differentiating into white adipose cells. The earliest studies indicated that STAT3 was necessary for proliferation of the preadipocytes to confluence and possibly needed for the proliferation of the preadipocytes during the MCE phase of differentiation (131). The authors noted that during induction STAT3 remained tyrosine phosphorylated for up to 3 days, which coincides with the MCE and early terminal differentiation phase. Using EMSA assays, STAT3 was bound to the DNA during the proliferation to confluence and to a minor extent during the MCE, but no binding was evident during the terminal differentiation phase. Thus, the authors concluded that STAT3 was only required for the proliferation of cells to confluence and possibly during the MCE, but is likely not required in the terminal differentiation phase.

Additional evidence of the importance of STAT3 for adipogenesis comes from a study of Protein Inhibitor of Activated STAT3 (PIAS3), a protein that binds to STAT3's DNA binding domain, which blocks STAT3's transcriptional activity. Overexpression of PIAS3 in preadipocytes led to reduced mRNA expression of PPAR γ and CEBP α , as well as the terminal markers aP2 and Adiponectin (132). Additionally, the authors found that ob/ob mice had natural overexpression of PIAS3 in WAT.

After establishing STAT3's importance in adipogenesis, other groups set out to determine what STAT3 was regulating during adipogenesis and what signaling molecules drive STAT3 activity. Leptin and LIF are two cytokines that bind to receptors that recruit STAT3. Leptin treatment in rat preadipocytes enhanced adipogenesis, while LIF had no major effect on adipogenesis per se, but did reduce the level of lipid accumulation in the mature adipocytes (133, 134). Midkine, also known as neurite growth-promoting factor 2 (NEGF2), was identified as an

autocrine/paracrine factor that is released upon induction of differentiation in 3T3-L1 cells and is the factor responsible for STAT3's tyrosine phosphorylation during the induction phase of adipogenesis; blocking antibodies to midkine reduced STAT3 phosphorylation, reduced the MCE, and reduced adipogenesis (135). How midkine signaling leads to tyrosine phosphorylation is unknown, as the receptor for midkine is considered to be a tyrosine phosphatase (136).

The mechanism of STAT3 in the regulation of adipogenesis is not well characterized. STAT3 was shown to transcriptionally regulate CEBP β , one of the first genes induced in adipogenesis (137). The authors also showed that STAT3 binds to the distal region of the promoter for CEBP β . Additional research indicated that STAT3 acts upstream of PPAR γ ; chemical inhibition of STAT3 or knockdown using siRNA reduced adipogenesis, but could be rescued by using a PPAR γ agonist (138).

In immortalized brown adipocytes, we previously published that STAT3 was downstream of Tyk2 and interacts and stabilizes PRDM16 (139). Moreover, expression of a constitutively activated STAT3 (STAT3C) in Tyk2 $^{-/-}$ was sufficient to rescue brown adipogenesis. Finally, STAT3C expression in the BAT of Tyk2 $^{-/-}$ animals can restore the expression of brown fat markers such as UCP1 and CIDEA.

In-vivo studies of STAT3 in the regulation of adipogenesis are lacking. Total STAT3 knockout causes embryonic lethality in mice, so tissue specific knockouts are required. An aP2 promoter driven Cre mouse was used to generate adipose tissue that lacks STAT3. The mice have increased weight and increased fat mass due to hypertrophy of the WAT- the hypertrophy was likely due to impaired lipolysis in response to leptin (140). However, aP2 is not specific to adipose tissue and is expressed relatively late in the development of adipose tissue and therefore

this mouse model may not capture the effects of STAT3 on differentiation of adipose tissue, but rather is a model of STAT3's role in the function of mature adipocytes (141).

1.5 The Wnt Pathway and its Role in Suppressing Adipogenesis

The Canonical Wnt/β-Catenin Signaling Pathway. The Wnt pathway is important for normal development of all metazoans; this pathway is responsible for diverse functions such as establishment of cell polarity in epithelium, cell fate, and maintenance of pluripotency of stem cells (142, 143).

The Wnt pathway contains 19 different secreted Wnt ligands (144). These are glycoproteins that all share conserved serine residues, which are acylated by the endoplasmic reticulum enzyme Porcupine (PORCN) (145). This acylation is necessary for secretion of Wnt ligands and for optimal binding of the ligands to their receptors (146). Once the Wnt ligands have been acylated, they are recognized by the carrier protein Wntless, which ferries the ligands through the Golgi and to the extracellular surface of the plasma membrane (147). Once released to the extracellular environment, they bind to their receptors, which is composed of two proteins called Frizzled (of which there are a number of different members) and Lipoprotein Receptor-Related Protein 5 and 6 (LRP5/6) (148). While there are a number of downstream effectors in the Wnt pathway, the most common is the canonical pathway involving β-catenin.

β-Catenin is a multifunctional protein. It is both a transcription factor and a component of cadherin junctions (149). **Figure 1.9** details how β-Catenin is regulated as a transcription factor. In the absence of Wnt ligand, β-catenin is marked for proteasomal degradation. A priming phosphorylation at serine 45 by Casein Kinase 1α allows β-catenin to be recognized by a destruction complex composed of the scaffold protein Axin2, Adenomatous Polyposis Coli (APC), and Glycogen Synthase Kinase 3β (GSK3β) (150). GSK3β phosphorylates β-catenin at serines 33 and 37; these serine sites serve as recognition sequences for an E3 Ubiquitin Ligase called βTrcp. Once ubiquitinated, β-catenin is rapidly degraded by the proteasome. However, if

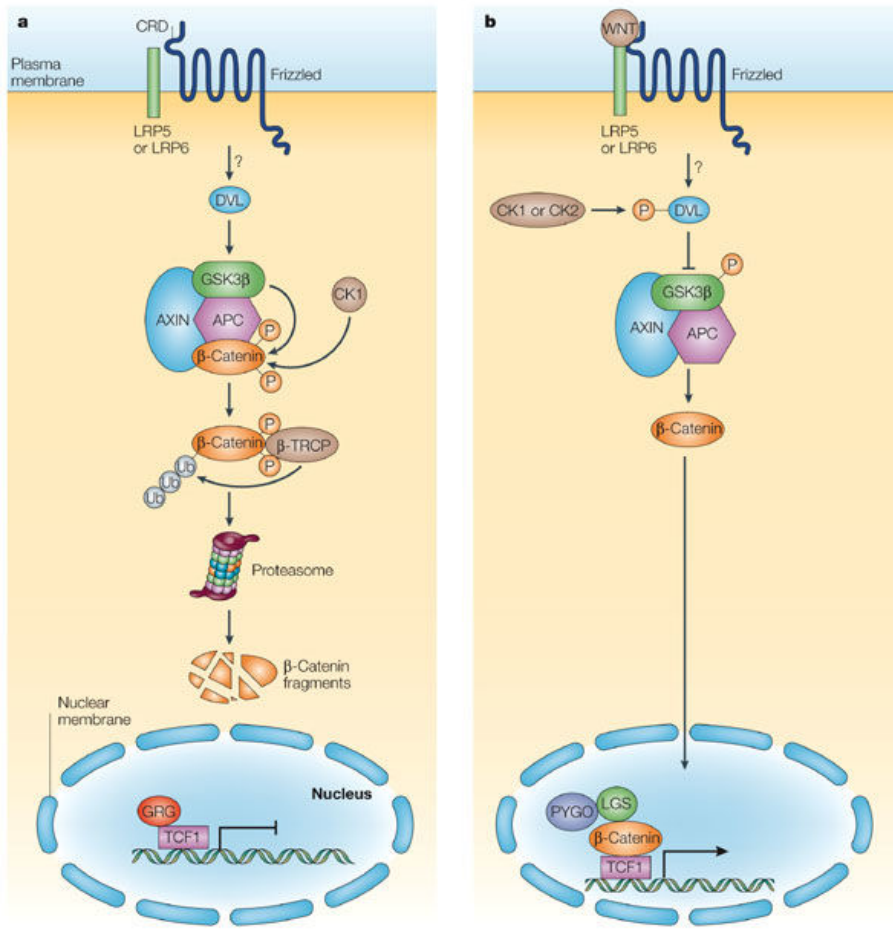
Wnt ligand is present, it signals through the Frizzled/LRP receptor, which allows recruitment of Axin to bind to LRP (151). The binding of the destruction complex to the receptor inactivates the destruction complex, allowing β -catenin to accumulate. Accumulating free cytosolic β -catenin is then available for transport to the nucleus, where it can bind to many partners to affect its nuclear function, but its most well defined partner is TCF (152). Additionally, β -Catenin turnover can be fine tuned by regulating different components of the destruction complex. For example, Axin2 stability can be altered by tankyrases 1 and 2 (153). Tankyrases are poly-ADP-Ribosylating enzymes; when Axin2 is ADP-Ribosylated it is marked for proteasomal degradation.

The Wnt Pathway in the Suppression of Adipogenesis. The Wnt pathway is well studied in the context of adipogenesis, and it is firmly established to be a negative regulator of adipogenesis. Treatment with Wnt1 or introduction of a stabilized form of beta-catenin is sufficient to suppress adipogenesis in 3T3-L1 cells (154). Specifically, this was due to a decrease in expression of PPAR γ and CEBP α , and adipogenesis could be rescued if either of these transcription factors were overexpressed. While Wnt1 can suppress adipogenesis, it is likely that Wnt10b is responsible for this repression as it is highly expressed in preadipocytes and as the cells differentiate levels of this ligand diminish (155). In brown fat, Wnt signaling reduces PGC1 α during differentiation, which is an important co-factor involved in the expression of UCP1 (156). Additionally, mature adipocytes treated with Wnt10a have suppressed UCP1 protein levels and *in-vivo* can convert brown adipocytes to a more white-like phenotype (157).

Non-canonical Wnt pathways can also modulate adipogenesis. Wnt5b antagonizes the canonical pathway through increased GSK3 β -mediated degradation activity and can partially restore adipogenesis with cells that are co-treated with Wnt3a (158). Wnts 2 and 11, part of the

Calcium/Calmodulin/Calcineurin non-canonical Wnt pathway, decrease adipogenesis in the 3T3-L1 cell line (159).

Normally, Wnt signaling is reduced during differentiation through silencing of Wnt ligand genes through the actions of the methyltransferase EZH2 tri-methylating Histone H3 K27 in the Wnt ligand promoters (160). The silencing of Wnt ligands should have the effect of reducing β -catenin, since without that signaling, the GSK3 β destruction complex will phosphorylate β -catenin to tag it for destruction by the proteasome. Further regulation of β -catenin comes through cross-talk with PPAR γ (161). Activation of PPAR γ with exogenous ligands leads to reduced β -catenin stability, possibly through a direct interaction between PPAR γ and β -catenin (162).



Nature Reviews | Immunology

Figure 1.9- The canonical Wnt/β-catenin pathway

Left Panel: When Wnt ligand is absent, the Axin2/APC/GSK3 β destruction complex is able to bind and phosphorylate β-catenin, which is a recognition mark for the E3 Ubiquitin Ligase βTRCP. β-Catenin is degraded by the proteasome and as a result does not transit to the nucleus. TCF1 interacts with Groucho (GRG), which represses Wnt regulated genes. **Right Panel:** When Wnt ligand is present, the Axin2/APC/GSK3 β destruction complex is inhibited and β-Catenin is left unphosphorylated, causing its levels to build up and eventually translocate to the nucleus. β-Catenin displaces Groucho and binds with TCF1, leading to upregulation of Wnt driven genes.

Adapted from (163), Copyright license 4302051187472.

1.6 Dissertation Rationale and Objectives

Previously, we observed that Tyk2 KO brown adipocytes do not differentiate and can be rescued with constitutively active STAT3 (139). How STAT3 was able to rescue the Tyk2 KO was not investigated, and the mechanism of STAT3 in adipogenesis has been poorly defined. This objective of this dissertation is to answer three questions, with each building upon the previous: 1) Is STAT3 needed for differentiation of primary brown adipocytes? 2) When is STAT3 required for differentiation- is it always required to maintain a brown adipocyte or is there a distinct period in development where STAT3 acts and then is no longer necessary? 3) What is STAT3 regulating during differentiation- does it regulate another known pathway that either positively or negatively regulates adipogenesis?

This dissertation provides evidence to all three questions posed. We show that STAT3 is indeed necessary for primary brown fat differentiation, that is only required during the induction phase, and that it functions to suppress Wnt/β-catenin signaling during the induction phase, likely through suppression of Wnt ligand expression.

Chapter 2: Materials and Methods

2.1 Generation of Mice

All mice were bred and maintained in the animal facility at MCV/VCU in accordance with the Institutional Animal Care and Use Committee (IACUC). Mice containing STAT3 with flanking Lox-P sites (Flox) were obtained from Jackson Laboratory- strain #016923. These mice were crossed with mice containing a ubiquitously expressed Tamoxifen induced Cre Recombinase in the ROSA locus (Jackson Laboratory)-strain #008463. The offspring were bred until they were homozygous for both the floxed STAT3 allele and Tamoxifen-inducible Cre Recombinase allele; these mice served as founders for the colony. Floxed Tyk2 mice were a gift from Brigit Strobel. These mice were crossed with the Tamoxifen-Inducible Cre Recombinase mice until mice that were homozygous for floxed Tyk2 and Tamoxifen Cre Recombinase. All mice were genotyped to confirm possession of the desired alleles.

2.2 Mouse Genotyping

The mice were genotyped using a modified HotSHOT genomic DNA isolation protocol. A 1-3mm tail snip was incubated with 75 μ L alkaline lysis buffer (25mM NaOH, 0.2mM EDTA, pH 12.0) at 95°C for 1 hour. After allowing the sample to cool to room temperature, 75 μ L of neutralization buffer (40mM Tris-HCl, pH 4.0) was added and the samples were briefly vortexed. The PCR reaction contained the following: 5 μ L of Genomic DNA sample, 12.5 μ L of 2x GoTaq Hot Start Green Master Mix (Promega), 2.5 μ L of a mixture containing the primers each at a concentration of 2.5 μ M, 0.625 μ L of 20mg/mL Bovine Serum Albumin (Sigma-

Aldrich), and 4.38 μ L of dH₂O. The following PCR conditions were used: 1) 95°C for 5 minutes, 2) 95°C for 30 seconds, 55°C for 30 seconds, 72°C for 30 seconds, repeated for 30 cycles, 3) 72°C for 10 minutes. The PCR products were run on a 1% Agarose (Fisher)/TBE (National Diagnostics) gel with 0.5 μ g/mL Ethidium Bromide (Fisher) at 100V for 1 hour. The sequences for the genotyping primers can be found in table 2.1.

2.3 Isolation of Primary Brown Preadipocytes

For Myf5⁺ Preadipocytes, one to three day-old pups were used to isolate primary preadipocytes. The pups were sacrificed by decapitation and the interscapular fat pad was harvested. Fat pads from different mice were pooled together during isolation; each pool is considered a biological replicate. Each pool contained a variable number of mice, but the minimum was three. The fat pads were minced and placed in isolation buffer (123mM NaCl, 5mM KCl, 1.3mM CaCl₂, 5mM Glucose, 100mM HEPES, 4g/100mL Bovine Serum Albumin, Antibiotics/Antimycotics) containing 1.5mg/mL of Collagenase A (Roche) and incubated for 40 minutes at 37°C with rocking. After the incubation period, the digestion was passed through a sterile 70 μ m nylon filter (Fisher) and the resulting filtrate was centrifuged at 500g for 5 minutes at room temperature. The supernatant was removed and the cell pellet (containing a mixture of preadipocytes and blood cells) was resuspended in 1mL of PBS for every fat pad in the pool (e.g. 5 fat pads processed-5mL of PBS resuspension). The cells were plated onto dishes such that the starting density would allow the cells to reach confluence between Day 5 and 7 after isolation; the volumes of the cell resuspension plated for each type of dish were determined empirically and are found in table 2.2. The cells were plated into DMEM (GIBCO) growth media containing 4.5g/L Glucose, 5nM Insulin (Sigma-Aldrich), Antibiotics/Antimycotics (GIBCO), and 20% FBS (Foundation Brand, Gemini Bio Products). Additionally, the media either contained 1 μ M of 4-OH Tamoxifen

(Sigma-Aldrich) to delete STAT3 or the ethanol vehicle. The cells were incubated with either Tamoxifen or vehicle for two days after isolation, and then were washed in PBS and fresh growth media was added. The media was changed every two days until confluence. Once the cell cultures reached confluence, the cells were induced to differentiate.

For Myf5⁻ (beige) preadipocytes, one-month-old mice were sacrificed and the inguinal fat pads were harvested and processed as above.

2.4 Induction of Differentiation

Once the cells reached confluence, they were induced to differentiate. The growth media was replaced with DMEM (GIBCO) differentiation media containing 4.5g/L Glucose, 20nM Insulin, 1nM T3, 10% FBS, and Antibiotics/Antimycotics. Additionally, the media contained a cocktail of 500μM IBMX, 125μM Indomethacin, 2mg/mL Dexamethasone, and 1μM Rosiglitazone (Sigma-Aldrich). The cells were incubated with the cocktail for 48 hours, and then aspirated and replaced with the base differentiation media lacking the cocktail. The cells were allowed to differentiate for five days after removal of the cocktail, with the media being replaced every two days. For Myf5⁻ preadipocytes, 1μM Rosiglitazone was kept in the media for the full seven days of differentiation. **Figure 2.1** is an illustration of the *in-vitro* time course that contains the date labeling used throughout the rest of the dissertation.

2.5 Temporal Knockout Studies

1μM 4-OH Tamoxifen was added for 48 hours on either Day 2 or Day 5 post-addition of induction cocktail. The media was removed and the cells were washed with PBS and replaced with fresh differentiation media.

2.6 In-Vitro Treatments

Unless otherwise stated, all treatments are applied for the full seven days of differentiation starting from the addition of the induction cocktail. Fresh inhibitor was added with each media change. Appropriate vehicles were used as controls. The following chemicals were used: IWP2 (Porcupine Inhibitor, 1µM, Selleckchem), C59-Wnt (Porcupine Inhibitor, 1µM, ApexBio), IWR1-endo (β -Catenin Inhibitor, 5µM, Selleckchem), FK506 (Calcineurin Inhibitor, 10ng/mL, Cayman Chemical), XAV939 (TANKYARASE Inhibitor, 1µM, Cayman Chemical), CHIR99021 (GSK3 β Inhibitor, 10µM, Cayman Chemical), PD0325901 (MEK Inhibitor, 10µM, Sigma-Aldrich), Isoproterenol (β -adrenoreceptor agonist, 10uM, Sigma-Aldrich), FCCP (chemical uncoupler, 10µM, Cayman Chemical), SAG (Smoothed Agonist/Hedgehog activator, 100nM, Calbiochem), DAPT (γ -Secretase Inhibitor/Notch Inhibitor, 5µM, Tocris), MG-132 (proteasome inhibitor, 10µM, Sigma-Aldrich), Cryptotanshinone (STAT3 inhibitor, 10µM, Selleckchem), Ruxolitinib (pan-JAK inhibitor, 2µM, Selleckchem), H₂O₂ (to induce apoptosis, 500µM, Sigma-Aldrich).

2.7 siRNA Transfection

siGenome SMARTpool control #1 and mouse specific β -catenin were purchased from Dharmacon and resuspended in siRNA buffer to 5µM. Primary cells were grown in 6 well plates. 48 hours before induction, the cells were washed three times with PBS and replaced with 1.6mL of antibiotic free primary media. The transfection cocktail was created as follows: for every well transfected, solution A contained 10µL of the siRNA and 190µL serum free media and solution B contained 4µL of Dharmafect Solution #1 and 196µL serum free media. After incubation for 5 minutes, solutions A and B were combined and incubated an additional 20 minutes at room temperature. 400µL of the transfection cocktail was added to each well and was left on the cells

for 48 hours. After the transfection, the cells were washed with PBS and then were directly induced to differentiate, or harvested in Trizol for mRNA analysis of the knockdown efficiency.

2.8 SDS-PAGE and Immunoblotting

Cells were washed in PBS and lysed on ice with 1x RIPA buffer containing protease and phosphatase inhibitors. The samples were incubated on ice for 30 minutes and then centrifuged for 10 minutes at 10,000g at 4°C. The supernatant was removed in such a way to minimize carry over of lipids from the differentiated cells. Protein concentration was measured using the BCA assay (Pierce). The lysates were combined with 4x Laemmli sample buffer (Bio-Rad) containing 1mM β -Mercaptoethanol. The samples were incubated at 65°C for 10 minutes and separated using SDS-PAGE electrophoresis using Tris-Glycine gels. Gels were transferred to PVDF membranes (Millipore) using a semi-dry transfer system (Bio-Rad). The membranes were blocked with either 5% milk or 5% BSA in 1x TBS + 0.05% Tween 20 (TBST) for 1 hour at room temperature. The membranes were incubated with primary antibodies in either milk or BSA TBST overnight at 4°C with gentle rocking. The membranes were washed and incubated with 1:5000 of anti-rabbit or anti-mouse HRP secondary antibody (GE Healthcare, #NA934 and #NA931) for 1 hour at room temperature with rocking. After washing, the membranes were incubated with either Amersham ECL (GE Healthcare), or ECL2 Reagent (ThermoFisher) and developed using CL-X Exposure Film (ThermoFisher). Films were scanned using an Epson Expression 1680 scanner in transmitted light mode at 16-bit greyscale with 300dpi resolution. Densitometry was performed using ImageJ software (National Institutes of Health). TATA Binding Protein (TBP) was used as the loading control. The primary antibodies used can be found in table 2.3.

2.9 RNA Extraction and Real-Time PCR

RNA was obtained using the Trizol method (Invitrogen). The RNA pellet was dissolved in DEPC-treated water (Sigma-Aldrich) and quantitated using absorbance at 260nm on a Nanodrop 200 (Thermo Fisher). 2 μ g of RNA was used in the first strand synthesis reaction. The High Capacity RNA-to-cDNA Kit (Applied Biosystems) was used according to manufacturer recommendations. The 20 μ L reaction volume was diluted with 380 μ L of dH₂O. 5 μ L of the cDNAs were combined with SYBR Green (SensiMix SYBR & Fluorescein Kit, Bioline), and with 250nM each of forward and reverse primers (table 2.4). The real-time PCRs were run on a CFX96 Real-Time PCR Detection System (Bio-Rad) using the following thermocycling conditions: 1) 95°C 10 minutes, 1x 2) 95°C 15 seconds, 57°C 15 seconds, 72°C 15 seconds, 40x. A melt curve analysis was included at the end of each run. No-transcript controls (NTC) were used to assess for genomic DNA contamination; the sample was considered pure if the NTCs amplified above 35 cycles or more than 6 cycles above the sample target (~100 fold less expression). The data was analyzed using the $\Delta\Delta C_t$ method.

2.10 Oil-Red O Staining

Fully differentiated Brown Adipocytes (Day 7 after induction) were fixed in 10% formaldehyde for 1 hour at room temperature. The fixed cells were washed with PBS and then incubated with 60% isopropanol for 5 minutes. Stock Oil Red O stain (3mg/mL, 100% isopropanol) was diluted using 3 parts of the stock stain to 2 parts dH₂O and filtered through a Whatman paper filter. The filtered stain was applied to the cells for 1 hour at room temperature. The stain was removed and the plate was washed several times with water. The plates were imaged using an AxioObserver A1 microscope with a 10x/0.12 Ph1 lens and AxioCam MRc5 camera (Zeiss). Plates were quantitated for the area of the plate occupied by the stain by the threshold/analyze particles

function in Image J (version 1.49, NIH). At least three random fields were imaged per sample. Whole plates were scanned with an Epson Expression 1680 scanner in reflective mode in 24 bit color at 300dpi resolution.

2.11 Proliferation Studies

For analysis of proliferation prior to confluence, cells were labeled on the day of isolation using the Tag-IT Violet™ Cell Proliferation Dye (Biolegend). Briefly, the primary cell pellet was resuspended in PBS containing 5 μ M of the dye and incubated for 20 minutes at 37°C with shaking. The cells were plated except for a sample that was retained for initial fluorescent measurement. Cells were fixed using 4% Formaldehyde for 10 minutes at room temperature and analyzed on the BD LSRFortessa-X20 system using the following laser and filter configuration: 405nm with BP 450/50. The data was analyzed using FCSExpress software. For proliferation during and after induction, confluent cells were washed with PBS and were incubated with 5 μ M of Tag-IT in HBSS with Calcium and Magnesium for 20 minutes at 37°C. The HBSS was replaced with media and control WT and KO cells were harvested and fixed as above to establish Day 0 fluorescence, while the rest of the cells were induced to differentiate.

2.12 Chromatin Immunoprecipitation Assays

Two confluent ten-centimeter dishes were used per sample. Cells were fixed for 10 minutes at room temperature with 1% formaldehyde, then 5 minutes of 150 mM glycine, and washed with PBS. The cells were incubated in Farnham lysis buffer (85mM KCl, 0.5% NP-40, 5mM PIPES pH 8.0) for 15 minutes on ice and spun down at 500g for 10 minutes to collect nuclei. The nuclei were lysed in sonication buffer (50 mM Tris-HCl pH 8.0, 10 mM EDTA, 1% SDS) and sonicated using a bioruptorpico sonicator (Diagenode) for 5 cycles of 30sec ON/30sec OFF. The sonicated lysate was diluted 1:10 in dilution buffer (20 mM Tris-HCl pH 8.0, 150 mM NaCl, 2

mM EDTA, 0.1% SDS, 1.0% Triton X-100) and manufacturer recommended amounts of antibodies were added and incubated overnight at 4 degrees. Non-specific matched species IgG was used as a control. 30 µL of 1% BSA blocked magnetic Protein A/G beads (Thermo-scientific) were added for 2 hours at 4 degrees then precipitated using a magnet and washed twice with dilution buffer and once with high salt wash (20 mM Tris-HCl pH 8.0, 500 mM NaCl, 2 mM EDTA, 0.1% SDS, 1.0% Triton X-100). The DNA was eluted using 1% SDS/ 0.1M Sodium Bicarbonate Buffer and de-crosslinked by heating overnight at 65 degrees. RNase A (ThermoScientific) and Proteinase K (New England Biolabs) were added, respectfully, for 1 hour each and the DNA was isolated using Qiaquick PCR Purification Kit (Qiagen). The real-time quantitative polymerase chain reaction (qPCR) reaction was performed on the CFX96 Real-Time PCR Detection System (Bio-Rad, Hercules, CA, USA), using the manufacturer recommendations from the SensiMix SYBR and Fluorescein Kit (Bioline). 5% of the input was saved for the calculations. The sequences for the ChIP primers can be found in **Table 2.5**.

2.13 Mitochondrial Isolation

Two 15cm dishes of cells were used per sample. Adherent cells were washed with PBS, trypsinized, and collected in ice-cold media containing serum. Cells were spun down at 500g for 5 minutes at 4°C and the pellets were washed 1x with PBS. Cells were spun down again at 500g and the supernatant was aspirated. The cells were resuspended in 1mL of sucrose buffer (10mM HEPES, pH 7.4, 250mM sucrose, 1mM EDTA, protease and phosphatase inhibitors) and incubated in ice for 10 minutes. Cells were then added to a metal douncer and cells were homogenized by hand on ice until approximately 90% of cells were broken (verified by trypan blue). The homogenate was spun down for 5 minutes at 800g at 4°C to pellet nuclei and intact cells. The supernatant was collected and spun down for 10 minutes at 8800g at 4°C to pellet

crude mitochondria. The supernatant was collected and labeled as the cytosolic fraction and spun an additional 10 minutes at 10,000g to remove any remaining organelle components. The supernatant was collected and frozen at -80°C for further analysis. The crude mitochondrial pellet was resuspended in 490µL sucrose buffer and 10µL of a 5mg/mL solution of trypsin was added to the sample. Samples were rotated for 10 minutes at 4°C after which 500µL of a 5% BSA solution was added to stop the trypsinization. Samples were rotated for an additional minute and then spun down at 10000g for 10 minutes at 4°C. The supernatant was aspirated (including the digested material around the mitochondria) and the pellet was washed 2x with 500µL of the sucrose buffer. After the final wash, the pellets were resuspended in an appropriate volume of sucrose buffer and stored at -80°C for further analysis.

2.14 Apoptosis Assays

Cells were incubated with AlexaFluor 488 annexin V/Propidium Iodide Kit (ThermoFisher) according to manufacturer protocols. The BD FACSCanto II analyzer was used for data acquisition. The following lasers and filter configurations were used: 488nm with BP 530/30 and BP 610/20. The data was analyzed using FCSExpress software. Cells incubated with 500µM H₂O₂ for 5 hours at 37°C was used as a positive control

2.15 *In-vivo* Beiging Studies

8 week old- Floxed STAT3-Tamoxifen Inducible Cre animals were orally gavaged once per day for 5 days with 5mg/20g body weight Tamoxifen (Cayman Chemicals). The mice were allowed to rest for 1 month. Afterwards, the mice were injected intraperitoneally (I.P.) once a day for seven days with either CL316,243 (Sigma-Aldrich) at a dose of 1mg/kg or an equivalent volume of PBS. The mice were then sacrificed and the inguinal fat pads were harvested and lysed in

RIPA buffer containing protease and phosphatase inhibitors. The lysates were stored at -80°C for further analysis.

2.16 Statistical Analysis

Data is presented as mean ± SEM, except for qPCR data which is expressed as mean ± SD.

Statistical Analysis was performed using Prism 7 (GraphPad) using the statistical tests indicated in figure legends. A p-value <0.05 was considered significant. N=3 unless otherwise indicated.

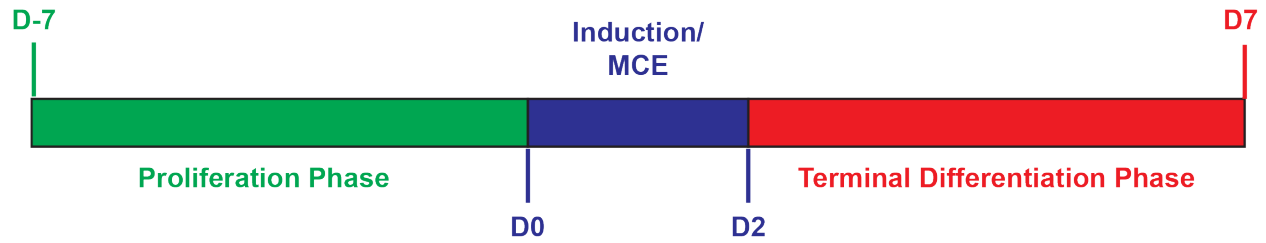


Figure 2.1- *In-Vitro* time course

Growth/Proliferation Phase is from isolation of the primary cells to confluence, which generally takes 7 days. When the cells reach confluence they are induced to differentiate, which lasts for 48 hours (D0-D2); the induction phase is also called the MCE. D2-D7 is the Terminal Differentiation Phase.

Gene	Primer Sequences	Notes
Flox STAT3	Forward: TTGACCTGTGCTCCTACAAAAA Reverse: CCCTAGATTAGGCCAGCACA	Floxed Allele: 600bp WT Allele: 400bp
Tamoxifen Cre	Forward: AAAGTCGCTCTGAGTTGTTAT Reverse: GGAGCGGGAGAAATGGATATG Mutant Reverse: CCTGATCCTGGCAATTTCG	Cre Allele: 825bp WT Allele: 603bp

Table 2.1- Genotyping Primers

Plate	Volume (µL)
35mm	150
60mm	350
10cm	750
24 well	75
12 well	150
6 well	250

Table 2.2- Plating Volumes for Primary Cells

Target	Company, catalog #, lot #	Species
UCP1	R&D Biosystems, MAB6158, CCNV0116081	Mouse
TBP	Cell Signaling Technology, 3544, 1	Rabbit
STAT3	Cell Signaling Technology, 9139, 8	Mouse
pSTAT3 Y705	Cell Signaling Technology, 9145, 31	Rabbit
pSTAT3 S727	Cell Signaling Technology, 9134, 21	Rabbit
β-Catenin	Cell Signaling Technology, 8480, 5	Rabbit
PPARγ	Cell Signaling Technology, 2443, 3	Rabbit
FABP4 (aP2)	Cell Signaling Technology, 3544, 2	Rabbit
CEBPα	Cell Signaling Technology, 8178, 3	Rabbit
STAT1	BD Biosciences	
NDUFA9	Santa Cruz Biotechnology	
Tubulin	Sigma-Aldrich, T8328	Mouse
GAPDH	Cell Signaling Technology, 5174	Rabbit

Table 2.3- Antibodies for Immunoblotting

Target	Sequence
18S	F: CCATCCAATCGGTAGTAGCG R: GTAACCCGTTGAACCCCATT
Adiponectin	F: TGACGACACCAAAAGGGCTC R: CACAAGTTCCCTTGGGTGGA
aP2	F: TGAAATCACCGCAGACGACA R: ACACATTCCACCACCAGCTT
Axin2	F: CAGCCCAAGAACCGGGAAAT R: AGCCTCCTCTCTTACAGCA
CEBPα	F: AATGGCAGTGTGCACGTCTA R: CCCCAGCCGTTAGTGAAGAG
CIDEA	F: GGCGTGTAAAGGAATCTGC R: GTATGTGCCGCATAGACCA
Dkk1	F: ACACCAAAGGACAAGAAAGGCT R: CTTGGTGCACACCTGACCTT
EBF2	F: GCTGCGGGAACCGGAACGAGA R: ACACGACCTGGAACCGCCTCA
PGC1α	F: TGAAAAAAGCTTGACTGGCGTC R: AGCAGCACACTCTATGTCACTC
PPARα	F: TGTGAACTGACGTTGTGGC R: CCACAGAGCGCTAAGCTGT
PPARγ	F: CTGTGAGACCAACAGCCTGAC R: TGGTTACCGCTCTTCAA
PRDM16	F: CAGCACGGTGAAGCCATT R: GCGTGCATCCGCTTGTG
Tbp	F: AGTCCCCAGCATCACTATTCA R: GTGGAAGGCTGTTGTCTGG
UCP1	F: CACGGGGACCTACAATGCTT R: TAGGGGTCGTCCCTTCAA
Wnt1	F: GATGGTGGGGCATCGTGAAC R: GTTCTGTCGGATCAGTCGCC
Wnt10b	F: TGTGGATCCTGCACCTGAAC R: TAGAGCCCGACTGAACAAAGC
Wnt3a	F: GGGTGTCAAAGCGGGCATCCA R: CCCGGGTGGCTTGTCCAGAA
β-Catenin	F: CCATTGTACGCACCATGCAG R: CCACTGGTGACCCAAGCATT

Table 2.4- Primers for Real-Time qPCR

Target	Sequence
Actin Promoter	F: AAATGCTGCACTGTGCAGCG R: AGGCAACTTCGGAACGGCG
PRDM16 Promoter	F: GAGGAAATCTATAGGGAGGACTCTCT R: AATCCGGTTAAAACAGCAATCC
UCP1 Enhancer	F: CTCCTCTACAGCGTCACAGAGG R: AGTCTGAGGAAAGGGTTGA
UCP1 Proximal Promoter	F: CCCACTAGCAGCTTTGGA R: CTGTGGAGCAGCTCAAAGGT

Table 2.5- Primers for Chromatin Immunoprecipitation

Chapter 3: Results

The data presented are in Myf5⁺ cells isolated from the interscapular region, unless otherwise indicated.

3.1 STAT3 is Phosphorylated During the Induction Period

To begin our study of STAT3 in brown adipose tissue development, we wanted to determine when STAT3 functions during differentiation. We took wild type primary cells, induced them to differentiate, and collected samples at different time points for analysis of total STAT3 and phosphorylated forms of STAT3. As seen in Figure 3.1, STAT3 is basally phosphorylated before addition of the induction cocktail, is rapidly dephosphorylated upon addition of the cocktail, then returns to basal levels for 24 hours, and still is detectable by 48 hours. Additionally, STAT3 serine phosphorylation rapidly increases upon addition of the induction cocktail and is elevated for 24 hours. This time course is in agreement with previous studies of STAT3 in the 3T3-L1 cell line (135, 164). Interestingly, total STAT3 amounts decrease after the induction period is complete and remain low throughout the rest of the terminal differentiation phase. These findings suggests that STAT3 is likely required during the induction phase (D0-D2) only.

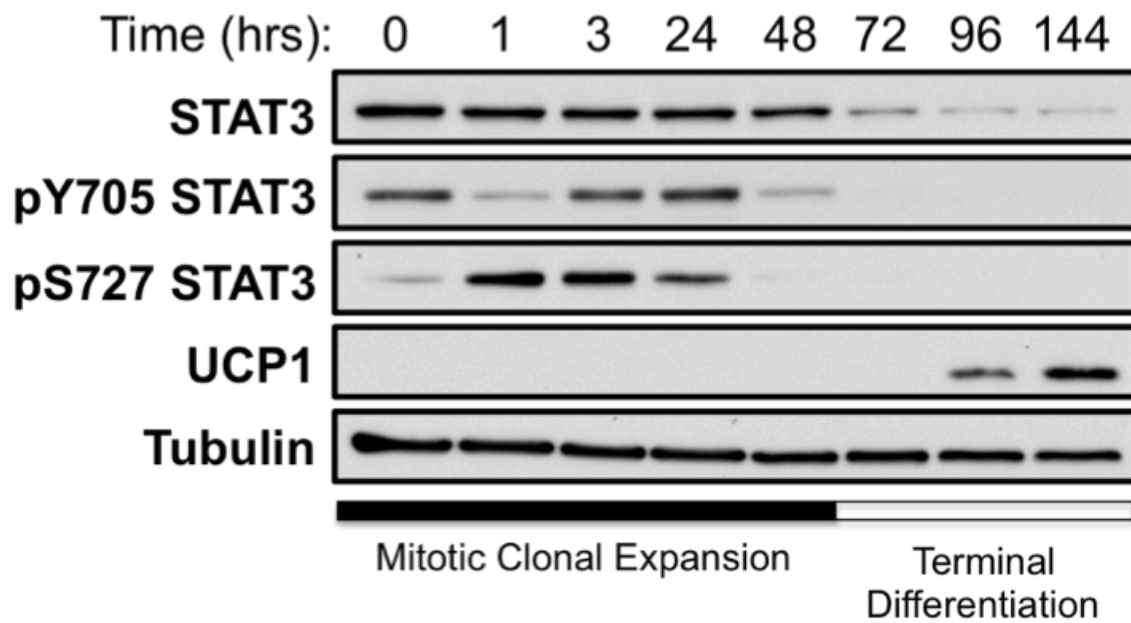


Figure 3.1- STAT3 levels during *in-vitro* differentiation

A representative immunoblot of whole cell extracts from wild type interscapular SVF. Time 0 are cells before induction, all time points are measured post-addition of induction cocktail. Tubulin is used as a loading control. N=3.

3.2 Inhibition of STAT3 Blocks Differentiation of Brown Adipocytes

To continue analysis of the role of STAT3 in the development of brown adipocytes, STAT3 was inhibited throughout the entire differentiation time course from addition of induction cocktail. We choose cryptotanshinone, a natural product inhibitor of STAT3 that prevents dimerization by binding the SH2 domain, as it was well tolerated by the cells for the entire time course. We treated the cells with 10 μ M cryptotanshinone and after 6 days, samples were collected samples for RT-qPCR. As shown in **Figure 3.2**, treatment with the STAT3 inhibitor reduces expression of both brown fat specific and general fat markers.

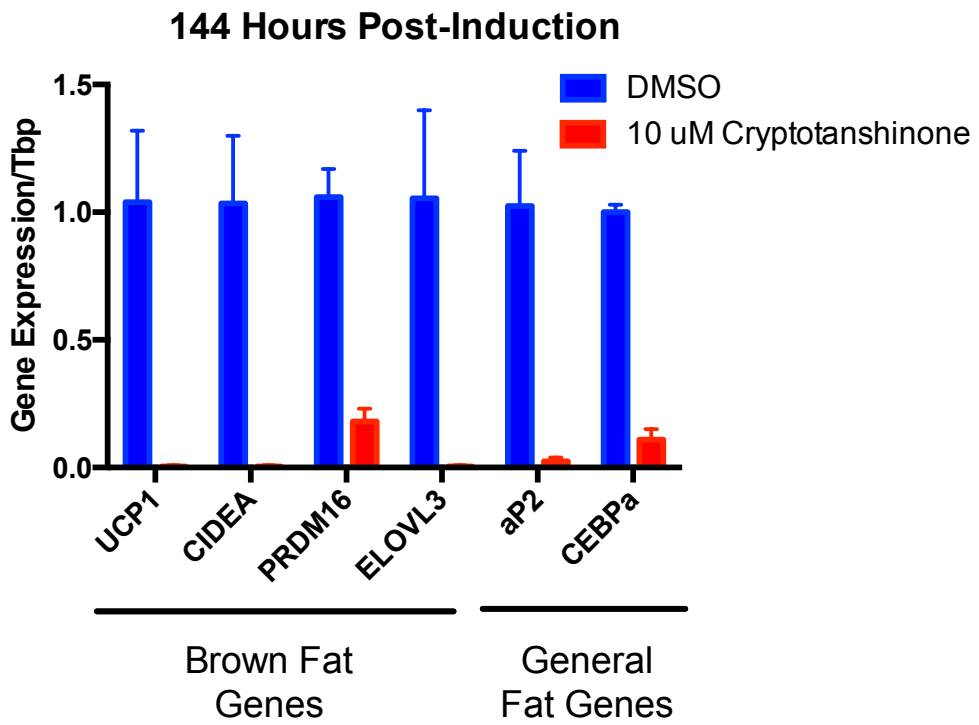


Figure 3.2- Inhibition of STAT3 suppresses expression of terminal adipogenic markers

Expression of brown fat specific and general adipocyte markers measured by RT-qPCR. N=2, data are expressed as mean \pm SD. Tbp was used as a loading control.

3.3 Inhibition of STAT3 During the Induction Period Only Blocks Differentiation

Since STAT3 is phosphorylated only during the induction period, we hypothesized that STAT3 is only required for differentiation during this period and that inhibition during the terminal differentiation phase (D2-D7) would have no effect. We used cryptotanshinone, a natural product inhibitor of STAT3 that prevents dimerization by binding to the SH2 domain, to investigate the temporal requirement for STAT3 (165). In **Figure 3.3**, 10 μ M of cryptotanshinone was added in 24-hour windows during the differentiation time course. To control for media changes, every sample was given fresh media every 24 hours and either the inhibitor or the DMSO vehicle. As expected, treatment with cryptotanshinone during the 24-hour windows that correspond to the induction period suppressed expression of UCP1, especially during the first 24 hours, but treatment during any 24-hour window after induction had no effect on UCP1. This is further evidence that STAT3 is only required during the differentiation period. However, cryptotanshinone is an SH2 domain inhibitor, and it likely has off-target effects, such as inhibition of STAT5, which is also important for adipogenesis (166).

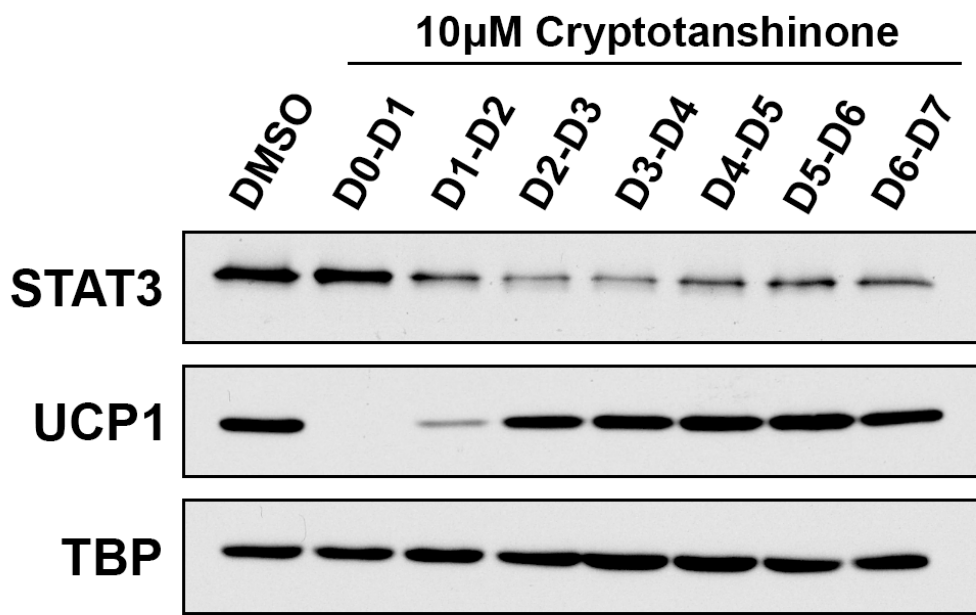


Figure 3.3- Inhibition of STAT3 during the induction phase reduces UCP1 expression

Representative immunoblot from Day 7 whole cell extracts of cells treated with the STAT3 inhibitor for the 24-hour window indicated above each lane. N=3. Tbp was used as a loading control.

3.4 Generation of a Floxed-STAT3, Tamoxifen Inducible Cre Leads to Efficient Total Knockout

The analysis thus of STAT3 in brown adipogenesis have utilized wild type brown preadipocytes and chemical inhibition of STAT3. However, in order to determine the mechanism of STAT3, a reproducible STAT3 Knockout (KO) primary cell system was needed. Therefore, mice that are homozygous for floxed STAT3 and a Tamoxifen- Inducible Cre Recombinase were generated for the study. The mice were viable and no defects were observed throughout the mouse lifespan. In **Figure 3.4**, harvested cells that were exposed to 1 μ M of 4-OH Tamoxifen for 48 hours have no detectable STAT3 at Day 0, when the cells are confluent but have yet to be induced. Interestingly, there are also reduced PRDM16, PPAR γ , and CEBP δ levels before the start of differentiation. The reduced levels of PRDM16 are in agreement with our prior published work (139).

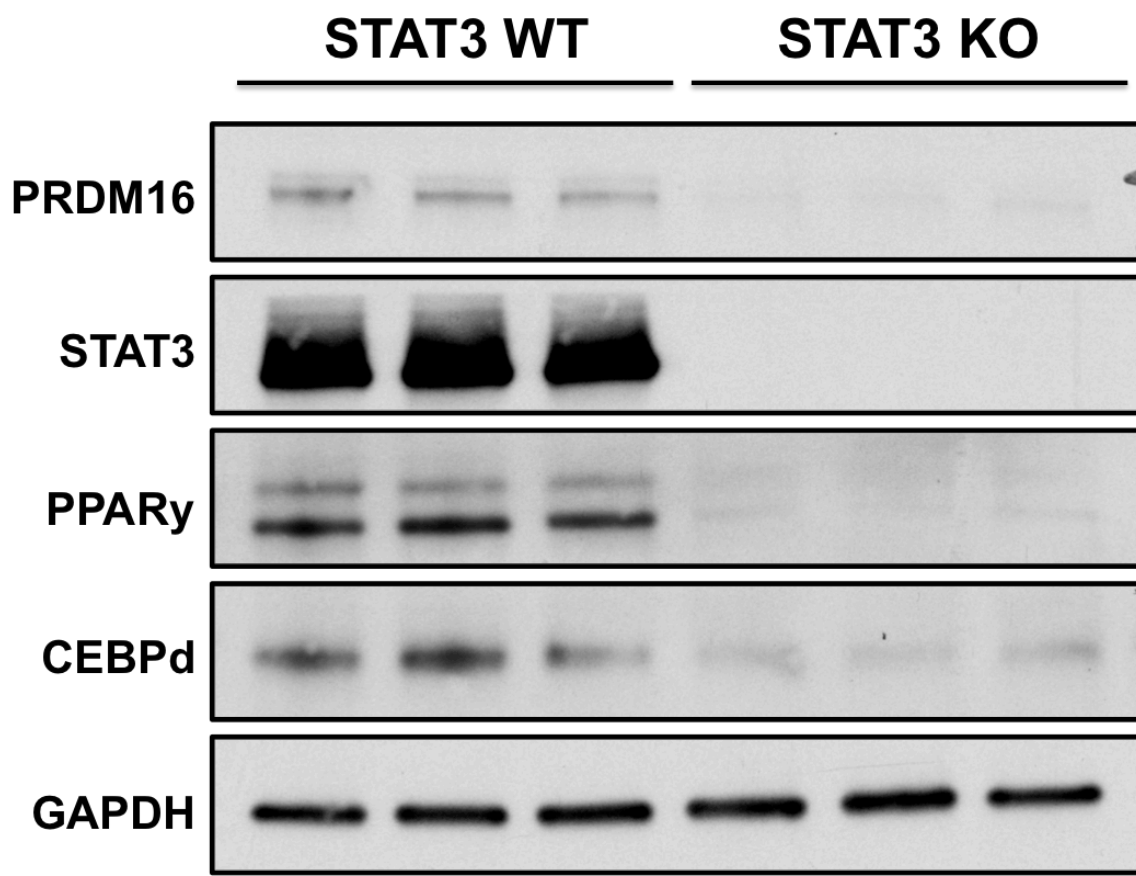


Figure 3.4- Treatment with 4-OH Tamoxifen efficiently reduces STAT3 and loss of STAT3 reduces levels of transcription factors important for differentiation.

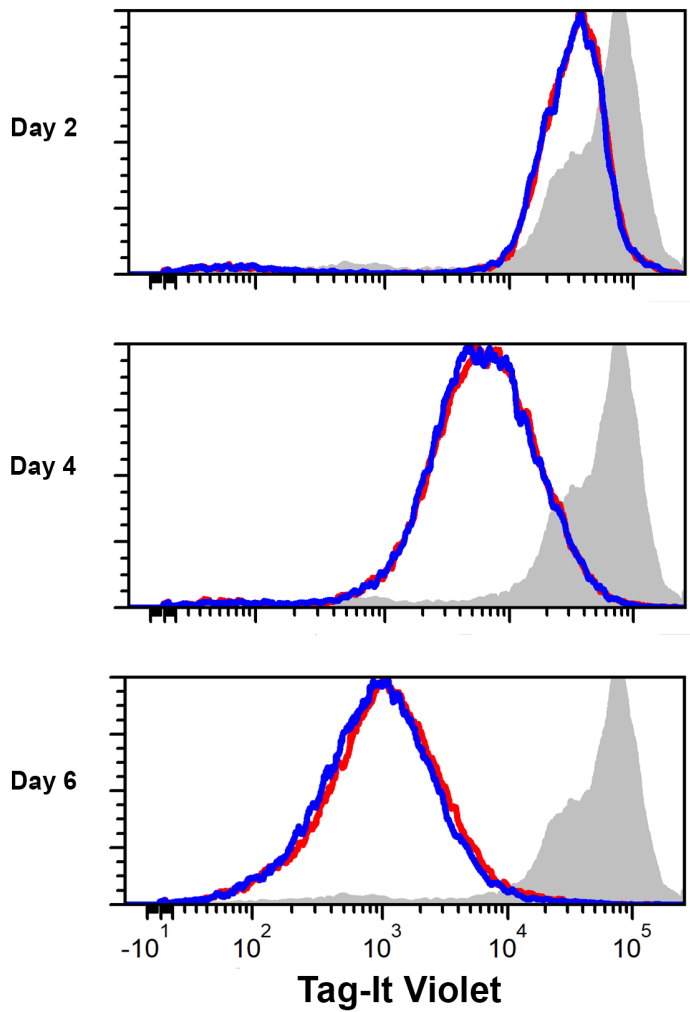
Immunoblot of three biological replicates of STAT3 WT and KO preadipocytes on Day 0.

GAPDH was used as a loading control.

3.5 Deletion of STAT3 Does Not Affect Proliferation of Preadipocytes in the Growth Phase

It has previously been reported that knockdown of STAT3 in the 3T3-L1 line reduces the proliferation rate of the cells compared to control during the growth phase to confluence (131). Any differences in proliferation during growth to confluence must be assessed as the cells are not primed to differentiate before they reach confluence and contact-growth inhibit each other, and any reduction in differentiation of the STAT3 KO must take this into consideration. Therefore, we assessed whether the STAT3 KO cells have reduced proliferation compared to wild type in the growth phase before differentiation. We used the Tag-IT Violet Dye system, a dye that covalently attaches to proteins in the cell and becomes diluted with each cell division, to track the proliferation rate of the cells from isolation to confluence. As seen in **Figure 3.5**, there is no difference in proliferation of the WT and KO cells during the growth phase.

A)



B)

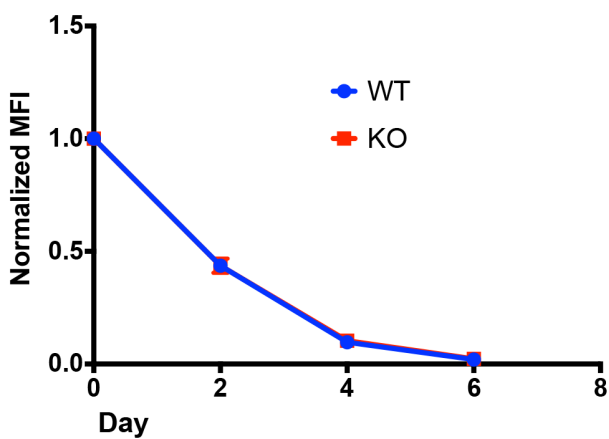


Figure 3.5- No difference in proliferation to confluence between WT and KO preadipocytes

A) Cells were labeled with 5 μ M Tag-It on the day of isolation (grey shaded distribution) and followed until they reached confluence 6 days later. WT is blue and KO is red. These are concatenated histograms that contain all 3 biological replicates within each panel. N=3 for each time point. **N.B.:** the days indicated here are measured from the date of isolation of the cells, this is in contrast to other figures where the days are measured starting from induction **B)** The relative change in mean fluorescence intensity from the day of isolation to confluence. Data is expressed as mean \pm SEM.

3.6 STAT3 KO Preadipocytes Have Reduced Proliferation After Induction

The induction phase, also known as the mitotic clonal expansion, is the 48 hours that the cells are incubated in the induction cocktail. During this time, the cells that were previously contact-growth inhibited divide 1-3 more times before entering the terminal differentiation phase (167). Previous work in the 3T3-L1 line indicates that STAT3 is required for the mitotic clonal expansion (164). To determine if primary brown adipocytes also require STAT3 for the mitotic clonal expansion, we again used the Tag-IT Violet dilution dye to measure proliferation. As shown in **Figure 3.6**, at the end of the Induction Phase (Day 2) there is no difference in loss relative loss of Tag-IT dye, indicating equal proliferation; however, by Day 4 the WT cells have undergone a few more rounds of proliferation than the KO. Therefore, we conclude that in the primary brown adipocyte system, STAT3 can modulate the proliferation of the primary brown preadipocytes after treatment with the induction cocktail.

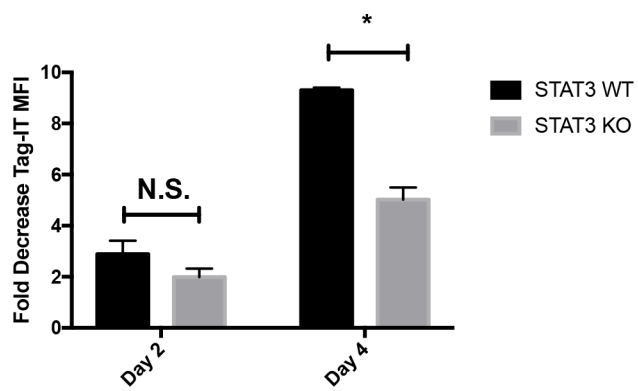


Figure 3.6- STAT3 KO brown adipocytes have reduced proliferation after induction

Cells were stained with 5 μ M Tag-IT Violet on Day 0 and then immediately induced to differentiate. A Day 0 WT and KO sample was collected and fixed to provide the baseline fluorescence. Data is calculated as mean fluorescent intensity of Day 0 divided by the mean fluorescent intensity of the sample day. N=3. * = p< 0.05, N.S. = not significant. Data is presented as mean \pm SEM.

3.7 Deletion of STAT3 Leads to Significant Reduction in Differentiation and Brown Specific Genes

With the Tamoxifen Cre system, the effects of STAT3 on differentiation of primary brown adipocytes can be studied without the off-target effects of a chemical inhibitor. We induced STAT3 WT and KO cells and analyzed Day 0 and Day 7 samples for markers of terminal adipocytes. In **Figure 3.7**, knockout of STAT3 reduces expression of UCP1 protein to near undetectable levels, similar to what we observed with the STAT3 inhibitor. Additionally, PPAR γ and CEBP α , two important transcription factors common to both WAT and BAT differentiation, are reduced. FABP4, a common fat marker, is slightly reduced. Because UCP1 is so dramatically decreased compared to the other markers of adipogenesis, we wanted to see if brown-specific markers are affected more by the STAT3 KO than common markers of adipogenesis. In **Figure 3.8**, we measured the mRNA expression of brown fat specific or selective markers and markers common to both WAT and BAT. Interestingly, brown fat markers are significantly reduced, while the general fat markers are only trending downward in their expression.

Visually, knockout of STAT3 led to a significant decrease in lipid accumulation compared to the WT STAT3 samples, as well as an apparent reduced number of cells while still confluent (**Figure 3.9**). Together, this data indicates that loss of STAT3 does not prevent the cells from attempting differentiation, however, full differentiation is suppressed and the thermogenic program is significantly affected.

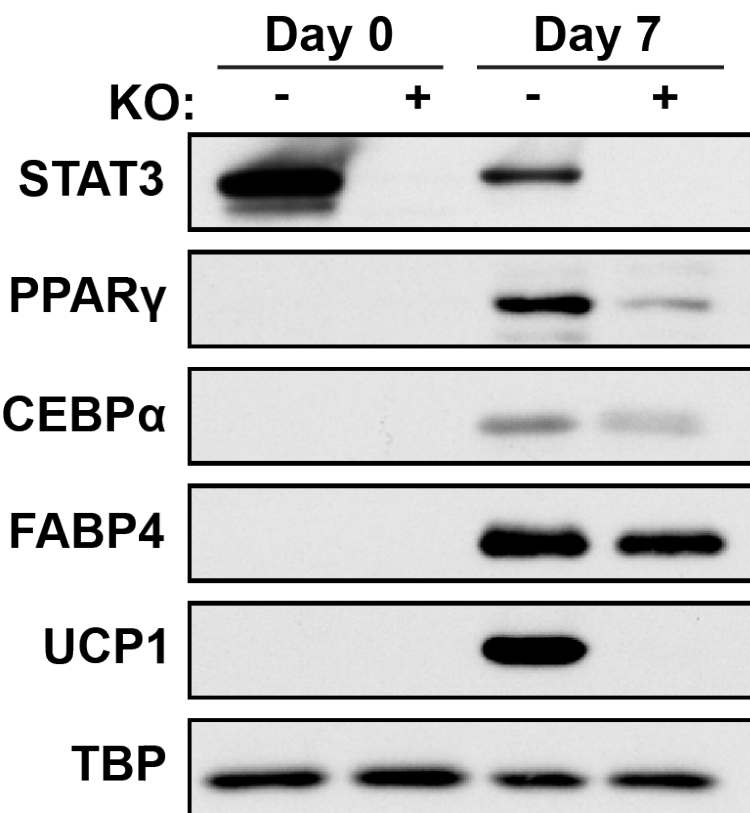


Figure 3.7- KO of STAT3 significantly reduces expression of UCP1

Representative immunoblot of Day 0 and Day 7 brown adipocytes for markers of brown fat and markers common to all types of fat. N=3.

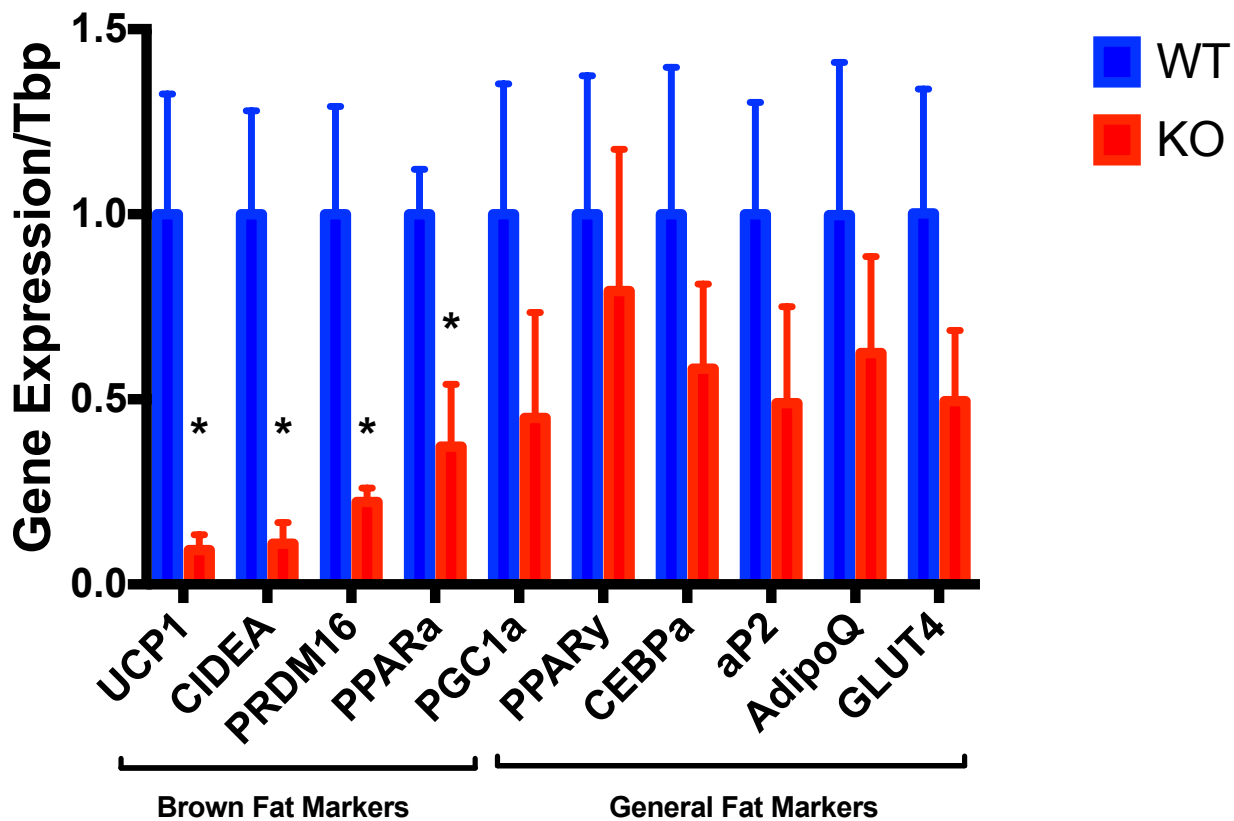
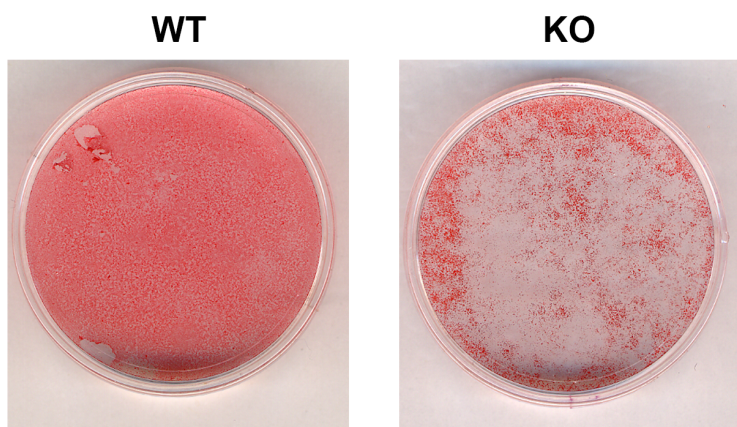


Figure 3.8- Expression of brown fat markers are more affected by knockout of STAT3 than general fat markers

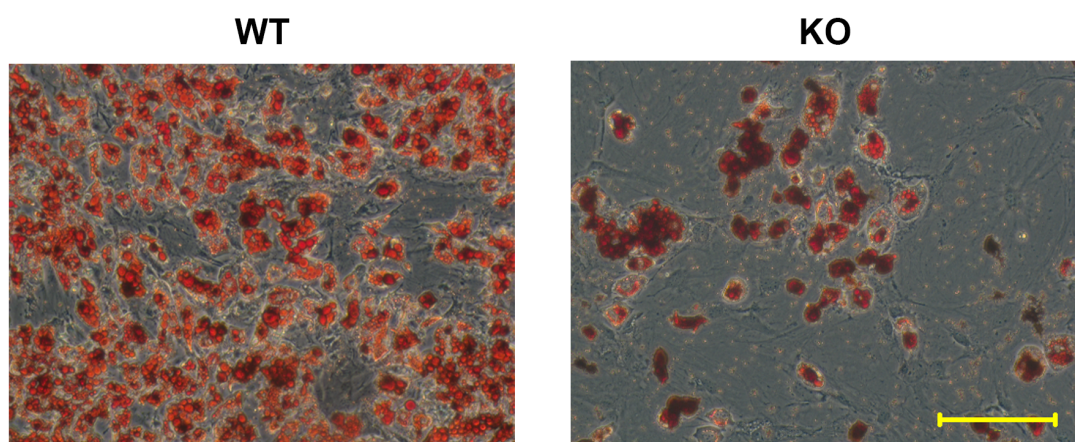
RT-qPCR of Day 7 adipocytes for markers of brown fat and markers common to all types of fat.

* indicate $p < 0.05$ compared to the wild type marker. Student's t-test. N=4. Data is expressed as mean \pm SD.

A)



B)



C)

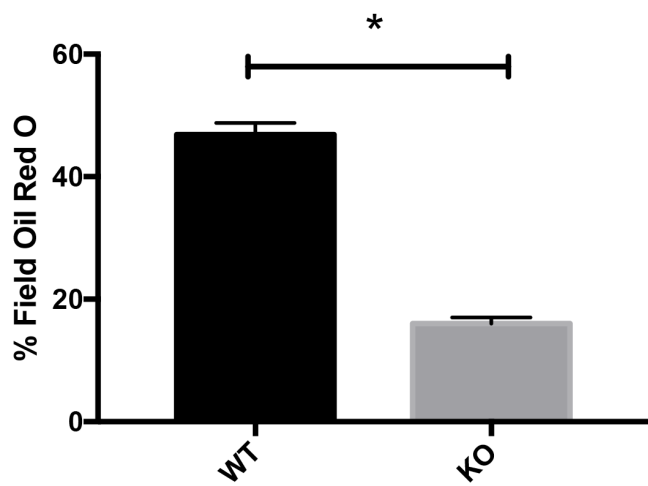


Figure 3.9- Knockout of STAT3 significantly reduces lipid accumulation

A) Representative plates of Day 7 adipocytes were fixed and stained with Oil-Red O, a dye that is retained in the neutral triglycerides of adipocyte lipid droplets. **B)** Day 7 adipocytes were imaged at 10x magnification, scale bar = 200 μ m. **C)** Quantitation of B). Student's t-test. N=3. * indicates p< 0.05. Data is presented as mean \pm SEM.

3.8 Tamoxifen is not Responsible for the Defects in Differentiation

While the Tamoxifen Cre system is a powerful tool to isolate the effects of STAT3 on differentiation of brown adipocytes, one weakness is that only one group receives tamoxifen while the other receives the ethanol vehicle. Because tamoxifen has been reported to affect UCP1 expression *in-vivo*, we wanted to rule out that the effects we see with the STAT3 KO are due to tamoxifen (168). In **Figure 3.10**, preadipocytes that contain floxed STAT3, but lack the Cre Recombinase, were treated with either ethanol or tamoxifen for 48 hours after isolation, exactly as is done for the STAT3 KO preadipocytes. Figure **3.10A** shows that treatment with tamoxifen does not alter the levels of UCP1 protein, and Figure **3.10B** shows that tamoxifen does not alter the ability of the cells to accumulate lipid. Thus, with these controls, we can conclude that the effects we see in the STAT3 KO are due to loss of STAT3 and not the tamoxifen treatment.

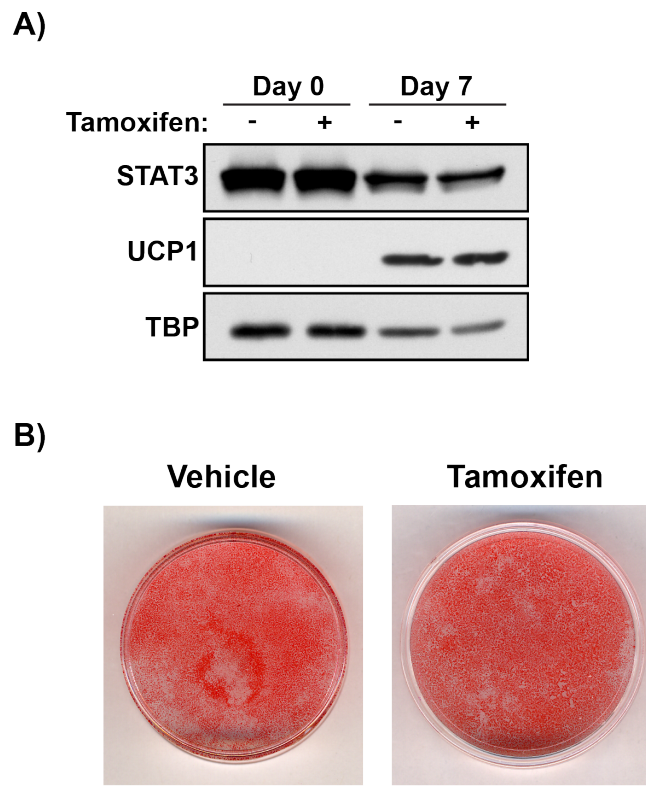


Figure 3.10- Tamoxifen treatment has no affect on brown preadipocytes ability to differentiate

A) Representative Immunoblot of whole cell lysates from Day 0 or Day 7. The cells were treated with 1 μ M 4-OH Tamoxifen for 48 hours after isolation, exactly as for the STAT3 KO, but these cells lack the Cre Recombinase. N= 3. **B)** Representative plates of Oil Red O Staining in cells lacking the Cre Recombinase treated with tamoxifen. N= 3.

3.9 PPAR γ is Less Stable in the STAT3 KO

We have observed that the levels of PPAR γ are reduced at Day 7 (**Figure 3.7**), and if we increase the exposure time, we can also see that at Day 0 there is already a reduction in PPAR γ levels (**Figure 3.4**). Since PPAR γ is considered a master regulator of adipogenesis, and previous work indicates that STAT3 is upstream of PPAR γ , we wanted to determine if STAT3 is involved in regulating PPAR γ expression. In **Figure 3.11A**, we analyzed Day 0 mRNA expression of PPAR γ and found no difference, indicating that STAT3 may regulate PPAR γ post-transcriptionally. There is a report that PPAR γ stability can be regulated by Interferon Gamma (IFN γ) (169). Specifically, IFN γ recruits ERKs 1 and 2 to phosphorylate PPAR γ , which marks PPAR γ for degradation by the proteasome. While we did not measure IFN γ levels in the media, we did measure expression of a marker of interferon signaling, ISG15, at Day 0 and found it to be highly up regulated in the STAT3 KO (**Figure 3.11B**). It should be noted that ISG15 expression is not specific to IFN γ , as other interferons can also increase expression of this gene (170). Therefore, we wanted to test if PPAR γ has a higher turnover rate in STAT3 KO cells, and if this is due to IFN γ /ERK signaling. In **Figure 3.11C** we treated Day 1 STAT3 WT and KO preadipocytes with 10 μ M MG-132 (Lanes 3 and 4), a proteasome inhibitor, for 8 hours. Treatment with MG-132 was able to restore levels of PPAR γ in the STAT3 KO; however, treatment with the MEK inhibitor PD0325901 for 8 hours had no affect on PPAR γ levels (Lanes 5 and 6), even though the MEK inhibitor did reduce phosphorylation of ERK1/2 (**Figure 3.11E**). During the treatment period levels of PPAR γ mRNA levels trended downward, but to the same extent on the WT and KO (**Figure 3.12E**). These results indicate that PPAR γ is undergoing increased degradation in the absence of STAT3, but it is not likely through the reported IFN γ /ERK pathway.

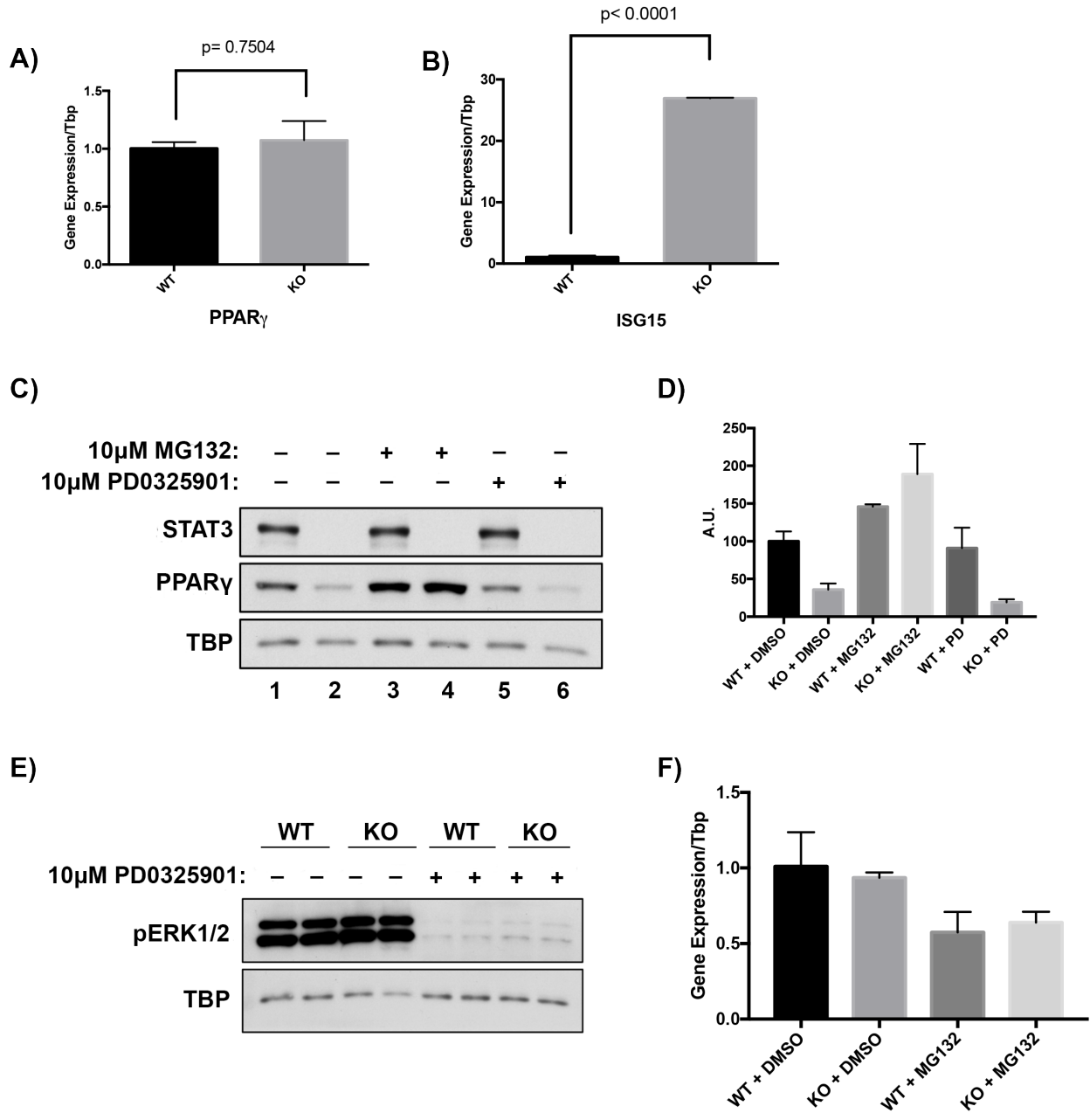


Figure 3.11- PPAR γ has increased turnover in the STAT3 KO preadipocytes

A) RT-qPCR of PPAR γ from Day 0 preadipocytes. N=3. Student's t test. **B)** RT-qPCR of ISG15 from Day 0 preadipocytes. N=3. Student's t test. Data is presented as the mean \pm SD **C)** Representative immunoblot of whole cell extracts from Day 1 preadipocytes treated with either 10 μ M MG132 or 10 μ M PD0325901 for 8 hours. N=2. TBP is used as a loading control. **D)** Densitometry of immunoblot in C). N=2. Data is expressed as mean \pm SEM. **E)** Immunoblot of two STAT3 WT and KO biological replicates from Day 1 whole cell lysates blotted for phosphorylated ERK1/2. Cells were treated with vehicle or PD0325901 for 8 hours. TBP is used as a loading control. **F)** RT-qPCR of PPAR γ from Day 1 STAT3 WT and KO treated with vehicle or MG132 for 8 hours. N=2. Data is expressed as mean \pm SD.

3.10 Deletion of STAT3 after the Induction Phase does not alter UCP1 levels

Although the STAT3 inhibitor studies (**Figure 3.3**) suggested that STAT3 was required only during the induction period, there is the possibility of non-specificity using a STAT3 inhibitor. Using the Tamoxifen-Inducible Cre system, we are able to delete STAT3 at different times during differentiation and avoid the problem of off target effects. Deletion of STAT3 prior to induction leads to loss of UCP1 levels and a reduction in PPAR γ (**Figure 3.12**, Lane 1). However, if tamoxifen is added at Day 2 or Day 5, there is no reduction in UCP1 or PPAR γ protein compared to the WT (lanes 2, 3, 4). This confirms that STAT3 is only required for differentiation during the induction phase, and is dispensable for UCP1 expression after the induction phase is complete.

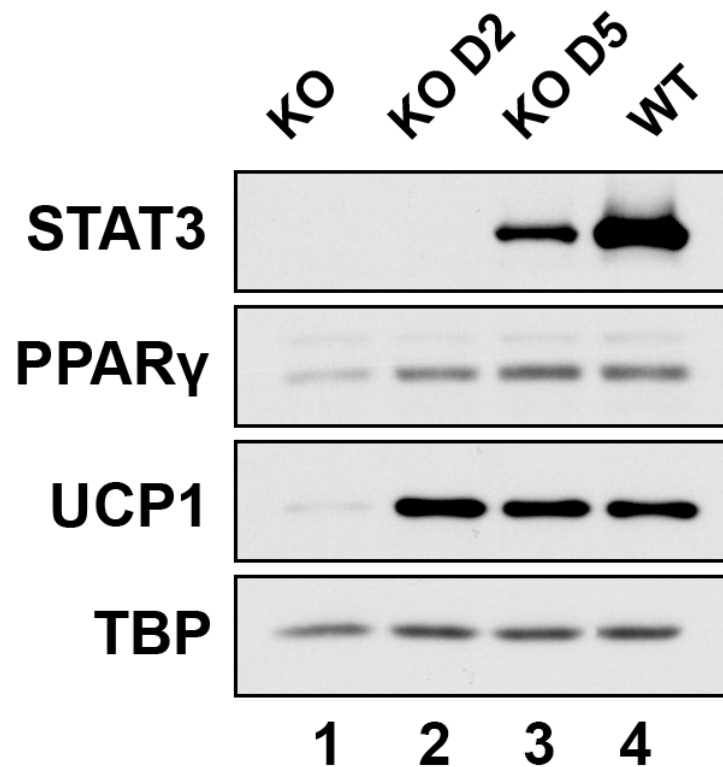


Figure 3.12- Deletion of STAT3 after the induction phase has no effect on UCP1 protein levels

Representative immunoblot of Day 7 whole cell extracts. D2= tamoxifen added to WT cells on Day 2, D5= tamoxifen added to WT cells on Day 5. N=3.

3.11 pan-JAK Inhibition Suggests that the JAK/STAT Pathway has a Biphasic Response to Differentiation

Since STAT3 is down regulated after the induction period, and deletion of STAT3 after induction does not affect total UCP1 amounts, it is possible that the JAK/STAT pathway may be pro-adipogenic during the induction period and anti-adipogenic after induction. To test this hypothesis, we treated the preadipocytes with 2 μ M of Ruxolitinib, a pan-JAK inhibitor, either during the induction phase (D0-D2), or after the induction phase (D2-D7). In **Figure 3.13**, treatment with 2 μ M of Ruxolitinib during the induction period results in reduced amounts of UCP1 in the STAT3 WT (Lane 3), which is expected as this should block both STAT3 and STAT5 signaling. Interestingly, treatment with Ruxolitinib during the terminal differentiation phase actually up regulated expression of UCP1 in the STAT3 WT (Lane 5). We have seen before that Ruxolitinib can increase UCP1 expression, but that was in an immortalized system and treatment improved UCP1 expression regardless of what stage of differentiation the cells were in (171). This indicates that: 1) The JAK/STAT pathway is either pro-adipogenic or anti-adipogenic depending on the stage of differentiation, and 2) that immortalization changes the cells in an unknown way that removes this biphasic response. Treatment with Ruxolitinib had no affect on the KO regardless of when the drug was added (Lanes 4 and 6).

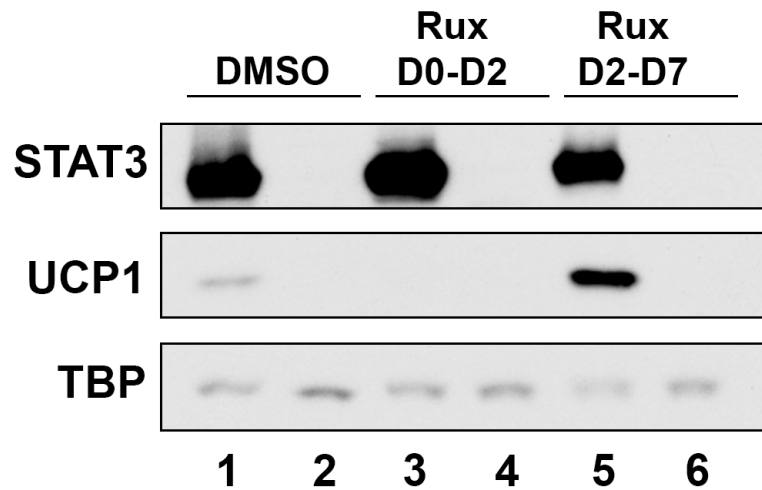


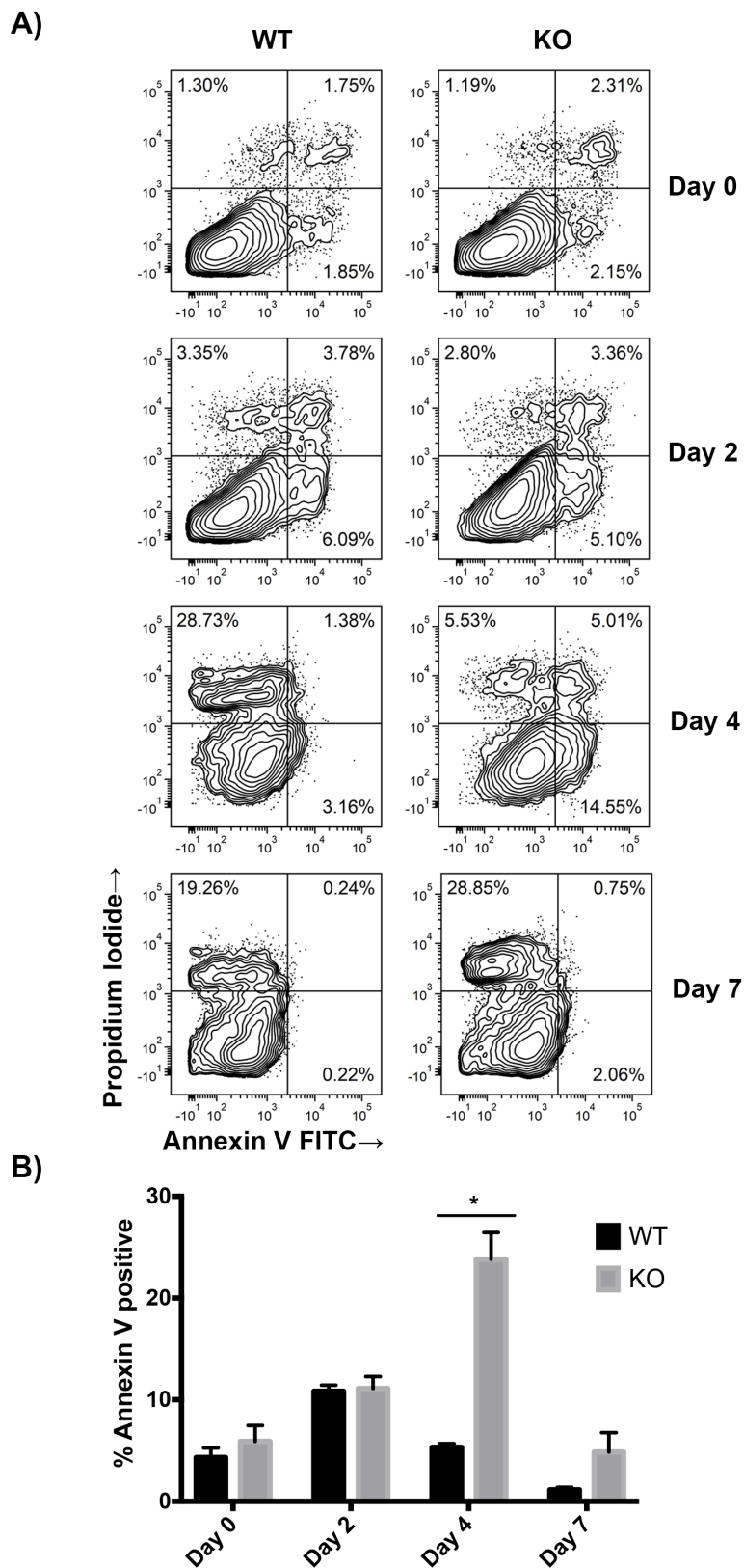
Figure 3.13- Inhibition of JAK shows a biphasic response

Representative Immunoblot of Day 7 lysates from STAT3 WT (Lanes 1, 3, 5) and KO (Lanes 2, 4, 6) cells treated with vehicle or 2 μ M Ruxolitinib during different periods of the differentiation time course. The exposure time was adjusted so that Lane 5 was not saturated; WT vehicle (Lane 1) appears to be decreased due to these exposure conditions but are likely not affected. N=2.

3.12 STAT3 KO Cells Have Increased Apoptosis in the Early Terminal Differentiation

Phase

We noticed that the number of cells on the STAT3 KO plate seemed to become less numerous as the differentiation time course proceeded, even though the cells start at a similar density to STAT3 WT cells. While part of this difference may be due to reduced proliferation of the STAT3 KO cells during the induction phase, we wanted to see if there were any differences in apoptosis between STAT3 WT and KO during the differentiation time course. In **Figure 3.14A and B**, we sampled different time points utilizing Annexin V/Propidium Iodide Flow Cytometry. We saw that the induction cocktail increased Annexin V staining equally in the WT and KO on Day 2 compared to pre-induction at Day 0. However, by Day 4, the levels of Annexin V staining decreased in the WT whereas levels doubled for the KO. By Day 7, the levels of Annexin V in the KO returned to WT levels. The increased Propidium Iodide positive/Annexin V negative staining seen in the WT and the KO at later time points are likely artifacts of processing cells as the adipocytes become more fragile and more likely to have a membrane rupture due to the increased lipid droplet accumulation. As a positive control, we treated WT Day 0 and Day 4 cells with 500 μ M H₂O₂ for 5 hours (**Figure 3.14B and C**). These results indicate that there is a defined window during the early terminal differentiation phase where the KO cells can initiate apoptosis. Not all cells initiate apoptosis, as the plate is still confluent by Day 7 (**Figure 3.9**). There is likely a spectrum of response in the STAT3 KO cells. Some cells may not respond to the induction cocktail and begin differentiation. Other cells respond and are able to fully differentiate by forming lipid droplets and expressing some UCP1. Most cells appear to fall in between, differentiating up to a point and then either stalling or initiating apoptosis.



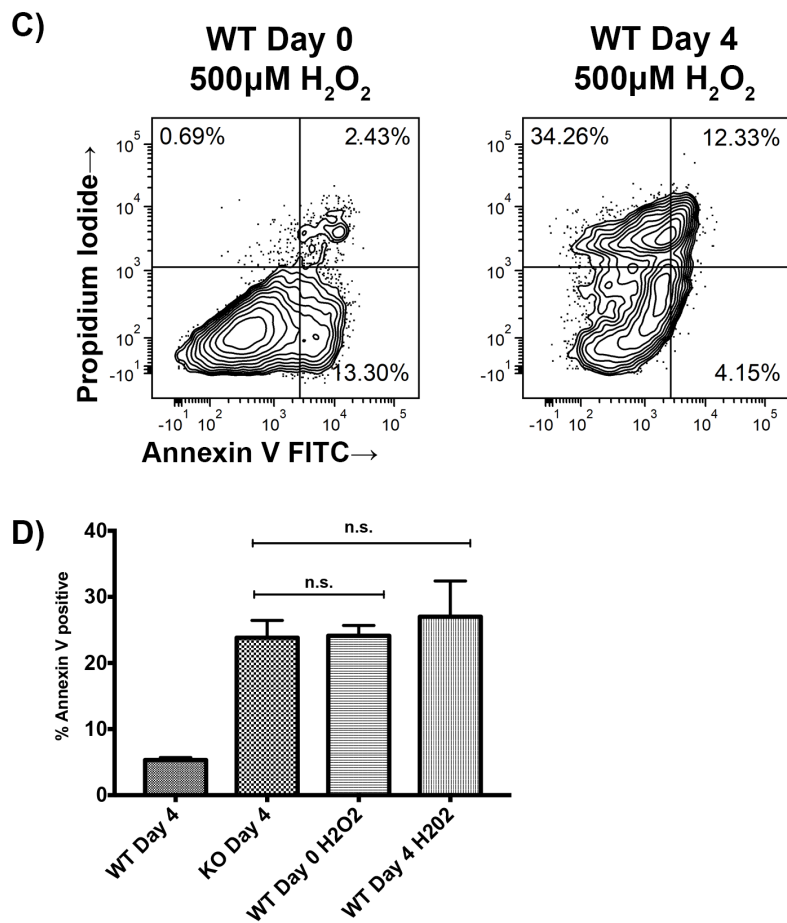


Figure 3.14- STAT3 KO have increased apoptosis during the early terminal differentiation phase

A) Annexin V/Propidium Iodide Flow Cytometry time course for WT and KO STAT3 adipocytes. The graph is a concatenation of 3 biological replicates per time point for both WT and KO. **B)** Quantitation of the Apoptosis time course. Two-way ANOVA with Sidak's multiple comparison's tests. * = p< 0.05. N=3 for each sample. Data is presented as the mean ± SEM. **C)** Positive controls for Apoptosis assay utilizing 500 μ M H₂O₂ for 5 hours. **D)** Quantitation of C). One-way ANOVA with Dunnett's multiple comparison's test. N.s. = not significant. N=3 for WT Day 0 and N=2 for WT Day 4. Data is presented as the mean ± SEM.

3.13 Inhibition of Wnt Ligand Secretion During Induction Rescues the Adipogenic and Thermogenic Program in STAT3 KO Preadipocytes

We wanted to determine if STAT3 regulates signaling pathways known to be important during the early stages of adipogenesis. We decided to use an inhibitor/activator screen to see if we could identify a pharmacological agent that could rescue adipogenesis in the STAT3 KO. We selected the following three agents for our first screen: IWP2, a general Wnt inhibitor; DAPT, an inhibitor of the Notch Pathway; and SAG, an agonist for the Hedgehog Pathway. We selected these three drugs after a literature search indicated that these three pathways (Wnt, Notch, and Hedgehog) can modulate adipogenesis and that these pathways have been reported to have cross-talk with the JAK/STAT pathway (172-178). We incubated the preadipocytes with these three drugs starting one day before induction and continuing throughout the full differentiation period. We found that inhibition of the Notch pathway or activation of the Hedgehog pathway did not rescue differentiation of STAT3 KO cells. However, treatment with 1 μ M of IWP2, an inhibitor of Porcupine (PORCN) in the Wnt signaling pathway, fully restored UCP1 expression in the STAT3 KO cells (**Figure 3.15A**, lanes 2 vs. 4). PORCN is an endoplasmic reticulum intramembrane O-serine palmityltransferase whose function is to add an acyl group to a conserved serine in all Wnt ligands (179). This acylation is necessary for proper secretion and signaling of Wnt ligands (145). IWP2 does not affect Wnt signaling from exogenous sources of Wnt, suggesting that the source of the Wnt that is suppressing STAT3 KO cells are from the cells themselves and not the media. We also tested another PORCN inhibitor, Wnt-C59, to confirm that the results are due to inhibition of PORCN and reduce the possibility of off-target effects. As expected, treatment with 1 μ M of this second PORCN inhibitor recapitulated the results seen with

IWP2 (**Figure 3.15B**). Treatment with IWP2 and Wnt-C59 also restored lipid droplet accumulation in the STAT3 KO cells (**Figure 3.15C**).

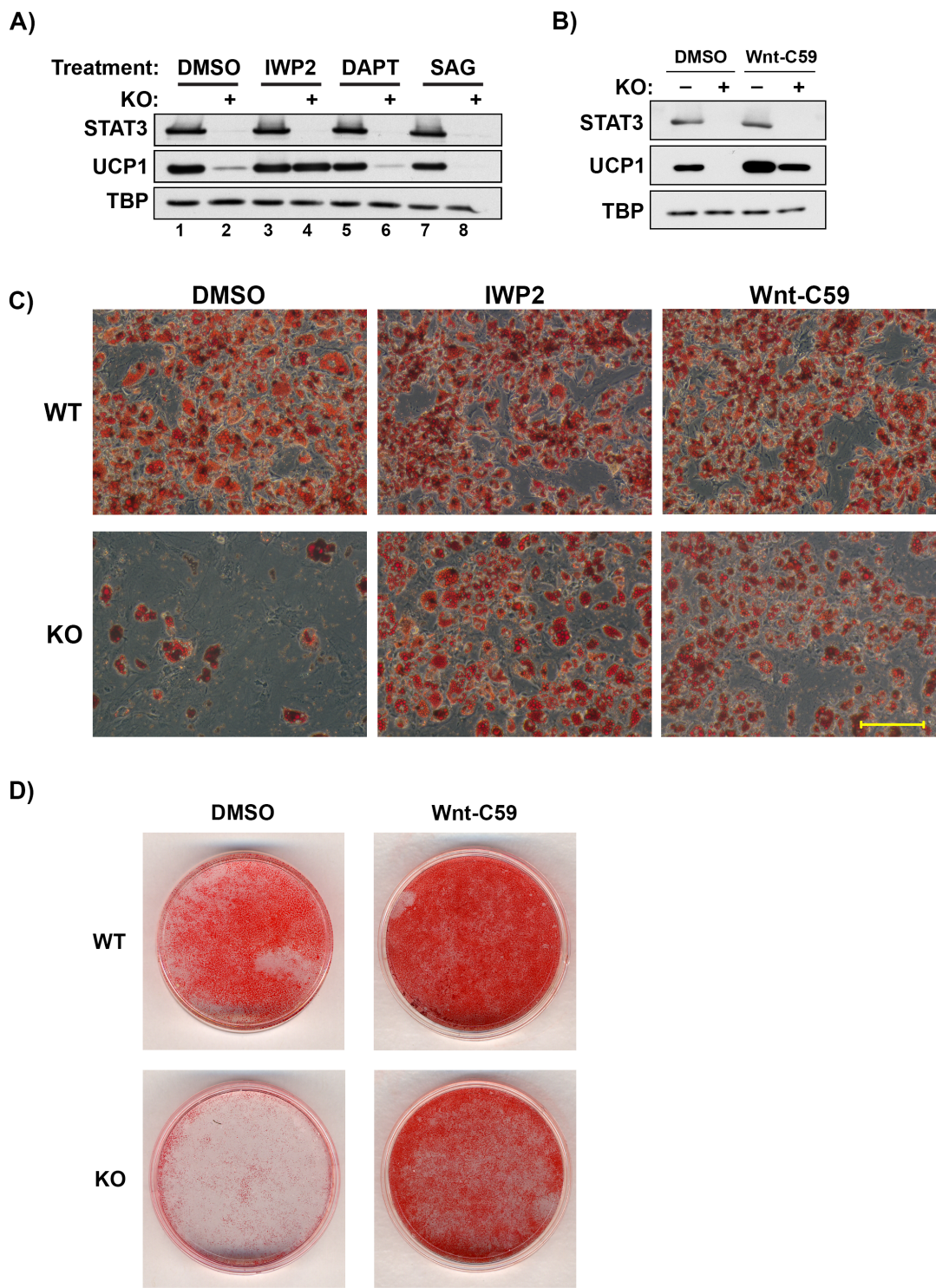


Figure 3.15- Inhibition of PORCN rescues STAT3 KO brown adipocytes

A) Representative immunoblot of Day 7 cells from an inhibitor/activator screen for drugs that can rescue STAT3 KO cells. Cells were treated for 7 days with either 1 μ M IWP2, 5 μ M DAPT, 100nM SAG, or DMSO control. N=3. **B)** Representative immunoblot of Day 7 cells treated with 1 μ M Wnt-C59 for 7 days. **C)** 10x micrograph of Oil Red O staining from Day 7 cells treated with IWP2 or Wnt-C59 for 7 days. Scale bar = 200 μ m. N=3. **D)** Whole plate Oil Red O Staining of Day 7 cells treated for 7 days with Wnt-C59. N=3.

3.14 STAT3 KO Cells have Reduced Histone H3K27 Acetylation at the UCP1 Promoter and Enhancer Regions and can be Rescued with IWP2

Epigenetic changes occur during adipogenesis that regulate access to cell-specific genes involved in the mature functioning brown adipocyte (180). We wanted to determine if STAT3 KO adipocytes have altered histone modifications at the UCP1 enhancer and proximal promoter regions, and whether rescue with Wnt inhibition can restore those histone modifications. ChIPs were performed using an antibody to H3K27Ac, a marker of open and active chromatin (181). In **Figure 3.16**, STAT3 KO cells have reduced levels of H3K27Ac in the enhancer and proximal promoter regions of UCP1, and treatment with IWP2 restores this histone modification.

PRDM16 mRNA expression is down 5-fold in the KO, so we also analyzed histone acetylation at the PRDM16 promoter. Although it failed to reach statistical significance, the same trend can be seen: STAT3 KO have less acetylation and IWP2 treatment can restore acetylation. The reduced acetylation is not a global depression as acetylation levels are equivalent between the WT and KO, and are also unchanged between vehicle and IWP2 treatment conditions. Additionally, we profiled a site that should not contain acetylated histone. IGX1A is a region in the mouse genome that is considered a “gene desert” as there are no known transcription start sites within 1 megabase of the region. As expected, histone acetylation is barely above the non-specific IgG background.

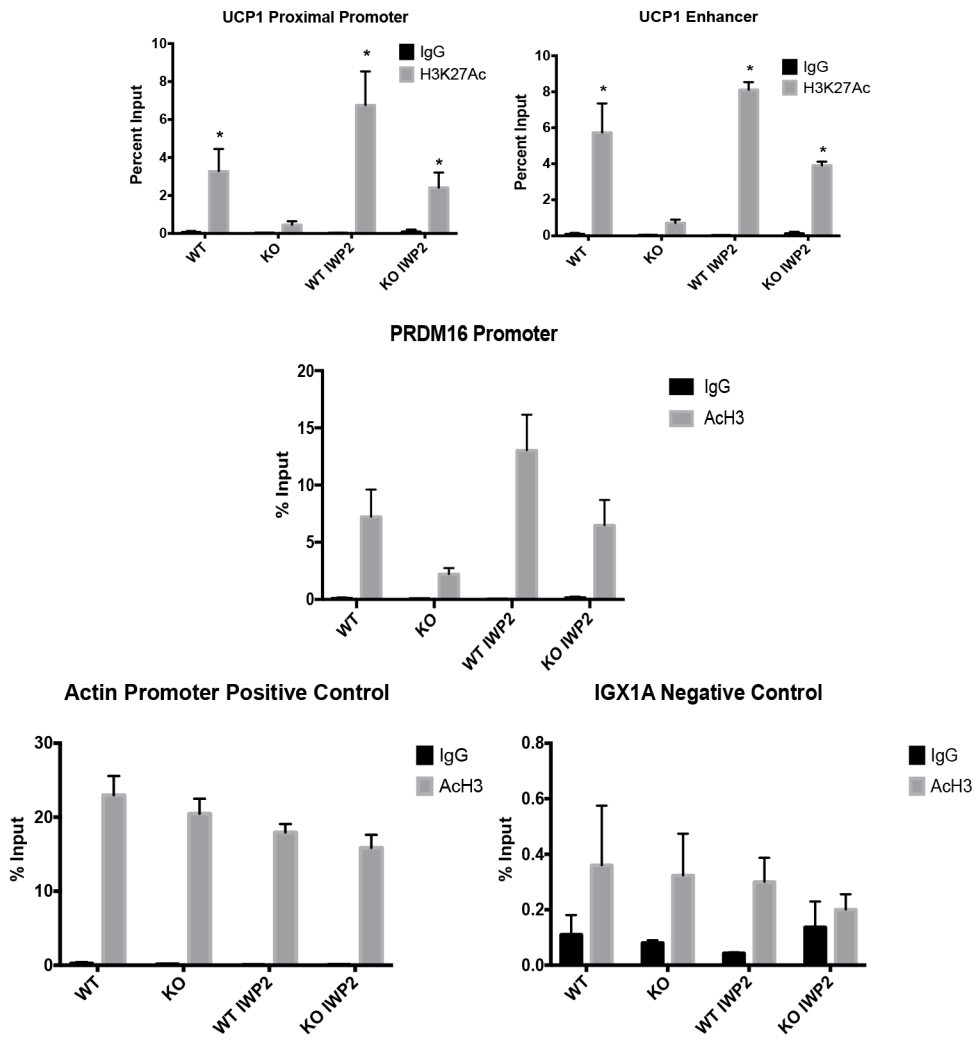


Figure 3.16- STAT3 KO cells have reduced H3K27Ac levels that can be rescued with IWP2

ChIP of the UCP1 Enhancer and Proximal Promoter regions, PRDM16 promoter, and positive (Actin Promoter) and negative (IGX1A) controls from Day 5 adipocytes treated with 1 μ M IWP2 or vehicle from D0-D5. Two-way ANOVA with post-hoc testing compared to the KO H3K27Ac sample. * = p < 0.05. N=3. Data is presented as the mean \pm SEM.

3.15 Wnt Inhibition is needed only during the Induction Period, showing temporal correlation with STAT3

We wanted to determine if inhibition of Wnt signaling during the induction period is sufficient to rescue STAT3 KO preadipocytes. STAT3 KO cells were incubated with IWP2 either during the induction phase (Day 0 to Day 2), after the induction phase (Day 2 to Day 7), or for the whole period (Day 0 to Day 7). Inhibition of Wnt signaling during the induction period is necessary and sufficient to rescue UCP1 in STAT3 KO cells, and is unable to rescue UCP1 after the induction period is completed (**Figure 3.17**). This result is in agreement with a previous study that determined that Wnt inhibition increases UCP1 expression in wild-type beige cells when added during the induction phase (182). Therefore, there is a temporal correlation between when STAT3 is required, and when Wnt inhibition can rescue STAT3 KO preadipocytes.

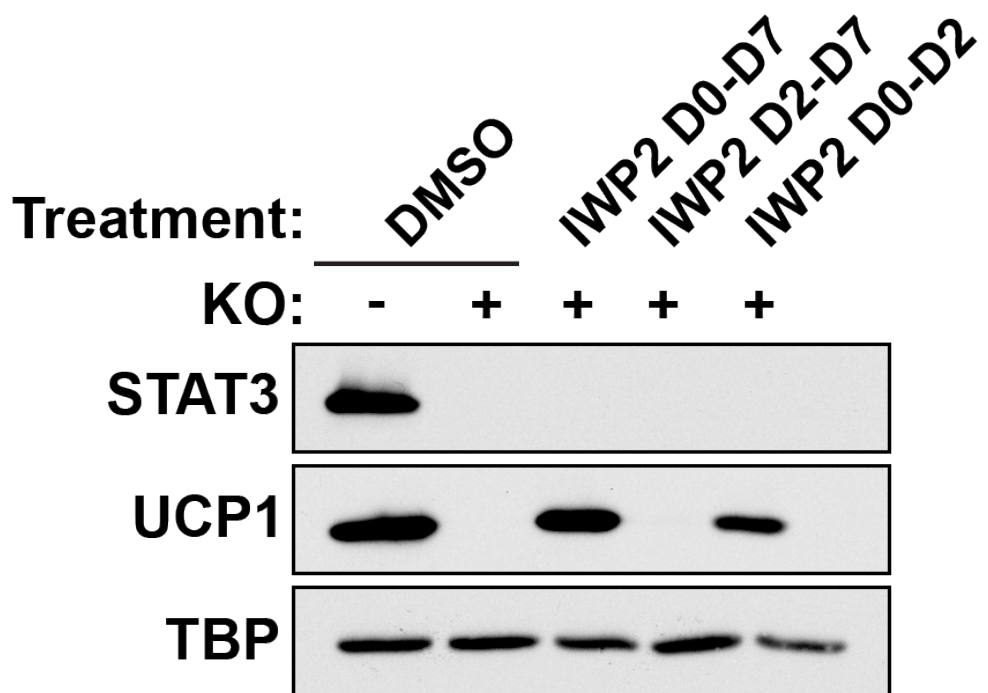


Figure 3.17- IWP2 can only rescue STAT3 KO preadipocyte differentiation when applied during the induction period

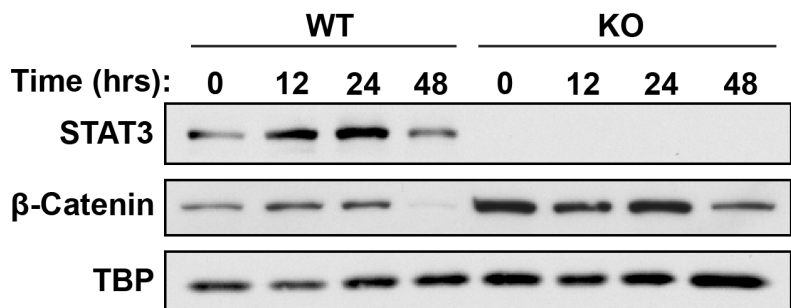
Immunoblot from Day 7 lysates of adipocytes treated with IWP2 during different phases of differentiation. The time range for IWP2 treatment is given relative to addition of the induction cocktail. N= 3.

3.16 β-Catenin Levels are not Down Regulated in the STAT3 KO

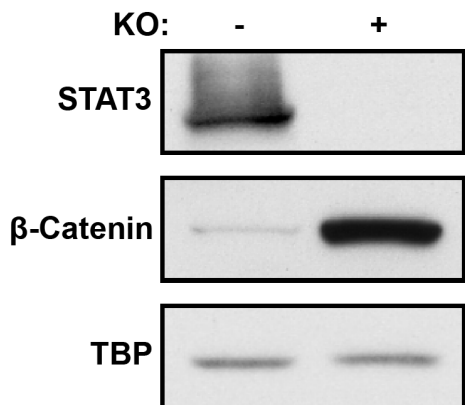
Inhibition of the Wnt pathway with IWP2 provides a way to rescue STAT3 KO preadipocytes, but this alone does not tell us which Wnt pathway is responsible as IWP2 suppresses secretion of Wnt ligands for both the β-catenin canonical pathways and the non-canonical β-catenin independent pathways. Previous studies have shown that the canonical β-catenin pathway and the non-canonical Calcium-Calmodulin/Calcineurin pathway both suppress adipogenesis in 3T3-L1 cells (159). Most of the literature to date has focused on the canonical β-catenin pathway in the suppression of adipogenesis, so we decided to analyze β-catenin levels over the course of differentiation.

In **Figure 3.18A**, by the end of the induction phase, β-catenin has been down regulated in the WT cells but not in the KO. There also appears to be a trend towards increased β-catenin levels in the KO during the induction period. Surprisingly, by Day 7 β-catenin is still detectable in the KO cells and is increased approximately 15 fold over the WT (**Figure 3.18B and C**). When the mRNA levels of β-catenin are measured at Day 7, we see no difference, indicating that the down regulation of β-catenin is occurring post-transcriptionally (**Figure 3.18D**).

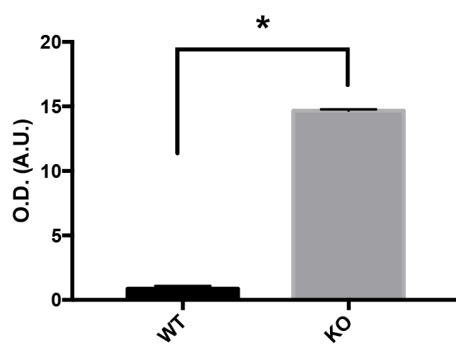
A)



B)



C)



D)

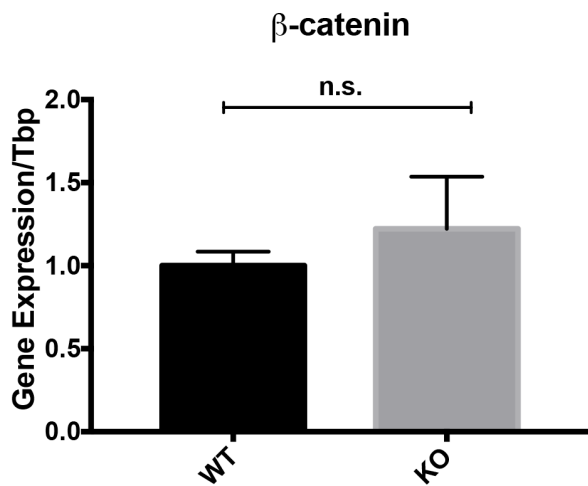


Figure 3.18 - β -Catenin is not down regulated in the STAT3 KO

A) Representative immunoblot of STAT3 WT and KO preadipocytes during the induction phase. Time is hours after addition of induction cocktail. N=3. **B)** Representative immunoblot of Day 7 STAT3 WT and KO adipocytes. N=5. **C)** Densitometry of B). O.D. (A.U.) = Optical Density, Arbitrary Units. N=5. * = p< 0.05. Student's t test. Data is presented as mean \pm SEM **D)** RT-qPCR of Day 7 STAT3 WT and KO adipocytes for β -Catenin. N=3. N.S.= not significant. Student's t test. Data is presented as mean \pm SD.

3.17 STAT3 KO adipocytes have increased Wnt/β-Catenin signaling during the induction phase

Since β-Catenin levels are not down regulated by the end of the induction phase, this suggested that there is increased Wnt/β-Catenin Signaling during the induction period. Measurement of mRNA levels for Axin2, a scaffold protein that is integral to the β-catenin destruction complex, and Dkk1, a natural antagonist to the Wnt pathway through sequestering of the co-receptor LRP6, are considered β-catenin regulated genes and are thus used to determine any differences in Wnt/β-catenin signaling (183, 184). In **Figure 3.19**, both Axin2 and Dkk1 are elevated in the STAT3 KO, confirming that the canonical Wnt pathway is elevated in the STAT3 KO adipocytes.

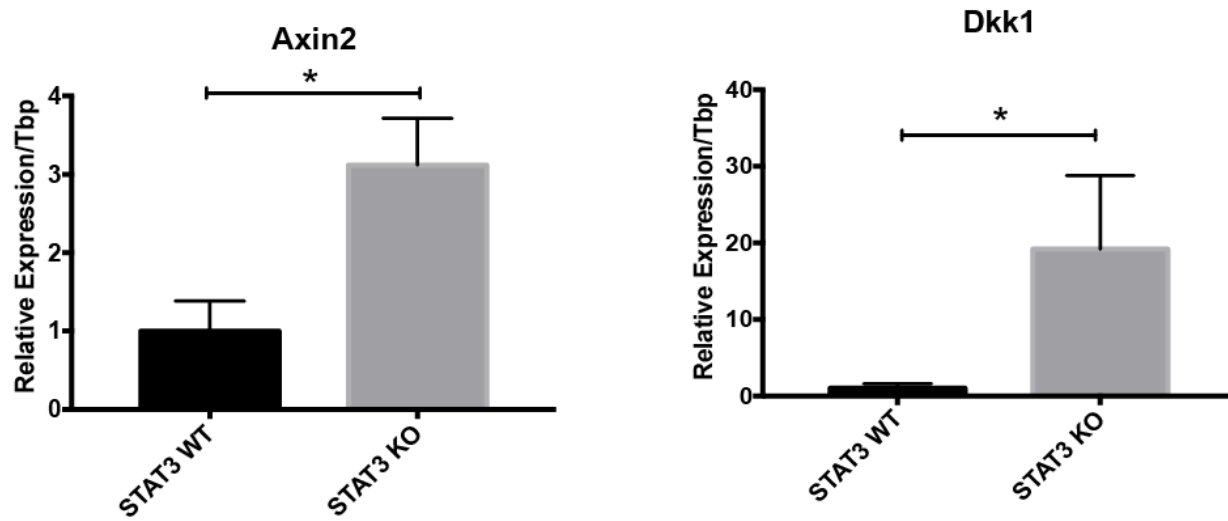


Figure 3.19- Wnt/β-catenin signaling is elevated during induction phase in STAT3 KO

RT-qPCR of Day 1 STAT3 WT and KO adipocytes profiled for β-catenin regulated genes Axin2 and Dkk1. N=3. * = p<0.05. Student's t-test. Data is presented as mean ±SD.

3.18 Wnt Ligands 3a, 1, and 10b are elevated in STAT3 KO adipocytes during the induction phase

Now that we have established increased canonical Wnt/β-Catenin Signaling, we wanted to determine if there is any increased expression in Wnt ligands in the STAT3 KO adipocytes. Recall from Figure 3.15 that the Wnt ligand secretion inhibitor IWP2 is able to rescue STAT3 KO adipocytes. As IWP2 only blocks Wnt signaling from endogenous sources of Wnt ligands, this suggested that the KOs may have increased synthesis and secretion of Wnt ligands during the induction phase. In **Figure 3.20**, mRNA levels of Wnts 1, 3a, and 10b were measured. All three signal through the canonical Wnt pathway and all three are elevated; in the case of Wnt3a the mRNA is up regulated in the STAT3 KO 50 fold.

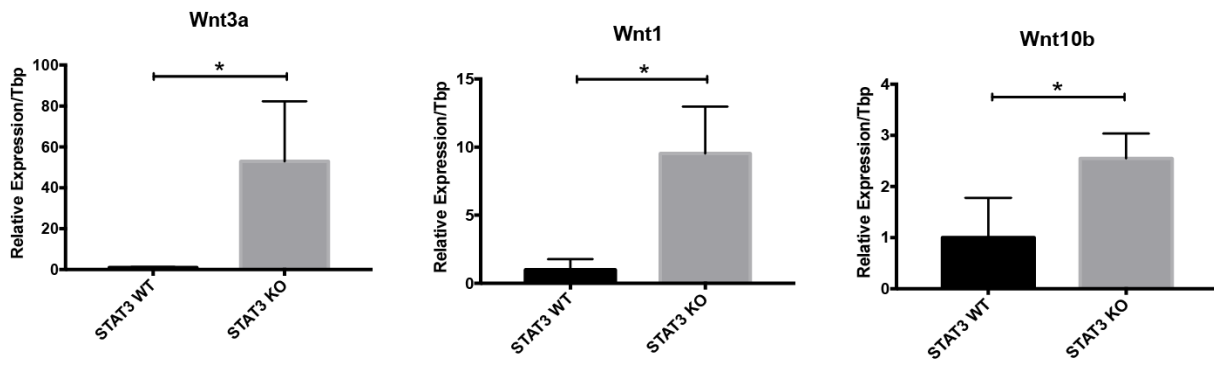


Figure 3.20- Canonical Wnt/ β -catenin ligands are up regulated during the induction phase in STAT3 KO adipocytes

RT-qPCR of Day 1 STAT3 WT and KO adipocytes for Wnt ligands that signal through the canonical β -catenin pathway. N=3. * = p<0.05. Student's t-test. Data is presented as mean \pm SD.

3.19 The Canonical β -Catenin Pathway is responsible for suppression of differentiation in STAT3 KO Brown Preadipocytes

Previous studies have established that the canonical β -catenin pathway and the non-canonical Calcium-Calmodulin/Calcineurin pathway suppress adipogenesis in 3T3-L1 cells (159). Since inhibition of Porcupine is a pan-Wnt inhibitor, we wanted to determine which pathway or pathways were responsible for suppression of UCP1 in STAT3 KO adipocytes. We selected IWR1-endo to target the canonical β -catenin pathway; the mechanism of action is through stabilization of Axin2, a scaffold protein of the β -Catenin destruction complex (185) . For the Calcium-Calmodulin/Calcineurin pathway, we selected FK506, an immunosuppressant that binds to FK506 Binding Protein (FKBP), which allows for FKBP to bind and inactivate calcineurin (186).

Treatment with 5 μ M of the β -catenin inhibitor IWR1-endo resulted in full rescue of UCP1 protein levels (**Figure 3.21A** Lanes 2 vs 8). The Calcineurin inhibitor FK506 (10ng/mL) produced a slight increase in UCP1 levels, which was statistically insignificant. Additionally, IWR1-endo rescued lipid accumulation in the STAT3 KO, whereas FK506 did not (**Figure 3.21 C-E**). We also profiled more brown fat selective/specific and general fat markers by RT-qPCR. In **Figure 3.22**, there is robust rescue of brown fat markers such as CIDEA, PRDM16, and PPAR α . Interestingly, the general fat markers were more mixed; some markers were down in the STAT3 KO and were rescued by Wnt/ β -Catenin inhibition, others appear to be unchanged in the WT versus the KO samples.

Since Wnt inhibition can rescue the expression of UCP1 and other aspects of adipocyte differentiation, we wanted to profile the other defects we have seen in the STAT3 KO to determine if the Wnt/ β -Catenin pathway is involved. In **Figure 3.23**, we analyzed Annexin

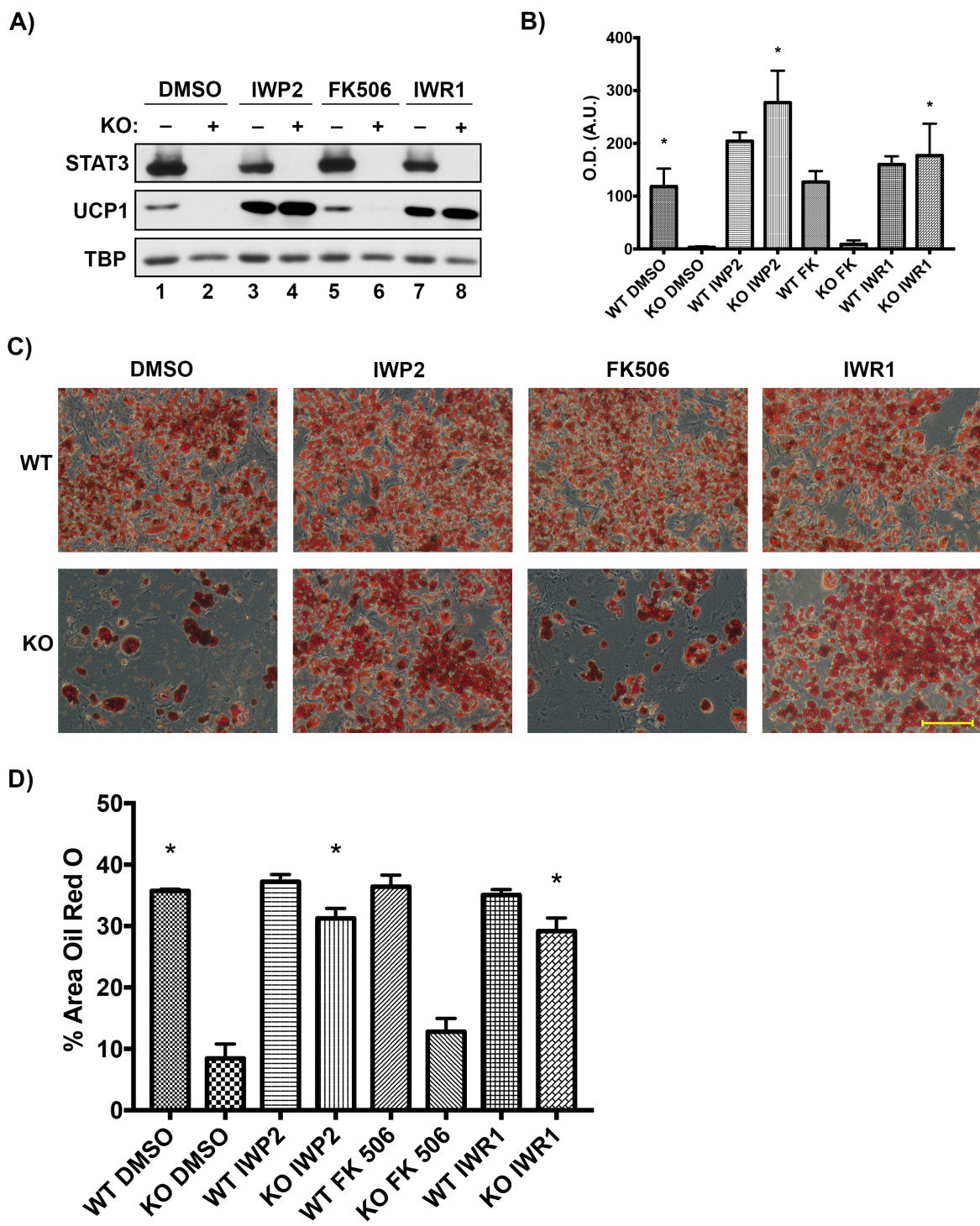
V/Propidium Iodide staining of Day 4 WT and KO STAT3 adipocytes. Treatment with IWP2 and IWR1-endo, but not FK506, is sufficient to reduce Annexin V staining. This indicates that the Wnt/β-catenin pathway is responsible for the increased marker of apoptosis we see in the STAT3 KO cells.

We also measured the proliferation of the cells treated with the inhibitors to determine if the proliferation defect seen in the STAT3 KO could be rescued by Wnt inhibitions. Day 4 adipocytes were analyzed with the dilutional dye Tag-IT in the presence of the inhibitors or vehicle (**Figure 3.24**). The proliferation defect was unaffected by treatment with the Wnt inhibitors, indicating that the proliferation defect is independent of the increased Wnt signaling in the STAT3 KO.

As a positive control, we took STAT3 KO Day 1 adipocytes treated with the inhibitors and profiled expression of Axin2. In **Figure 3.25**, Axin2 levels are decreased in the IWP2 and IWR1-endo conditions, but not in the FK506 condition. FK506 targets a non-canonical β-catenin independent pathway so the unchanged expression of Axin2 is as expected.

To confirm our results that it is the β-catenin pathway that is specifically involved, we selected a second β-catenin inhibitor, XAV939. In **Figure 3.26A-C**, treatment with 1μM of XAV939 was also able to rescue UCP1 protein levels, decrease β-Catenin levels, and restore lipid accumulation in the STAT3 KO cells. Conversely, we inhibited GSK3β in WT cells using 10μM CHIR99021 for just the induction period (D0-D2). It is well known that inhibiting GSK3β can stabilize β-catenin levels and suppress adipogenesis *in-vitro*, and here we see no exception (187). In **Figure 3.26D-F**, GSK3β inhibition results in total suppression of differentiation in the WT STAT3 brown adipocytes and also stabilizes β-catenin levels out to Day 7. Altogether, these

results indicate that Wnt/β-catenin inhibition is sufficient to restore differentiation in STAT3 KO cells.



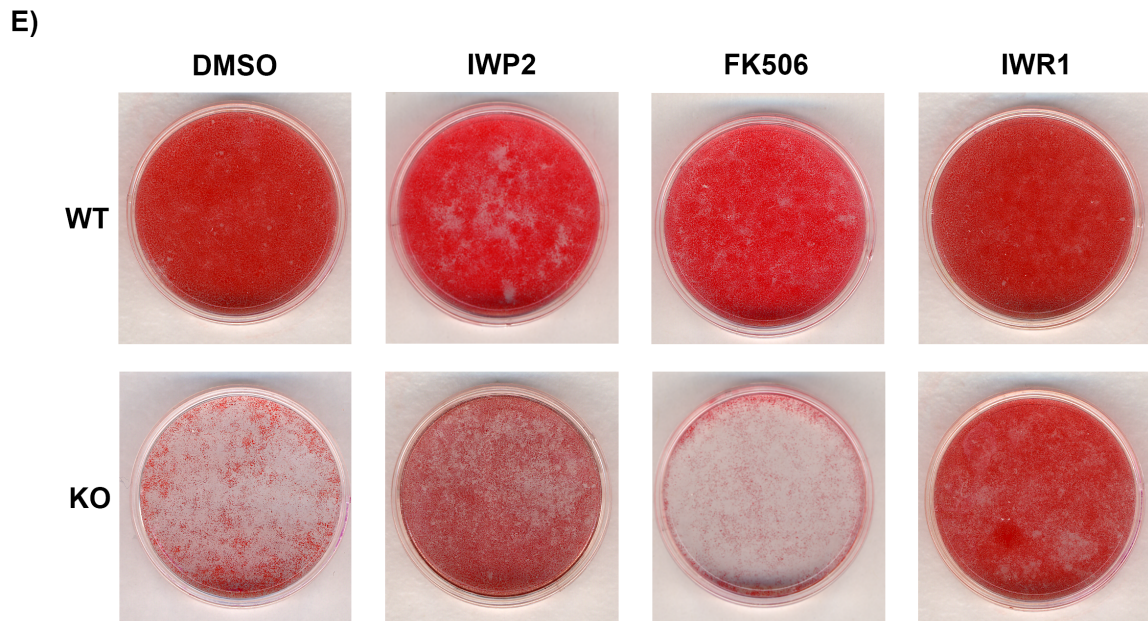


Figure 3.21- β -catenin pathway inhibitors rescue STAT3 KO brown adipocytes

A) Representative immunoblot of Day 7 WT and KO STAT3 brown adipocytes treated with different inhibitors or vehicle for 7 days. N=4-5 for each treatment. **B)** Densitometry of A). O.D. (A.U.) = Optical Density (Arbitrary Units). N=4-5 for each treatment. * = p< 0.05 compared to KO DMSO. One-Way ANOVA with Sidak Multiple Comparison Test. Data is presented as mean \pm SEM. **C)** 10x micrographs of Oil Red O staining of Day 7 WT and KO STAT3 brown adipocytes. Scale bar = 200 μ m. **D)** Quantitation of percent of field positive for Oil Red O stain in C). N=3-4 per treatment. * = p< 0.05 compared to KO DMSO. One-Way ANOVA with Sidak Multiple Comparison Test. Data is presented as mean \pm SEM. **E)** Whole Plate Oil Red O staining of Day 7 WT and KO STAT3 brown adipocytes.

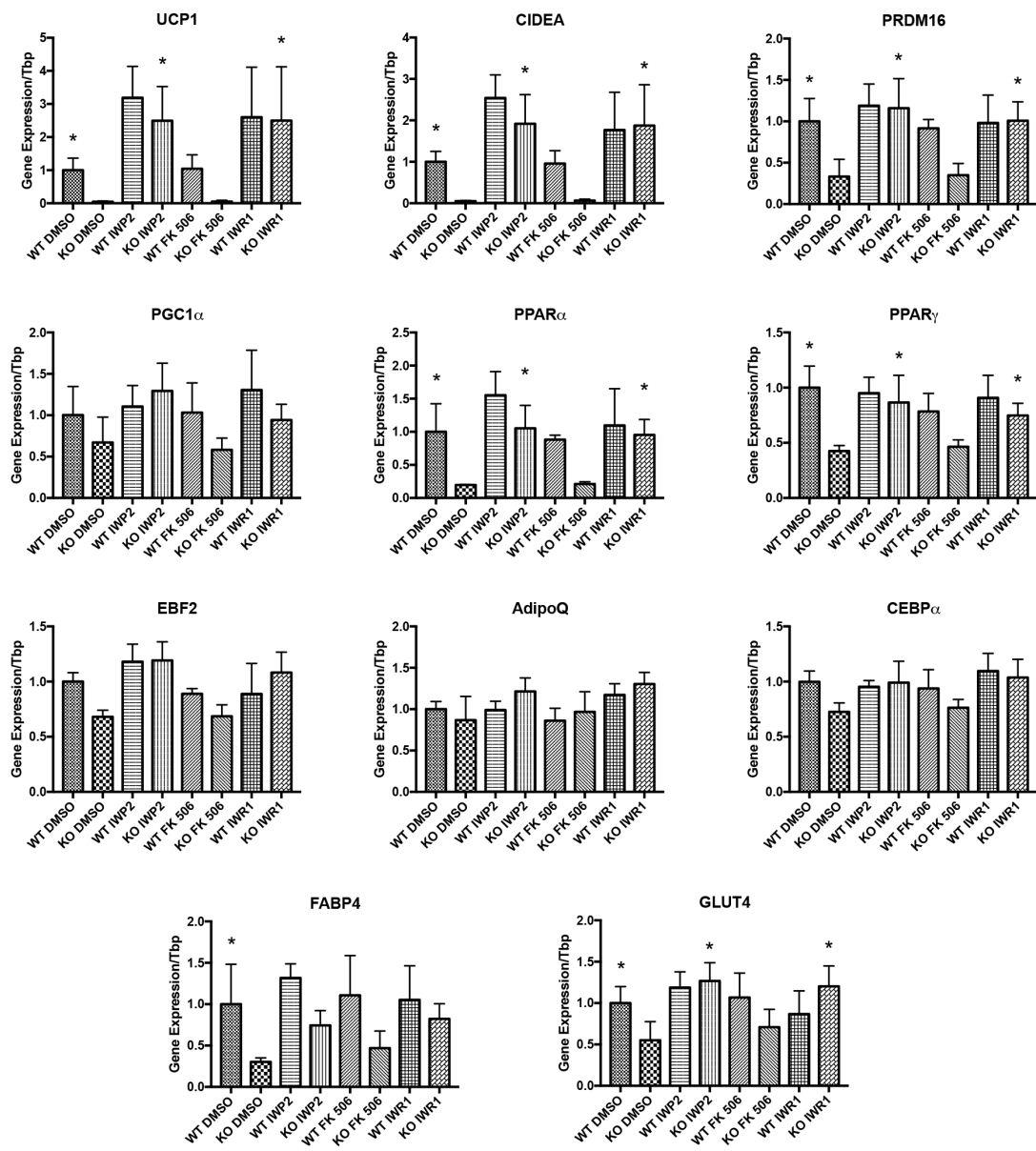
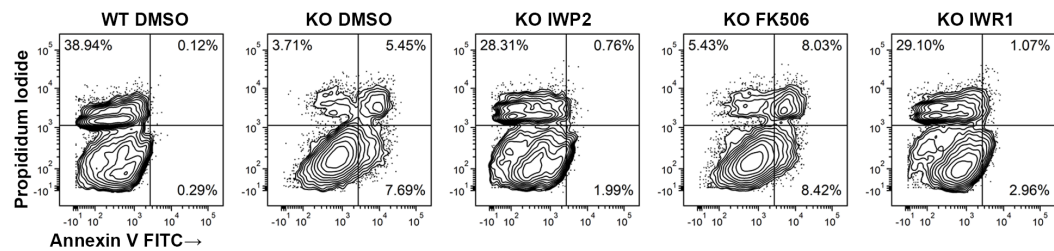


Figure 3.22- RT-qPCR analysis of Wnt inhibitors

Day 7 STAT3 WT and KO Cells were treated with the Wnt inhibitors for 7 days or vehicle. RT-qPCR was performed on various targets important in brown- and general-adipocyte development. N=4. * = $p < 0.05$ compared to KO DMSO. One-Way ANOVA with Sidak's Multiple Comparison Tests. Data is presented as mean \pm SD. Tbp was used as a loading control.

A)



B)

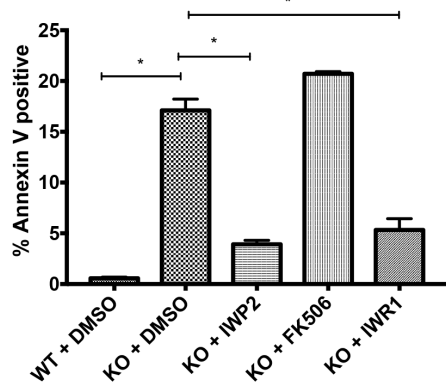


Figure 3.23- Treatment with Wnt inhibitors reduces Annexin V staining in the KO brown adipocytes

A) Flow Cytometry Annexin V/Propidium Iodide of Day 4 primary cells treated with the Wnt inhibitors or vehicle for 4 days. Each panel is a concatenation of three independent biological replicates. **B)** Quantitation of A). One-Way ANOVA with Sidak's Multiple Comparison Test.

* = p< 0.05. N=3. Data is presented as mean ± SEM.

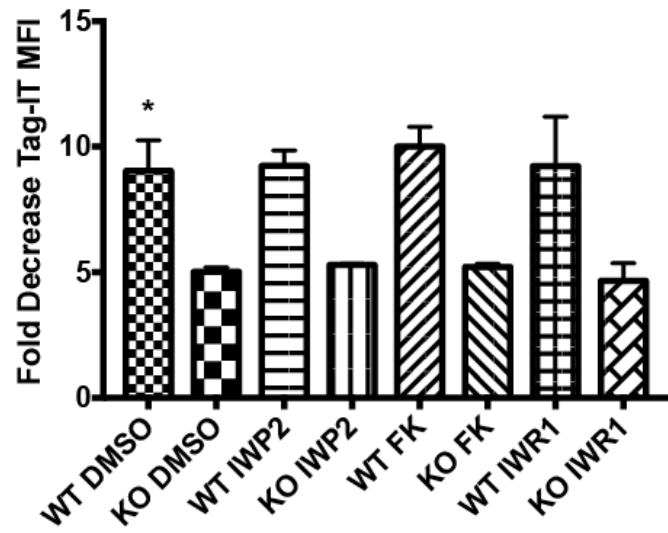


Figure 3.24- Wnt inhibition fails to rescue proliferation defect in STAT3 KO

Tag-IT assay of Day 4 STAT3 WT and KO adipocytes treated with the Wnt inhibitors. N=3. * = p<0.05, compared to KO DMSO. N=3. One-way ANOVA. Data is presented as mean ±SEM.

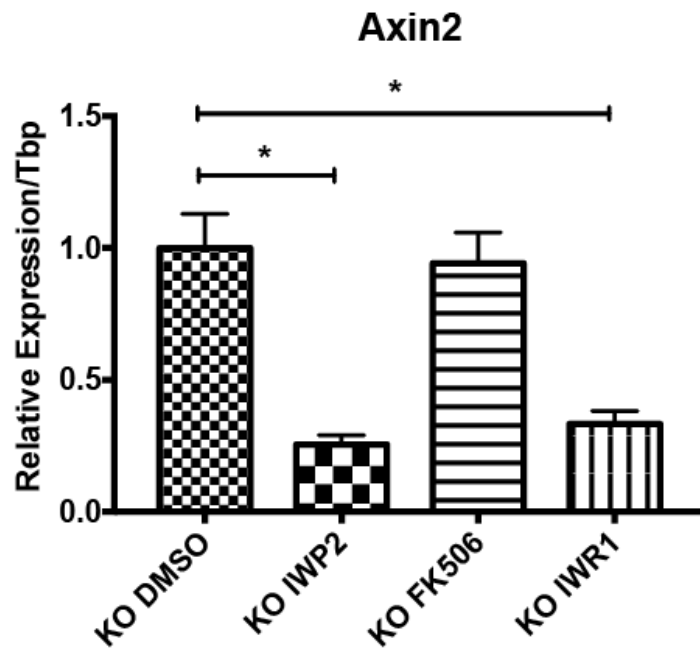


Figure 3.25- Canonical Wnt inhibitors block β -catenin signaling

RT-qPCR of Day 1 STAT3 KO adipocytes treated with the Wnt inhibitors or vehicle. N=4. * = p<0.05. One-way ANOVA. Data is presented as mean \pm SD.

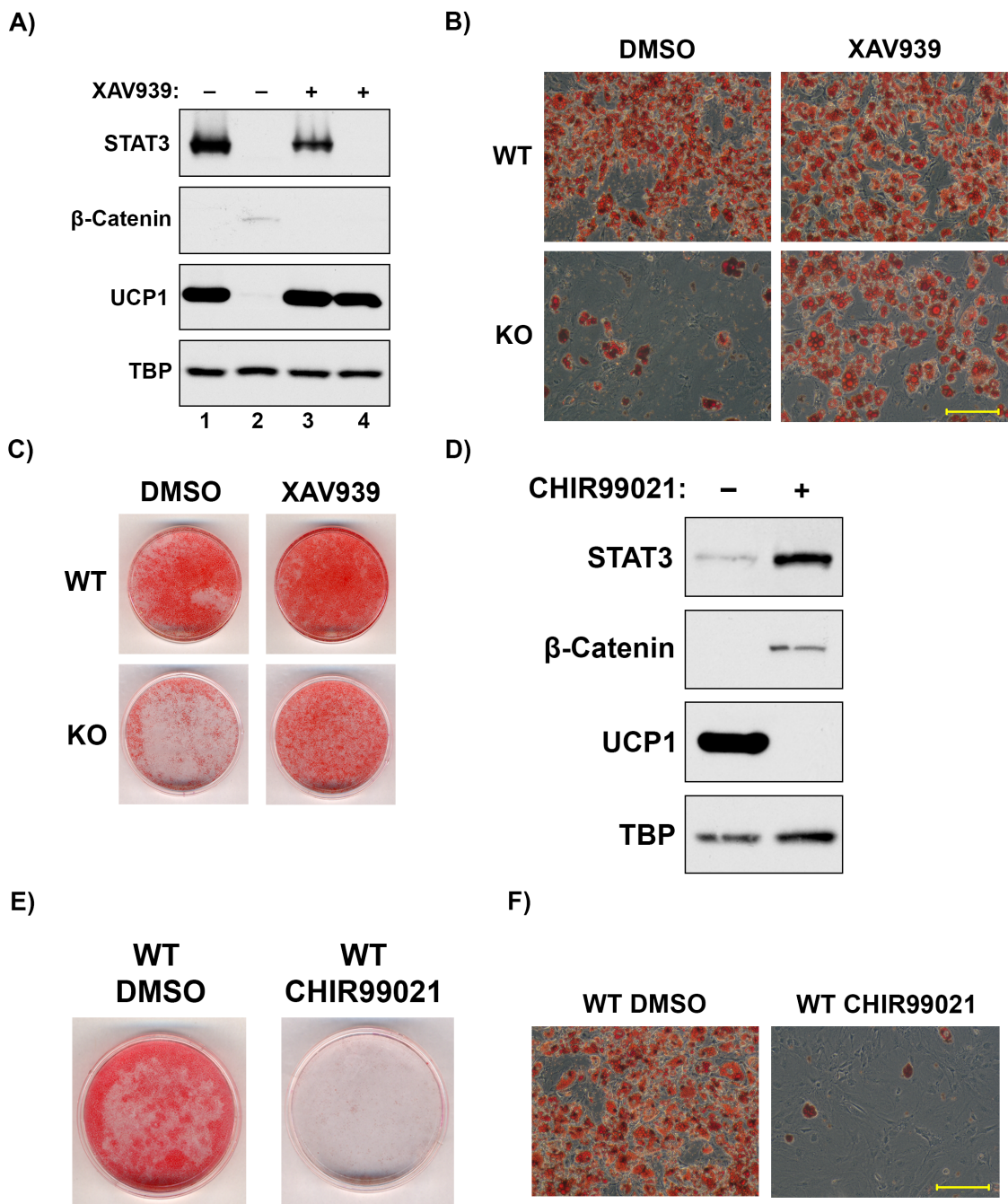


Figure 3.26- XAV939, a second β -catenin inhibitor, rescues STAT3 KO while a GSK3 β inhibitor, CHIR99021, blocks differentiation in WT STAT3 brown adipocytes

A) Representative immunoblot of Day 7 STAT3 WT and KO cells treated for 7 days with 1 μ M XAV939 or vehicle. N=2. **B)** Oil Red O micrographs of Day 7 STAT3 WT and KO cells treated for 7 days with XAV939 or vehicle. 10x magnification, scale bar = 200 μ m. N= 3. **C)** Whole plate Oil Red O of cells treated with XAV939 for 7 days or vehicle. N=3. **D)** Representative immunoblot of Day 7 STAT3 WT cells treated only during the induction with 10 μ M CHIR99021 or vehicle. N=3. **E)** Whole plate image of Day 7 WT STAT3 cells treated with CHIR99021 or vehicle. N=3. **F)** Oil Red O micrographs of Day 7 WT STAT3 cells treated with CHIR99021 or vehicle. 10x magnification, scale bar = 200 μ m. N=3.

3.20 Knockdown of β-Catenin Before Induction Fully Rescues UCP1 Levels

So far we have demonstrated that inhibitors to the Wnt/β-catenin pathway are able to rescue adipogenesis in the STAT3 KO cells. Even though we have targeted different aspects of the pathway with different drugs, there is still a small chance that these inhibitors could be doing something else to the STAT3 KO to effect rescue independent of β-catenin. Therefore, the definitive test that it is the inability to suppress β-catenin that is causing the block in differentiation is to knockdown β-catenin through RNA interference.

48 hours before induction, we transfected either non-targeting control siRNA or β-catenin specific siRNA and let the transfection proceed for 2 days. When the transfection was complete, the cells were either induced to differentiate, or Day 0 mRNA was collected for β-catenin knockdown efficiency analysis. In **Figure 3.27A**, we saw that the siRNA was effective in reducing levels of β-catenin approximately 20 fold compared to the non-targeting siRNA. In **Figure 3.27B**, the levels of β-catenin in the β-catenin siRNA STAT3 KO sample are still undetectable at Day 7 compared to control siRNA STAT3 KO (Lanes 2 and 4). Additionally, we see full recovery of UCP1 in the STAT3 KO where β-catenin is absent. With these results, combined with the Wnt inhibitor studies, we can confidently conclude that the block in adipogenesis in the STAT3 KO adipocytes is singly due to the inability to down regulate β-catenin during the induction phase and that full restoration of the adipogenic and thermogenic program can be rescued in primary Myf5+ brown adipocytes by blocking Wnt/β-catenin.

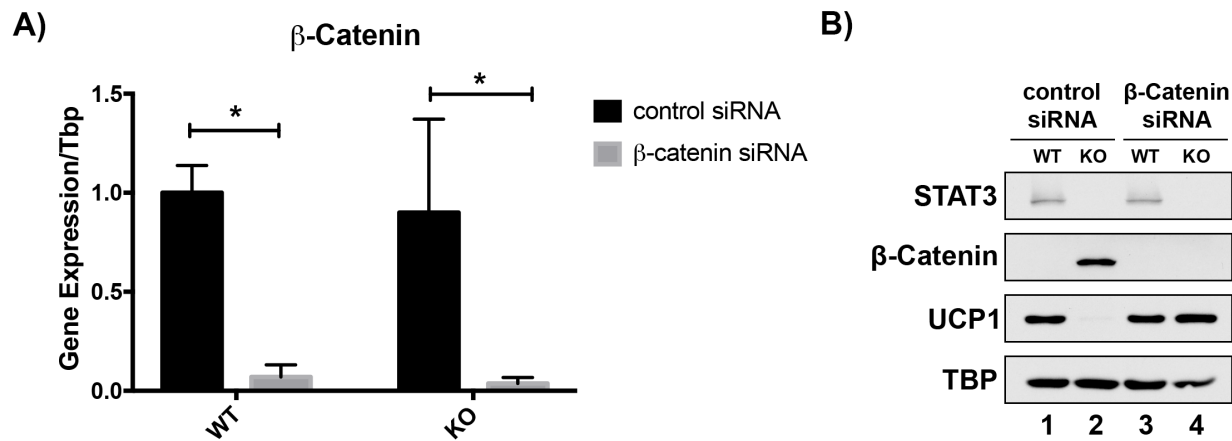


Figure 3.27- Knockdown of β -catenin can fully rescue UCP1 in the STAT3 KO brown adipocyte

A) Day 0 STAT3 WT and KO samples were collected and analyzed by RT-qPCR for β -catenin knockdown efficiency. N=3. * = p< 0.05. Student's t test. Data is presented as mean \pm SD. **B)** Representative immunoblot of Day 7 STAT3 WT and KO Adipocytes. N=2.

3.21 Beige Cells also Require STAT3 Prior to Induction and can be Partially Rescued with Wnt Inhibition

The results so far have all been in the Myf5+ lineage of thermogenic adipocytes. However, as stated in the introduction, beige cells likely have more human relevance as the UCP1+ adipocytes in humans are Myf5- (77, 81). Therefore, using the results generated in the Myf5+ lineage, we wanted to determine if STAT3 is also required for beige development, is it also only required during the induction period, and can Wnt inhibition also rescue STAT3 KO beige adipocytes.

The SVF from the inguinal fat pads from 1-month-old mice was isolated and STAT3 was deleted using tamoxifen in an identical fashion to the Myf5+ cells. In **Figure 3.28A**, we performed a knockout time course where we either knocked out STAT3 prior to induction or at Days 2 and 5 after induction. In agreement with the Myf5+ cells, STAT3 is required for UCP1 expression and must be present during the induction period. Deletion of STAT3 after the induction period also has no deleterious effect on UCP1 protein levels, and if anything, deleting STAT3 after induction seems to improve UCP1 levels. Also, we see the levels of β -catenin are elevated in the STAT3 KO beige cells compared to the WT cells, just as it was for the Myf5+ cells.

In **Figure 3.28B**, we treated the STAT3 WT and KO cells with the Wnt inhibitors. We used the same treatment conditions as we did for the Myf5+ cells. Interestingly, while IWP2 and IWR1-endo can increase UCP1 in the STAT3 KO cells, the rescue is not as robust as in the Myf5+ cells.

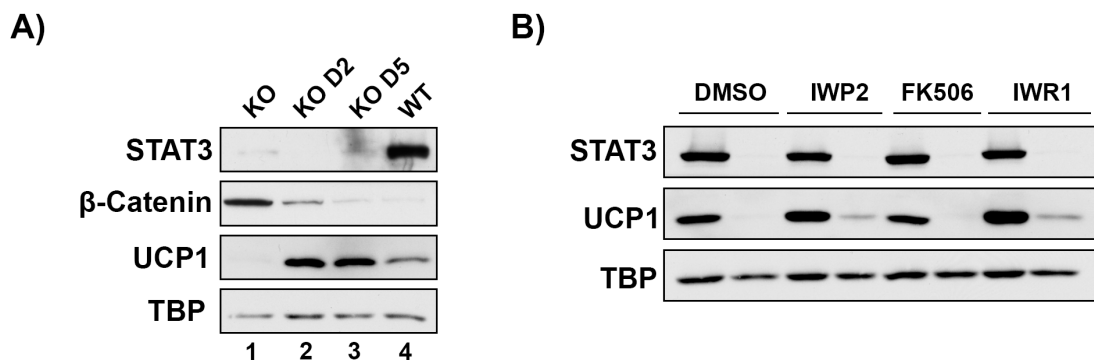


Figure 3.28 Beige cells also require STAT3 during the induction period, but Wnt inhibition is not as robust

A) Representative immunoblot of Day 7 STAT3 WT and KO beige cells. D2= Tamoxifen added to WT on Day 2, D5= Tamoxifen added to WT on Day 5. N=3. **B)** Representative immunoblot of Day 7 STAT3 WT and KO beige cells treated for 7 days with the indicated inhibitor. N=2.

3.22 Pilot *In-Vivo* Beiging Study Shows Equal Induction of UCP1 in the STAT3 WT and KO animals

We were unable to generate any viable pups from a Myf5+ promoter driven Cre, Floxed STAT3 animal. Because our Tamoxifen Cre mouse has Cre Recombinase ubiquitously expressed in every tissue, we were hesitant to attempt to knockout STAT3 in the entire adult animal. We decided to attempt a pilot study where we orally gavaged three 8-week-old mice once a day for five days at a dose of 5mg/20g body weight. One mouse died within a week of administration of the tamoxifen, while the other two mice were viable. We waited four weeks with the remaining two mice to allow tamoxifen to clear the system, since it is reported that tamoxifen can induce browning in the inguinal fat pad (168). For one mouse, we injected I.P. once daily a 1mg/kg body weight dosage of CL316,243, a β 3 agonist, to induce browning of the inguinal fat pads for a total of 7 days. The other mouse received an equivalent dosage of PBS. As controls, we took two mice that had not been gavaged with tamoxifen and injected one with CL316,243 and the other with PBS at the same dosage as the KO mice. We harvested the fat pads and ran immunoblots for STAT3 and UCP1. In **Figure 3.29**, the tamoxifen was effective in knocking down STAT3 expression (Lanes 2 and 4), however, the mice still induced UCP1 protein levels to an equal extent to the WT controls (Lanes 3 and 4). The PBS mice as expected show no evidence of browning.

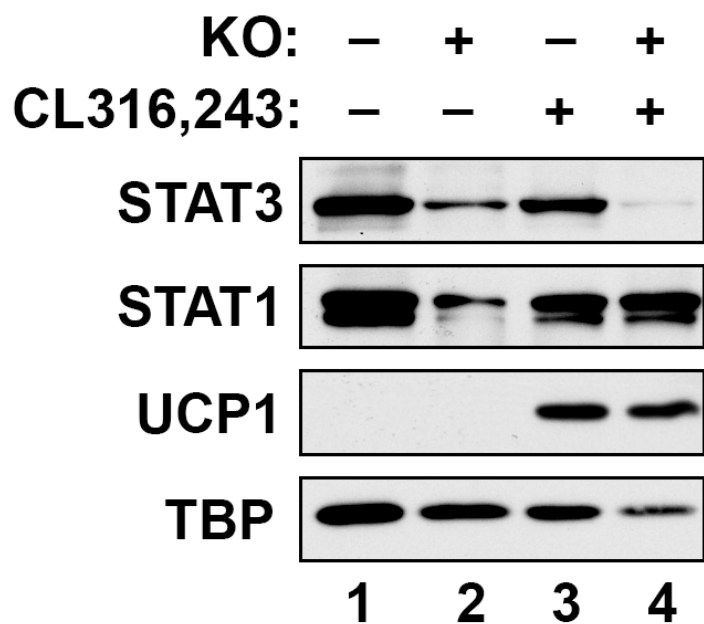


Figure 3.29- Deletion of STAT3 in inguinal fat pad of 8 week old mice appears to not affect UCP1 induction with the β 3 agonist CL316,243

Immunoblot of mouse inguinal pads from WT and KO STAT3 mice treated once per day for 7 days with 1mg/kg CL316,243 by I.P., or with PBS control. N=1 mouse for each condition.

3.23 Primary Tyk2 KO cells Differentiate Normally

Previously, our lab had investigated the role of Tyk2 in brown adipocyte differentiation .

Most of the cell work involved SV40 immortalized Tyk2 WT and KO cells. We decided to continue the project utilizing primary cells. However, in the primary cell system, we were unable to recapitulate our prior results. We isolated SVF from interscapular fat pads of newborn mice from either a Tyk2 WT or total Tyk2 KO line. We grew them to confluence and induced them to differentiate and analyzed the cells by RT-qPCR. In **Figure 3.30**, the expression levels of UCP1 and CIDEA are not different between the Tyk2 WT and Tyk2 KO lines.

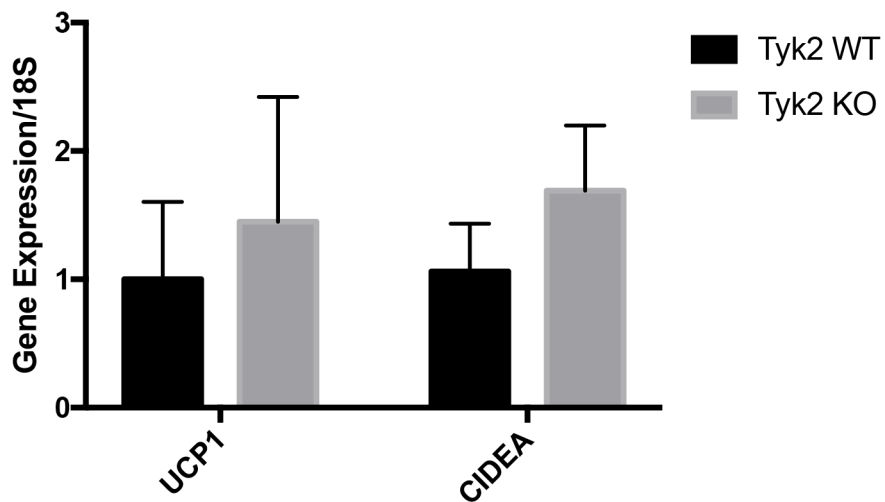


Figure 3.30- Primary Tyk2 KO brown adipocytes have equal UCP1 and CIDEA expression to the WT

RT-qPCR of Day 6 Tyk2 WT and KO adipocytes. N=4. Data is presented as mean \pm SD. 18S rRNA was used as a loading control.

3.24 Tyk2 KO animals Appear to Beige Normally under β 3 Agonist Stimulation

We also attempted to determine if Tyk2 is required for beiging under stimulation by the β 3 agonist CL316,243. We treated WT and KO Tyk2 mice to once daily I.P. injections of either PBS or 1mg/kg body weight CL316,243 for 7 days and then harvested the inguinal fat pad for analysis by RT-qPCR for UCP1 expression. In **Figure 3.31**, the WT and the KO Tyk2 animals induced equal expression of UCP1 under stimulation from the β 3 agonist.

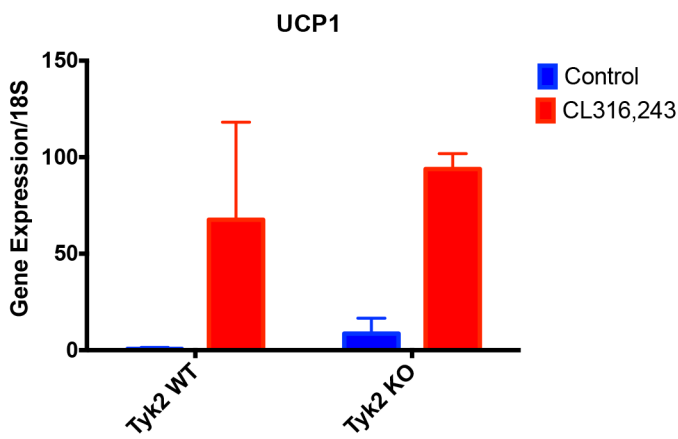


Figure 3.31- Induction of UCP1 mRNA by CL316,243 in Tyk2 KO mice appear to be normal

RT-qPCR for UCP1 expression in the inguinal fat pads of mice treated with either PBS or 1mg/kg CL316,243 once a day for 7 days by I.P. injection. N=2 mice per group. 18S was used as a loading control. Data is presented as mean \pm SD; normalized to Tyk2 WT control.

3.25 Immortalization of STAT3 Preadipocytes Appears to Remove the Requirement for STAT3 in Differentiation

Use of primary cells allows for robust differentiation of adipocytes and expression of UCP1; however there are downsides. The primary cells only become available when there are newborn pups available, which makes the frequency of obtaining samples difficult to predict; therefore, a large breeding colony has to be maintained to ensure constant supply of primary cells. Additionally, primary cells lose their ability to differentiate the longer they are in culture. In our hands, the WT cells start to significantly lose their ability to express UCP1 after more than one week in culture (data not shown). For these reasons, many investigators create cell lines of adipocytes through immortalization using Murine Stem Cell Virus containing the SV40 Large T Antigen. Our prior work in adipocytes utilized immortalized lines, and we began the project with the intent to create an immortalized STAT3 line. However, as **Figure 3.32** shows, once the cells are immortalized, the difference seen in UCP1 mRNA expression levels in primary cells is lost.

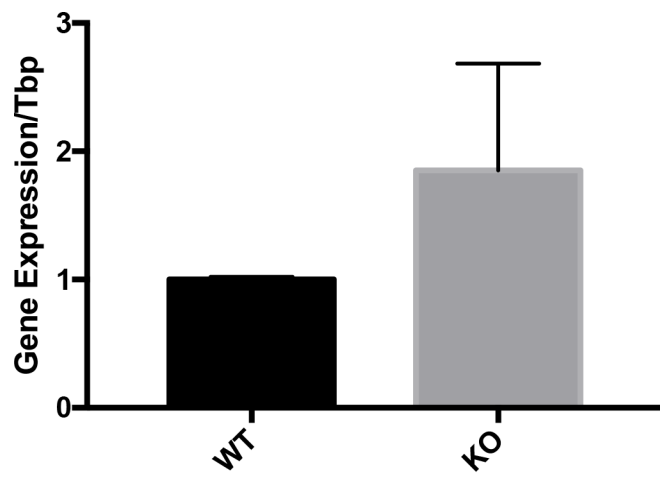


Figure 3.32- UCP1 mRNA expression appears to be equal in SV40 immortalized WT and KO STAT3 brown adipocytes

RT-qPCR of UCP1 mRNA in Day 7 WT and KO STAT3 immortalized brown fat cells. N=2.

Data is expressed as mean \pm SD. Tbp was used as a loading control.

3.26 Mitochondrial STAT3 Levels Decrease During the Induction Period and Remained Depressed Throughout the Terminal Differentiation Phase

Previous work in our lab has identified that STAT3 can localize to the mitochondria, where it can affect functions such as ROS production, ETC activity, and binding to Cyclophilin D, part of the Mitochondrial Permeability Transition Pore (MPTP) (188-190). Therefore, we wanted to determine whether STAT3 localizes to the mitochondria in brown adipocytes and how its levels change during differentiation. In **Figure 3.33**, STAT3 rapidly exits the mitochondria during the induction phase and appears to stay depressed throughout the terminal differentiation phase. This rate of loss from the mitochondria appears to be more rapid than the reduction in cytosolic fractions. In contrast, levels of STAT1 in the mitochondria appear to be relatively unchanged during the time course.

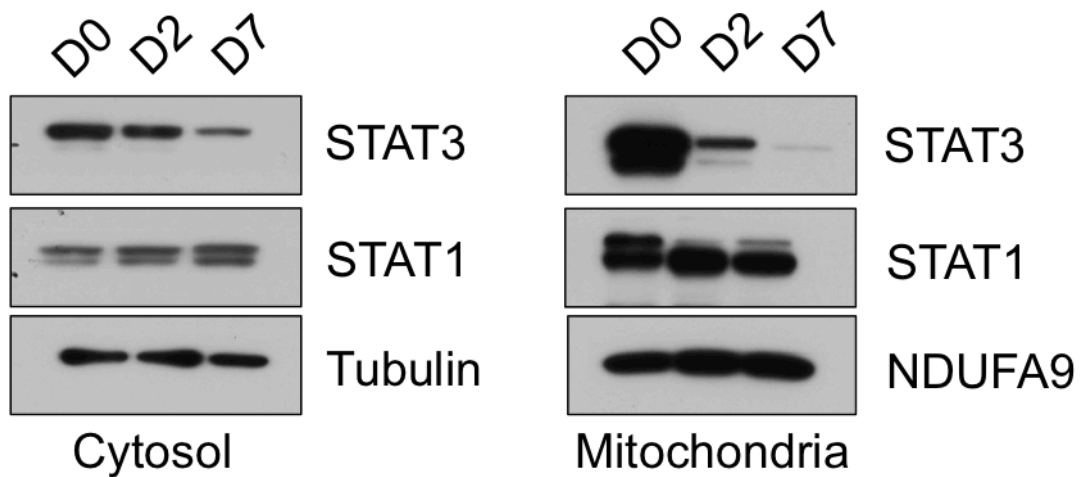


Figure 3.33- STAT3 rapidly exits the mitochondria during brown adipocyte differentiation

Representative immunoblot of cytosolic and mitochondrial fractions from primary adipocytes at the indicated time points along the differentiation time course. N=2.

Chapter 4: Discussion

We have shown for the first time that STAT3 is necessary for differentiation of primary brown adipocytes. Loss of STAT3 leads to a more than 10 fold loss of UCP1 and CIDEA, and 5 fold reduction in PRDM16 and PPAR α expression (**Figure 3.8**). Interestingly, the general fat genes show more variability; this is a result we have seen before in a STAT3 shRNA immortalized cell system (139). One interpretation is that STAT3 may have brown fat specific effects in addition to its role in the general adipogenic program; our previous results did show that STAT3 physical interacts with and stabilizes PRDM16, which lends support to this model. However, another equally valid model is that the cells are encountering a decision point early in the differentiation program before the thermogenic program is fully initiated so that cells can gain access to the chromatin of brown fat specific genes. **Figure 3.16** showed that at Day 5, Histone H3K27Ac is decreased in the STAT3 KO at the UCP1 promoter and enhancer regions. We have attempted to ChIP the UCP1 promoter and enhancer before Day 5, but we were unable to detect any significant histone acetylation (data not shown). The reduction in histone acetylation would presumably make access to the promoter and enhancer binding sites for transcription factors like PPAR γ , PPAR α , PGC1 α , and PRDM16 much more difficult. Also supporting this model is the increase in apoptosis seen at Day 4 in the STAT3 KO (**Figure 3.14**). The increased apoptosis could be due to conflicting signals in the cells. The STAT3 KO cells are clearly attempting to differentiate as markers of adipocytes are not present in Day 0 lysates, but present in Day 7 and show little difference (**Figure 3.4**). However, if they are also receiving

suppressive signals, for example from the Wnt/β-Catenin pathway, the cells undergo a stochastic decision point to either halt differentiation and remain in a quasi-adipocyte state, or initiate apoptosis.

Since STAT3 has first been studied in the 3T3-L1 system, it has been hypothesized that STAT3 only functions during the induction phase in *in-vitro* differentiation of adipocytes . However, to our knowledge, no one has directly tested that hypothesis through either pharmacological inhibition time courses or gene deletion time courses. We therefore believe we are the first to confirm this hypothesis. It is also interesting that the JAK/STAT pathway appears to have a biphasic response during differentiation of brown fat. In **Figure 3.13**, Ruxolitinib increased UCP1 protein levels in WT STAT3 cells over the vehicle control. This effect has been seen before in immortalized systems of brown and beige (171). However, the decrease with Ruxolitinib during the induction phase is a new finding, and not surprising given the role that STAT3 and STAT5 play in adipogenesis. What complicates these findings are *in-vivo* studies that show that cytokines like IL-6, which signal in part through STAT3, generally increase UCP1 levels (191). It could be that the *in-vitro* system is exposed to cytokines in the serum or released from the cells themselves that suppress full expression of UCP1, while other cytokines that are not present *in-vitro* but are present *in-vivo* would always be pro-thermogenic and adipogenic no matter what phase of development the tissue is in. Another explanation is the *in-vitro* model of adipogenesis fails to adequately recapitulate what is seen *in-vivo*, which is certainly possible. This is concerning about the applicability of our findings to *in-vivo* models, however, this pilot study has some caveats. First, we do not know which cells in the tissue actually were knocked out with STAT3. Some cells may not have been exposed to tamoxifen, and these cells were enough to produce UCP1 under β3 agonism. Tissue immunofluorescence for STAT3 after

addition of tamoxifen would determine what percentage of cells in the tissue are STAT3 KO. Additionally, we may have deleted STAT3 at a point in the development of the tissue where STAT3 is no longer required. We unfortunately were unable to create a tissue specific knockout line of STAT3 using an early acting Cre. While another STAT3 adipose specific knockout mouse exists, it is driven by the aP2 promoter- a terminal marker of adipocytes. If our *in-vitro* results do correlate to an *in-vivo* system, then by the time aP2 is turned on, STAT3 has already fulfilled its function in adipogenesis and any effects seen are defects in the functioning of mature adipocytes. Currently, other than Myf5 Cre, with which we failed to generate any viable pups, there is no early acting Cre that would be limited to BAT that could be used to test the *in-vivo* role of STAT3 in brown adipose development.

Until now the function of STAT3 during the induction phase was not well characterized. There was a report that PPAR γ was downstream of STAT3 and STAT3 KO cells can be rescued by application of a PPAR γ agonist. Our protocol involves treating the cells with rosiglitazone, a PPAR γ agonist, during the induction period. We have attempted to leave rosiglitazone in the cells for the entire 7 days, but we have seen that most replicates are unable to be rescued by continuous PPAR γ agonism. In fact, our beige *in-vitro* system involves leaving rosiglitazone in the entire 7 days to maximize UCP1 expression, but rosiglitazone still failed to rescue UCP1 levels in the beige cells.

With our results, we now show that the major function of STAT3 during *in-vitro* differentiation is to suppress β -catenin levels. Through both pharmacological inhibition and knockdown studies, we were able to completely restore UCP1 protein levels, and mRNA expression of other markers of brown adipocytes like PRDM16 and CIDEA. Therefore, we

conclude that the single block to differentiation of STAT3 KO primary brown adipocytes is the inability to suppress β -catenin.

In hindsight, it is not surprising that STAT3 would be involved in cross talk with β -catenin; there are multiple papers in the literature describing cross talk between β -catenin and STAT3 (192, 193). However our results are novel, because research to date has usually shown STAT3 and Wnt co-operatively functioning rather than in opposition (178, 193-195). Why there is this difference between STAT3 and Wnt interaction in adipocytes versus other systems requires further study.

Another interesting finding is that STAT3's regulation of β -catenin is post-transcriptional. β -catenin mRNA amounts at Day 7 are not different between the STAT3 WT and the STAT3 KO (**Figure 3.18**). This is likely due to increased synthesis and secretion of Wnt ligands, especially Wnt3a, as the presence of Wnt ligands stabilizes β -catenin (**Figure 3.20**). That β -catenin is still elevated at Day 7 indicates that Wnt ligands are still present in the STAT3 KO. There are multiple reports describing long-term regulation of Wnt ligand expression in adipocytes. Specifically, EZH2, a methyltransferase that is part of the polycomb repressor complex 2 (PRC2), methylates Histone H3 K27 in the promoters of Wnt ligands as differentiation progresses, which results in silencing of those genes (160, 196). This could indicate that in the absence of STAT3, the long-term suppression of Wnt signaling is affected. The elevated β -catenin could also be the result of suppressed proteasomal degradation. It is known that STAT3 can crosstalk with GSK3 β , which is part of the β -catenin destruction complex, and they can appear to regulate each other (197, 198). Additionally, a recent report determined that STAT3 interacts with and stabilizes an E3 Ubiquitin Ligase, SIAH1 (199). The stabilized SIAH1 then leads to increased proteasomal degradation of β -catenin.

Our findings also show that STAT3 is required for full UCP1 expression in beige cells, and indeed, KO of STAT3 also led to increased β -catenin in the beige cells (**Figure 3.28**). However, rescue with Wnt inhibition was only partial. There are several possible explanations here. The first is that the mechanism of STAT3 in beige fat is slightly different and does not depend as much on suppressing β -catenin. Another explanation is that the inhibitors are not adequate in beige fat and knockdown or deletion of β -catenin is necessary for full restoration. Additionally, we are isolating the SVF from one month old mice for beige studies and newborn pups for the Myf5+ studies. This difference in isolation protocols exists because at birth the Myf5+ interscapular fat pad is present, while the inguinal fat pad is not. We must wait for the fat pad to develop before we can harvest and adequate number of preadipocytes for experiments. It is possible that the Wnt pathway plays a stronger role in suppression of differentiation in the younger cells.

Immortalization of primary brown adipocytes removed all differences between the WT and KO STAT3 cells, which is what necessitated the use of primary cells. One explanation is that the β -catenin pathway is suppressed or bypassed in SV40 immortalized cells. However, that is not the case. The explanation is that immortalization affects the WT more than the KO. When the Ct values of primary and immortalized lines are compared, we see that the Ct value increases in the WT, but remains unchanged in the KO. Immortalization therefore negatively affects the WT to the point that it differentiates comparably to a primary KO STAT3 cell.

Finally, the inability to replicate the results in the Tyk2 primary system is disappointing. We have no explanation as to why the results were unable to be replicated. The Tyk2 KO mice are knockout from conception, so it cannot be that the cells have passed a cell fate point where Tyk2 is no longer needed. One possible explanation is that immortalization may render Tyk2

more important than in primary cells. As stated above, immortalized WT cells have a reduced ability to differentiate. We use a retrovirus in our immortalization protocol and we have found that after immortalization, ISG15, a marker of interferon signaling, is elevated in immortalized cells compared to primary cells (data not shown). It could be that Tyk2 is needed to attenuate this “inflammatory” signaling. It is known that interferons can suppress adipogenesis (200, 201). The suppression of this interferon response in brown adipocytes seems to be through PRDM16 (202). We have published that deletion of Tyk2 can lead to reduction in PRDM16, but perhaps there is more complexity to this regulation than is currently understood.

We propose that the function of STAT3 is to repress expression of select Wnt ligands during the induction phase of adipogenesis. Our model is presented as Figure 4.1. Once the cells are induced to differentiate, STAT3 is activated through phosphorylation and translocates to the nucleus, where through either direct or indirect means leads to repression of Wnt ligand expression. Loss of STAT3 relieves that suppression, leading to increased expression and secretion of Wnt ligands—particularly Wnt3a which was 50 fold up regulated. The increased Wnt ligands signal in an autocrine/paracrine manner leading to stabilization and nuclear translocation of β -catenin. β -catenin then suppresses the expression and activity of transcription factors important for adipogenesis and the thermogenic program, such as PPAR γ , CEBP α , PRDM16, and PGC1 α .

Future work in understanding how STAT3 regulates adipogenesis will require adequate *in-vivo* models to confirm that this STAT3/Wnt/ β -catenin regulatory pathway is important in the development of brown and beige adipose tissue. This can be accomplished through adipose tissue selective STAT3 KO animals treated with either Wnt inhibitors, or by combining the STAT3 KO animals with a targeted knockout of PORCN, the Wnt ligand acylating enzyme.

Additionally, how STAT3 regulates Wnt ligand expression is unknown. A pilot *in-silico* analysis of the Wnt3a promoter identified putative STAT3 binding motifs within 1000bp of the transcription start site (data not shown). Finally, more work is required in the primary beige *ex-vivo* system to determine if the Wnt suppression mechanism is not conserved in this lineage.

The data presented here advance our understanding of how the JAK/STAT pathway, and STAT3 in particular, regulates brown adipogenesis. While still in the pre-clinical stages, methods to increase BAT mass in humans holds potential as an adjunct treatment of obesity, when combined with diet and exercise. Additionally, increased BAT mass in rodents led to better glucose control while on a high fat diet; therapies to increase BAT mass could also be used in the treatment of T2D. Targeted activation of STAT3 at the proper time point in development of these adipocytes, or inhibition Wnt signaling could be one treatment avenue towards increasing UCP1+ fat tissue in humans.

Sympathetic Input, β 3 Agonist,
Induction Cocktail

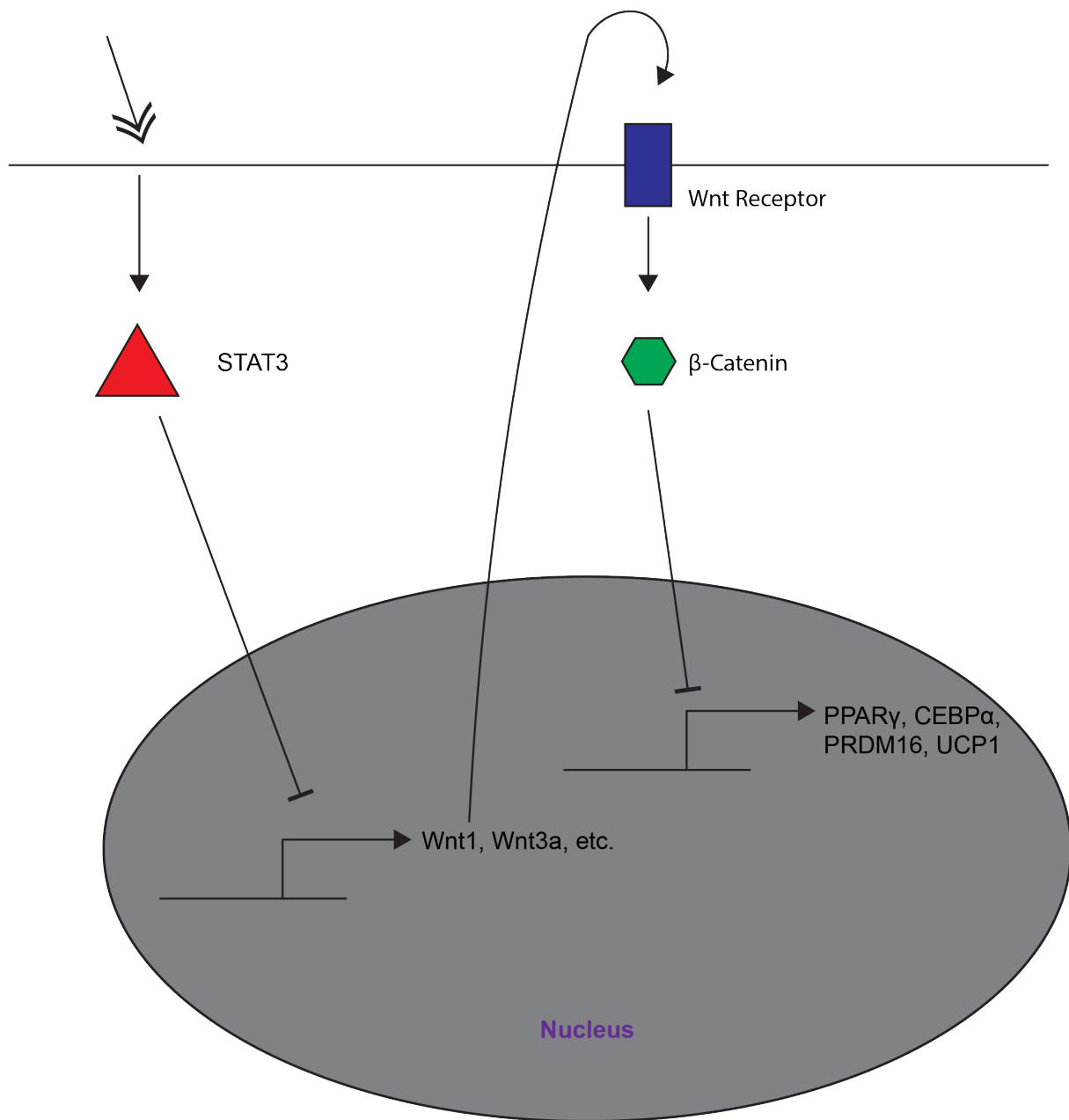


Figure 4.1- Model of STAT3 Suppressing β -Catenin in Brown Adipogenesis

When the preadipocytes are induced to differentiate, STAT3 is activated and through either direct or indirect means inhibits the expression of select Wnt ligands, leading to reduction in Wnt/ β -Catenin Signaling. The resulting suppression of β -Catenin levels leads to promotion of adipogenesis.

References

1. Seidell, J. C. (2005) Epidemiology of Obesity. *Seminars in Vascular Medicine* **5**, 3-14
2. Upadhyay, J., Farr, O., Perakakis, N., Ghaly, W., and Mantzoros, C. (2018) Obesity as a Disease. *The Medical clinics of North America* **102**, 13-33
3. Cawley, J., and Meyerhoefer, C. (2012) The medical care costs of obesity: an instrumental variables approach. *Journal of health economics* **31**, 219-230
4. Cannon, B., and Nedergaard, J. (2004) Brown adipose tissue: function and physiological significance. *Physiological reviews* **84**, 277-359
5. Cypess , A. M., Lehman , S., Williams , G., Tal , I., Rodman , D., Goldfine , A. B., Kuo , F. C., Palmer , E. L., Tseng , Y.-H., Doria , A., Kolodny , G. M., and Kahn , C. R. (2009) Identification and Importance of Brown Adipose Tissue in Adult Humans. *New England Journal of Medicine* **360**, 1509-1517
6. Health, N. I. o. (2017) Vol. 2018
7. Organization, W. H. (2017) Vol. 2018
8. Prevention, C. f. D. C. a. (2018) Vol. 2018
9. Flegal, K. M., Kruszon-Moran, D., Carroll, M. D., Fryar, C. D., and Ogden, C. L. (2016) Trends in Obesity Among Adults in the United States, 2005 to 2014. *Jama* **315**, 2284-2291
10. Nguyen, D. M., and El-Serag, H. B. (2010) The Epidemiology of Obesity. *Gastroenterology clinics of North America* **39**, 1-7
11. Le, A., Judd, S. E., Allison, D. B., Oza-Frank, R., Affuso, O., Safford, M. M., Howard, V. J., and Howard, G. (2014) The Geographic Distribution of Obesity in the US and the Potential Regional Differences in Misreporting of Obesity. *Obesity (Silver Spring, Md.)* **22**, 300-306
12. Kim, J. H., Kim, S. H., Song, S. Y., Kim, W. S., Song, S. U., Yi, T., Jeon, M. S., Chung, H. M., Xia, Y., and Sung, J. H. (2014) Hypoxia induces adipocyte differentiation of adipose-derived stem cells by triggering reactive oxygen species generation. *Cell biology international* **38**, 32-40
13. Ogden, C. L., Carroll, M. D., Lawman, H. G., and et al. (2016) Trends in obesity prevalence among children and adolescents in the united states, 1988-1994 through 2013-2014. *Jama* **315**, 2292-2299
14. Jo, J., Gavrilova, O., Pack, S., Jou, W., Mullen, S., Sumner, A. E., Cushman, S. W., and Periwal, V. (2009) Hypertrophy and/or Hyperplasia: Dynamics of Adipose Tissue Growth. *PLoS Computational Biology* **5**, e1000324
15. Farooqi, I. S., and O'Rahilly, S. (2004) Monogenic Obesity in Humans. *Annual Review of Medicine* **56**, 443-458
16. Schwartz, M. W., Woods, S. C., Porte, D., Jr., Seeley, R. J., and Baskin, D. G. (2000) Central nervous system control of food intake. *Nature* **404**, 661-671
17. Dubern, B., and Clement, K. (2012) Leptin and leptin receptor-related monogenic obesity. *Biochimie* **94**, 2111-2115

18. Farooqi, I. S., Matarese, G., Lord, G. M., Keogh, J. M., Lawrence, E., Agwu, C., Sanna, V., Jebb, S. A., Perna, F., Fontana, S., Lechler, R. I., DePaoli, A. M., and O'Rahilly, S. (2002) Beneficial effects of leptin on obesity, T cell hyporesponsiveness, and neuroendocrine/metabolic dysfunction of human congenital leptin deficiency. *J Clin Invest* **110**, 1093-1103
19. Wang, B., P, C. C., and Pippin, J. J. (2014) Leptin- and Leptin Receptor-Deficient Rodent Models: Relevance for Human Type 2 Diabetes. *Current Diabetes Reviews* **10**, 131-145
20. Farooqi , I. S., Keogh , J. M., Yeo , G. S. H., Lank , E. J., Cheetham , T., and O'Rahilly , S. (2003) Clinical Spectrum of Obesity and Mutations in the Melanocortin 4 Receptor Gene. *New England Journal of Medicine* **348**, 1085-1095
21. Tao, Y.-X. (2010) The Melanocortin-4 Receptor: Physiology, Pharmacology, and Pathophysiology. *Endocrine Reviews* **31**, 506-543
22. Cheung, C. C., Clifton, D. K., and Steiner, R. A. (1997) Proopiomelanocortin Neurons Are Direct Targets for Leptin in the Hypothalamus. *Endocrinology* **138**, 4489-4492
23. Fan, W., Boston, B. A., Kesterson, R. A., Hruby, V. J., and Cone, R. D. (1997) Role of melanocortinergic neurons in feeding and the agouti obesity syndrome. *Nature* **385**, 165
24. Frazier-Wood, A. C., and Wang, Z. (2016) Genetics of Obesity. In *Metabolic Syndrome: A Comprehensive Textbook* (Ahima, R. S., ed) pp. 123-140, Springer International Publishing, Cham
25. Dina, C., Meyre, D., Gallina, S., Durand, E., Korner, A., Jacobson, P., Carlsson, L. M., Kiess, W., Vatin, V., Lecoeur, C., Delplanque, J., Vaillant, E., Pattou, F., Ruiz, J., Weill, J., Levy-Marchal, C., Horber, F., Potoczna, N., Hercberg, S., Le Stunff, C., Bougnères, P., Kovacs, P., Marre, M., Balkau, B., Cauchi, S., Chevre, J. C., and Froguel, P. (2007) Variation in FTO contributes to childhood obesity and severe adult obesity. *Nature genetics* **39**, 724-726
26. Frayling, T. M., Timpson, N. J., Weedon, M. N., Zeggini, E., Freathy, R. M., Lindgren, C. M., Perry, J. R. B., Elliott, K. S., Lango, H., Rayner, N. W., Shields, B., Harries, L. W., Barrett, J. C., Ellard, S., Groves, C. J., Knight, B., Patch, A.-M., Ness, A. R., Ebrahim, S., Lawlor, D. A., Ring, S. M., Ben-Shlomo, Y., Jarvelin, M.-R., Sovio, U., Bennett, A. J., Melzer, D., Ferrucci, L., Loos, R. J. F., Barroso, I., Wareham, N. J., Karpe, F., Owen, K. R., Cardon, L. R., Walker, M., Hitman, G. A., Palmer, C. N. A., Doney, A. S. F., Morris, A. D., Smith, G. D., Hattersley, A. T., and McCarthy, M. I. (2007) A Common Variant in the FTO Gene Is Associated with Body Mass Index and Predisposes to Childhood and Adult Obesity. *Science* **316**, 889-894
27. Jebb, S. A., and Moore, M. S. (1999) Contribution of a sedentary lifestyle and inactivity to the etiology of overweight and obesity: current evidence and research issues. *Medicine and science in sports and exercise* **31**, S534-541
28. Vilchis-Gil, J., Galván-Portillo, M., Klünder-Klünder, M., Cruz, M., and Flores-Huerta, S. (2015) Food habits, physical activities and sedentary lifestyles of eutrophic and obese school children: a case-control study. *BMC Public Health* **15**, 124
29. Martínez-González, M. Á., Alfredo Martínez, J., Hu, F. B., Gibney, M. J., and Kearney, J. (1999) Physical inactivity, sedentary lifestyle and obesity in the European Union. *International Journal Of Obesity* **23**, 1192
30. Hu, F. B. (2003) Sedentary lifestyle and risk of obesity and type 2 diabetes. *Lipids* **38**, 103-108

31. Hu, F. B., Li, T. Y., Colditz, G. A., Willett, W. C., and Manson, J. E. (2003) Television watching and other sedentary behaviors in relation to risk of obesity and type 2 diabetes mellitus in women. *Jama* **289**, 1785-1791
32. John, G. K., and Mullin, G. E. (2016) The Gut Microbiome and Obesity. *Current oncology reports* **18**, 45
33. Maruvada, P., Leone, V., Kaplan, L. M., and Chang, E. B. (2017) The Human Microbiome and Obesity: Moving beyond Associations. *Cell host & microbe* **22**, 589-599
34. Parekh, P. J., Balart, L. A., and Johnson, D. A. (2015) The Influence of the Gut Microbiome on Obesity, Metabolic Syndrome and Gastrointestinal Disease. *Clinical And Translational Gastroenterology* **6**, e91
35. Pinhas-Hamiel, O., and Zeitler, P. Acute and chronic complications of type 2 diabetes mellitus in children and adolescents. *The Lancet* **369**, 1823-1831
36. Katsarou, A., Gudbjörnsdottir, S., Rawshani, A., Dabelea, D., Bonifacio, E., Anderson, B. J., Jacobsen, L. M., Schatz, D. A., and Lernmark, Å. (2017) Type 1 diabetes mellitus. *Nature Reviews Disease Primers* **3**, 17016
37. Kahn, S. E., Cooper, M. E., and Del Prato, S. (2014) Pathophysiology and treatment of type 2 diabetes: perspectives on the past, present, and future. *Lancet (London, England)* **383**, 1068-1083
38. Rabe, K., Lehrke, M., Parhofer, K. G., and Broedl, U. C. (2008) Adipokines and Insulin Resistance. *Molecular Medicine* **14**, 741-751
39. Huang, S., and Czech, M. P. (2007) The GLUT4 Glucose Transporter. *Cell Metabolism* **5**, 237-252
40. Hotamisligil, G. S., Arner, P., Caro, J. F., Atkinson, R. L., and Spiegelman, B. M. (1995) Increased adipose tissue expression of tumor necrosis factor-alpha in human obesity and insulin resistance. *The Journal of Clinical Investigation* **95**, 2409-2415
41. Uysal, K. T., Wiesbrock, S. M., Marino, M. W., and Hotamisligil, G. S. (1997) Protection from obesity-induced insulin resistance in mice lacking TNF- α function. *Nature* **389**, 610
42. Roden, M., Price, T. B., Perseghin, G., Petersen, K. F., Rothman, D. L., Cline, G. W., and Shulman, G. I. (1996) Mechanism of free fatty acid-induced insulin resistance in humans. *The Journal of Clinical Investigation* **97**, 2859-2865
43. Boden, G., She, P., Mozzoli, M., Cheung, P., Gumireddy, K., Reddy, P., Xiang, X., Luo, Z., and Ruderman, N. (2005) Free Fatty Acids Produce Insulin Resistance and Activate the Proinflammatory Nuclear Factor- κ B Pathway in Rat Liver. *Diabetes* **54**, 3458-3465
44. Lauby-Secretan, B., Scoccianti, C., Loomis, D., Grosse, Y., Bianchini, F., and Straif, K. (2016) Body Fatness and Cancer — Viewpoint of the IARC Working Group. *New England Journal of Medicine* **375**, 794-798
45. Louie, S. M., Roberts, L. S., and Nomura, D. K. (2013) Mechanisms linking obesity and cancer. *Biochimica et Biophysica Acta (BBA) - Molecular and Cell Biology of Lipids* **1831**, 1499-1508
46. Park, J., Morley, T. S., Kim, M., Clegg, D. J., and Scherer, P. E. (2014) Obesity and cancer—mechanisms underlying tumour progression and recurrence. *Nature Reviews Endocrinology* **10**, 455
47. Schelbert, K. B. (2009) Comorbidities of obesity. *Primary care* **36**, 271-285
48. Legro, R. S. (2012) Obesity and PCOS: Implications for Diagnosis and Treatment. *Seminars in reproductive medicine* **30**, 496-506

49. Grodstein, F., Goldman, M. B., and Cramer, D. W. (1994) Body mass index and ovulatory infertility. *Epidemiology (Cambridge, Mass.)* **5**, 247-250
50. Best, D., and Bhattacharya, S. (2015) Obesity and fertility. *Hormone molecular biology and clinical investigation* **24**, 5-10
51. Schwartz, M. W., and Gelling, R. W. (2002) Rats lighten up with MCH antagonist. *Nature medicine* **8**, 779
52. Fruebis, J., Tsao, T. S., Javorschi, S., Ebbets-Reed, D., Erickson, M. R., Yen, F. T., Bihain, B. E., and Lodish, H. F. (2001) Proteolytic cleavage product of 30-kDa adipocyte complement-related protein increases fatty acid oxidation in muscle and causes weight loss in mice. *Proceedings of the National Academy of Sciences of the United States of America* **98**, 2005-2010
53. Diez, J. J., and Iglesias, P. (2003) The role of the novel adipocyte-derived hormone adiponectin in human disease. *European journal of endocrinology* **148**, 293-300
54. Munzberg, H., Bjornholm, M., Bates, S. H., and Myers, M. G., Jr. (2005) Leptin receptor action and mechanisms of leptin resistance. *Cellular and molecular life sciences : CMLS* **62**, 642-652
55. Gao, Q., Wolfgang, M. J., Neschen, S., Morino, K., Horvath, T. L., Shulman, G. I., and Fu, X. Y. (2004) Disruption of neural signal transducer and activator of transcription 3 causes obesity, diabetes, infertility, and thermal dysregulation. *Proceedings of the National Academy of Sciences of the United States of America* **101**, 4661-4666
56. Tam, C. S., Lecoultre, V., and Ravussin, E. (2012) Brown Adipose Tissue. *Mechanisms and Potential Therapeutic Targets* **125**, 2782-2791
57. Fruhbeck, G., Becerril, S., Sainz, N., Garrastachu, P., and Garcia-Veloso, M. J. (2009) BAT: a new target for human obesity? *Trends in pharmacological sciences* **30**, 387-396
58. Cioffi, F., Senese, R., de Lange, P., Goglia, F., Lanni, A., and Lombardi, A. (2009) Uncoupling proteins: a complex journey to function discovery. *BioFactors (Oxford, England)* **35**, 417-428
59. Fedorenko, A., Lishko, Polina V., and Kirichok, Y. Mechanism of Fatty-Acid-Dependent UCP1 Uncoupling in Brown Fat Mitochondria. *Cell* **151**, 400-413
60. Klingenspor, M. (2003) Cold-induced recruitment of brown adipose tissue thermogenesis. *Experimental physiology* **88**, 141-148
61. Arsenijevic, D., Onuma, H., Pecqueur, C., Raimbault, S., Manning, B. S., Miroux, B., Couplan, E., Alves-Guerra, M. C., Goubern, M., Surwit, R., Bouillaud, F., Richard, D., Collins, S., and Ricquier, D. (2000) Disruption of the uncoupling protein-2 gene in mice reveals a role in immunity and reactive oxygen species production. *Nature genetics* **26**, 435-439
62. Brand, M. D., and Esteves, T. C. (2005) Physiological functions of the mitochondrial uncoupling proteins UCP2 and UCP3. *Cell Metabolism* **2**, 85-93
63. Nussbaum, R. L. (2005) Mining yeast in silico unearths a golden nugget for mitochondrial biology. *The Journal of Clinical Investigation* **115**, 2689-2691
64. Stanford, K. I., Middelbeek, R. J., Townsend, K. L., An, D., Nygaard, E. B., Hitchcox, K. M., Markan, K. R., Nakano, K., Hirshman, M. F., Tseng, Y. H., and Goodyear, L. J. (2013) Brown adipose tissue regulates glucose homeostasis and insulin sensitivity. *J Clin Invest* **123**, 215-223
65. Kharitonenkova, A., Shiyanova, T. L., Koester, A., Ford, A. M., Micanovic, R., Galbreath, E. J., Sandusky, G. E., Hammond, L. J., Moyers, J. S., Owens, R. A., Gromada, J.,

- Brozinick, J. T., Hawkins, E. D., Wroblewski, V. J., Li, D. S., Mehrbod, F., Jaskunas, S. R., and Shanafelt, A. B. (2005) FGF-21 as a novel metabolic regulator. *J Clin Invest* **115**, 1627-1635
66. Liu, X., Wang, S., You, Y., Meng, M., Zheng, Z., Dong, M., Lin, J., Zhao, Q., Zhang, C., Yuan, X., Hu, T., Liu, L., Huang, Y., Zhang, L., Wang, D., Zhan, J., Jong Lee, H., Speakman, J. R., and Jin, W. (2015) Brown Adipose Tissue Transplantation Reverses Obesity in Ob/Ob Mice. *Endocrinology* **156**, 2461-2469
67. Yuan, X., Hu, T., Zhao, H., Huang, Y., Ye, R., Lin, J., Zhang, C., Zhang, H., Wei, G., Zhou, H., Dong, M., Zhao, J., Wang, H., Liu, Q., Lee, H. J., Jin, W., and Chen, Z.-J. (2016) Brown adipose tissue transplantation ameliorates polycystic ovary syndrome. *Proceedings of the National Academy of Sciences* **113**, 2708
68. Gunawardana, S. C., and Piston, D. W. (2012) Reversal of Type 1 Diabetes in Mice by Brown Adipose Tissue Transplant. *Diabetes* **61**, 674-682
69. Kikai, M., Yamada, H., Wakana, N., Terada, K., Yamamoto, K., Wada, N., Motoyama, S., Saburi, M., Sugimoto, T., Irie, D., Kato, T., Kawahito, H., Ogata, T., and Matoba, S. (2017) Transplantation of brown adipose tissue inhibits atherosclerosis in apoE^{-/-} mice: contribution of the activated FGF-21-adiponectin axis. *Cardiovascular research*
70. van Marken Lichtenbelt, W. D., Vanhommerig, J. W., Smulders, N. M., Drossaerts, J. M., Kemerink, G. J., Bouvy, N. D., Schrauwen, P., and Teule, G. J. (2009) Cold-activated brown adipose tissue in healthy men. *The New England journal of medicine* **360**, 1500-1508
71. Lee, P., Smith, S., Linderman, J., Courville, A. B., Brychta, R. J., Dieckmann, W., Werner, C. D., Chen, K. Y., and Celi, F. S. (2014) Temperature-acclimated brown adipose tissue modulates insulin sensitivity in humans. *Diabetes* **63**, 3686-3698
72. Klaus, S., Seivert, A., and Boeuf, S. (2001) Effect of the beta(3)-adrenergic agonist CI316,243 on functional differentiation of white and brown adipocytes in primary cell culture. *Biochimica et biophysica acta* **1539**, 85-92
73. Krief, S., Lönnqvist, F., Raimbault, S., Baude, B., Van Spronsen, A., Arner, P., Strosberg, A. D., Ricquier, D., and Emorine, L. J. (1993) Tissue distribution of beta 3-adrenergic receptor mRNA in man. *The Journal of Clinical Investigation* **91**, 344-349
74. Warren, K., Burden, H., and Abrams, P. (2016) Mirabegron in overactive bladder patients: efficacy review and update on drug safety. *Therapeutic Advances in Drug Safety* **7**, 204-216
75. Cypess, Aaron M., Weiner, Lauren S., Roberts-Toler, C., Elía, Elisa F., Kessler, Skyler H., Kahn, Peter A., English, J., Chatman, K., Trauger, Sunia A., Doria, A., and Kolodny, Gerald M. Activation of Human Brown Adipose Tissue by a β_3 -Adrenergic Receptor Agonist. *Cell Metabolism* **21**, 33-38
76. Seale, P., Bjork, B., Yang, W., Kajimura, S., Kuang, S., Scime, A., Devarakonda, S., Chin, S., Conroe, H. M., Erdjument-Bromage, H., Tempst, P., Rudnicki, M. A., Beier, D. R., and Spiegelman, B. M. (2008) PRDM16 Controls a Brown Fat/Skeletal Muscle Switch. *Nature* **454**, 961-967
77. Wu, J., Boström, P., Sparks, Lauren M., Ye, L., Choi, Jang H., Giang, A.-H., Khandekar, M., Virtanen, Kirsi A., Nuutila, P., Schaart, G., Huang, K., Tu, H., van Marken Lichtenbelt, Wouter D., Hoeks, J., Enerbäck, S., Schrauwen, P., and Spiegelman, Bruce M. (2012) Beige Adipocytes Are a Distinct Type of Thermogenic Fat Cell in Mouse and Human. *Cell* **150**, 366-376

78. Park, A., Kim, W. K., and Bae, K.-H. (2014) Distinction of white, beige and brown adipocytes derived from mesenchymal stem cells. *World Journal of Stem Cells* **6**, 33-42
79. Klaus, S., Ely, M., Encke, D., and Heldmaier, G. (1995) Functional assessment of white and brown adipocyte development and energy metabolism in cell culture. Dissociation of terminal differentiation and thermogenesis in brown adipocytes. *Journal of cell science* **108 (Pt 10)**, 3171-3180
80. Ohno, H., Shinoda, K., Spiegelman, B. M., and Kajimura, S. (2012) PPARgamma agonists induce a white-to-brown fat conversion through stabilization of PRDM16 protein. *Cell Metab* **15**, 395-404
81. Shinoda, K., Luijten, I. H., Hasegawa, Y., Hong, H., Sonne, S. B., Kim, M., Xue, R., Chondronikola, M., Cypess, A. M., Tseng, Y. H., Nedergaard, J., Sidossis, L. S., and Kajimura, S. (2015) Genetic and functional characterization of clonally derived adult human brown adipocytes. *Nat Med* **21**, 389-394
82. Betz, M. J., and Enerbäck, S. (2015) Human Brown Adipose Tissue: What We Have Learned So Far. *Diabetes* **64**, 2352
83. Tsukada, J., Yoshida, Y., Kominato, Y., and Auron, P. E. (2011) The CCAAT/enhancer (C/EBP) family of basic-leucine zipper (bZIP) transcription factors is a multifaceted highly-regulated system for gene regulation. *Cytokine* **54**, 6-19
84. Lane, M. D., Tang, Q. Q., and Jiang, M. S. (1999) Role of the CCAAT enhancer binding proteins (C/EBPs) in adipocyte differentiation. *Biochemical and biophysical research communications* **266**, 677-683
85. Yamada, T., Tobita, K., Osada, S., Nishihara, T., and Imagawa, M. (1997) CCAAT/enhancer-binding protein delta gene expression is mediated by APRF/STAT3. *Journal of biochemistry* **121**, 731-738
86. Tang, Q.-Q., and Lane, M. D. (1999) Activation and centromeric localization of CCAAT/enhancer-binding proteins during the mitotic clonal expansion of adipocyte differentiation. *Genes & Development* **13**, 2231-2241
87. Yeh, W. C., Cao, Z., Classon, M., and McKnight, S. L. (1995) Cascade regulation of terminal adipocyte differentiation by three members of the C/EBP family of leucine zipper proteins. *Genes Dev* **9**, 168-181
88. Tanaka, T., Yoshida, N., Kishimoto, T., and Akira, S. (1997) Defective adipocyte differentiation in mice lacking the C/EBPbeta and/or C/EBPdelta gene. *The EMBO journal* **16**, 7432-7443
89. Wu, Z., Xie, Y., Bucher, N. L., and Farmer, S. R. (1995) Conditional ectopic expression of C/EBP beta in NIH-3T3 cells induces PPAR gamma and stimulates adipogenesis. *Genes & Development* **9**, 2350-2363
90. Wu, Z., Bucher, N. L., and Farmer, S. R. (1996) Induction of peroxisome proliferator-activated receptor gamma during the conversion of 3T3 fibroblasts into adipocytes is mediated by C/EBPbeta, C/EBPdelta, and glucocorticoids. *Mol Cell Biol* **16**, 4128-4136
91. Bernlohr, D. A., Bolanowski, M. A., Kelly, T. J., and Lane, M. D. (1985) Evidence for an increase in transcription of specific mRNAs during differentiation of 3T3-L1 preadipocytes. *Journal of Biological Chemistry* **260**, 5563-5567
92. Timchenko, N. A., Wilde, M., Nakanishi, M., Smith, J. R., and Darlington, G. J. (1996) CCAAT/enhancer-binding protein alpha (C/EBP alpha) inhibits cell proliferation through the p21 (WAF-1/CIP-1/SDI-1) protein. *Genes & Development* **10**, 804-815

93. Hwang, C. S., Mandrup, S., MacDougald, O. A., Geiman, D. E., and Lane, M. D. (1996) Transcriptional activation of the mouse obese (ob) gene by CCAAT/enhancer binding protein alpha. *Proceedings of the National Academy of Sciences* **93**, 873-877
94. Lin, F. T., and Lane, M. D. (1992) Antisense CCAAT/enhancer-binding protein RNA suppresses coordinate gene expression and triglyceride accumulation during differentiation of 3T3-L1 preadipocytes. *Genes Dev* **6**, 533-544
95. Wang, N. D., Finegold, M. J., Bradley, A., Ou, C. N., Abdelsayed, S. V., Wilde, M. D., Taylor, L. R., Wilson, D. R., and Darlington, G. J. (1995) Impaired energy homeostasis in C/EBP alpha knockout mice. *Science* **269**, 1108-1112
96. Tyagi, S., Gupta, P., Saini, A. S., Kaushal, C., and Sharma, S. (2011) The peroxisome proliferator-activated receptor: A family of nuclear receptors role in various diseases. *Journal of Advanced Pharmaceutical Technology & Research* **2**, 236-240
97. Rosen, E. D., Hsu, C. H., Wang, X., Sakai, S., Freeman, M. W., Gonzalez, F. J., and Spiegelman, B. M. (2002) C/EPalpha induces adipogenesis through PPARgamma: a unified pathway. *Genes Dev* **16**, 22-26
98. Janani, C., and Ranjitha Kumari, B. D. (2015) PPAR gamma gene--a review. *Diabetes & metabolic syndrome* **9**, 46-50
99. Zhu, Y., Qi, C., Korenberg, J. R., Chen, X. N., Noya, D., Rao, M. S., and Reddy, J. K. (1995) Structural organization of mouse peroxisome proliferator-activated receptor gamma (mPPAR gamma) gene: alternative promoter use and different splicing yield two mPPAR gamma isoforms. *Proceedings of the National Academy of Sciences* **92**, 7921-7925
100. Lefterova, M. I., Zhang, Y., Steger, D. J., Schupp, M., Schug, J., Cristancho, A., Feng, D., Zhuo, D., Stoeckert, C. J., Jr., Liu, X. S., and Lazar, M. A. (2008) PPARgamma and C/EBP factors orchestrate adipocyte biology via adjacent binding on a genome-wide scale. *Genes Dev* **22**, 2941-2952
101. Sears, I. B., MacGinnitie, M. A., Kovacs, L. G., and Graves, R. A. (1996) Differentiation-dependent expression of the brown adipocyte uncoupling protein gene: regulation by peroxisome proliferator-activated receptor gamma. *Mol Cell Biol* **16**, 3410-3419
102. Mueller, E., Drori, S., Aiyyer, A., Yie, J., Sarraf, P., Chen, H., Hauser, S., Rosen, E. D., Ge, K., Roeder, R. G., and Spiegelman, B. M. (2002) Genetic analysis of adipogenesis through peroxisome proliferator-activated receptor gamma isoforms. *The Journal of biological chemistry* **277**, 41925-41930
103. Tontonoz, P., Hu, E., and Spiegelman, B. M. (1994) Stimulation of adipogenesis in fibroblasts by PPAR gamma 2, a lipid-activated transcription factor. *Cell* **79**, 1147-1156
104. Puigserver, P., Wu, Z., Park, C. W., Graves, R., Wright, M., and Spiegelman, B. M. (1998) A cold-inducible coactivator of nuclear receptors linked to adaptive thermogenesis. *Cell* **92**, 829-839
105. Wu, Z., Puigserver, P., Andersson, U., Zhang, C., Adelman, G., Mootha, V., Troy, A., Cinti, S., Lowell, B., Scarpulla, R. C., and Spiegelman, B. M. (1999) Mechanisms controlling mitochondrial biogenesis and respiration through the thermogenic coactivator PGC-1. *Cell* **98**, 115-124
106. St-Pierre, J., Lin, J., Krauss, S., Tarr, P. T., Yang, R., Newgard, C. B., and Spiegelman, B. M. (2003) Bioenergetic analysis of peroxisome proliferator-activated receptor gamma

- coactivators 1alpha and 1beta (PGC-1alpha and PGC-1beta) in muscle cells. *The Journal of biological chemistry* **278**, 26597-26603
107. Zhou, Z., Yon Toh, S., Chen, Z., Guo, K., Ng, C. P., Ponniah, S., Lin, S. C., Hong, W., and Li, P. (2003) Cidea-deficient mice have lean phenotype and are resistant to obesity. *Nature genetics* **35**, 49-56
 108. Seale, P., Kajimura, S., Yang, W., Chin, S., Rohas, L. M., Uldry, M., Tavernier, G., Langin, D., and Spiegelman, B. M. (2007) Transcriptional control of brown fat determination by PRDM16. *Cell Metab* **6**, 38-54
 109. Seale, P., Conroe, H. M., Estall, J., Kajimura, S., Frontini, A., Ishibashi, J., Cohen, P., Cinti, S., and Spiegelman, B. M. (2011) Prdm16 determines the thermogenic program of subcutaneous white adipose tissue in mice. *The Journal of Clinical Investigation* **121**, 96-105
 110. Cohen, P., Levy, J. D., Zhang, Y., Frontini, A., Kolodin, D. P., Svensson, K. J., Lo, J. C., Zeng, X., Ye, L., Khandekar, M. J., Wu, J., Gunawardana, S. C., Banks, A. S., Camporez, J. P., Jurczak, M. J., Kajimura, S., Piston, D. W., Mathis, D., Cinti, S., Shulman, G. I., Seale, P., and Spiegelman, B. M. (2014) Ablation of PRDM16 and beige adipose causes metabolic dysfunction and a subcutaneous to visceral fat switch. *Cell* **156**, 304-316
 111. Seale, P., Bjork, B., Yang, W., Kajimura, S., Chin, S., Kuang, S., Scime, A., Devarakonda, S., Conroe, H. M., Erdjument-Bromage, H., Tempst, P., Rudnicki, M. A., Beier, D. R., and Spiegelman, B. M. (2008) PRDM16 controls a brown fat/skeletal muscle switch. *Nature* **454**, 961-967
 112. Iida, S., Chen, W., Nakadai, T., Ohkuma, Y., and Roeder, R. G. (2015) PRDM16 enhances nuclear receptor-dependent transcription of the brown fat-specific Ucp1 gene through interactions with Mediator subunit MED1. *Genes & Development* **29**, 308-321
 113. Harms, M. J., Lim, H.-W., Ho, Y., Shapira, S. N., Ishibashi, J., Rajakumari, S., Steger, D. J., Lazar, M. A., Won, K.-J., and Seale, P. (2015) PRDM16 binds MED1 and controls chromatin architecture to determine a brown fat transcriptional program. *Genes & Development* **29**, 298-307
 114. Harms, M. J., Ishibashi, J., Wang, W., Lim, H. W., Goyama, S., Sato, T., Kurokawa, M., Won, K. J., and Seale, P. (2014) Prdm16 is required for the maintenance of brown adipocyte identity and function in adult mice. *Cell Metab* **19**, 593-604
 115. Rajakumari, S., Wu, J., Ishibashi, J., Lim, H. W., Giang, A. H., Won, K. J., Reed, R. R., and Seale, P. (2013) EBF2 determines and maintains brown adipocyte identity. *Cell Metab* **17**, 562-574
 116. Shapira, S. N., Lim, H.-W., Rajakumari, S., Sakers, A. P., Ishibashi, J., Harms, M. J., Won, K.-J., and Seale, P. (2017) EBF2 transcriptionally regulates brown adipogenesis via the histone reader DPF3 and the BAF chromatin remodeling complex. *Genes & Development*
 117. Stark, George R., and Darnell, James E. (2012) The JAK-STAT Pathway at Twenty. *Immunity* **36**, 503-514
 118. O'Shea, J. J., Schwartz, D. M., Villarino, A. V., Gadina, M., McInnes, I. B., and Laurence, A. (2015) The JAK-STAT Pathway: Impact on Human Disease and Therapeutic Intervention. *Annual Review of Medicine* **66**, 311-328
 119. Yamaoka, K., Saharinen, P., Pesu, M., Holt, V. E. T., Silvennoinen, O., and O'Shea, J. J. (2004) The Janus kinases (Jaks). *Genome Biology* **5**, 253-253

120. Ghoreschi, K., Laurence, A., and O'Shea, J. J. (2009) Janus kinases in immune cell signaling. *Immunological reviews* **228**, 273-287
121. Levy, D. E., and Darnell, J. E., Jr. (2002) Stats: transcriptional control and biological impact. *Nature reviews. Molecular cell biology* **3**, 651-662
122. Lim, C. P., and Cao, X. (2006) Structure, function, and regulation of STAT proteins. *Molecular BioSystems* **2**, 536-550
123. Ceresa, B. P., and Pessin, J. E. (1996) Insulin Stimulates the Serine Phosphorylation of the Signal Transducer and Activator of Transcription (STAT3) Isoform. *Journal of Biological Chemistry* **271**, 12121-12124
124. Kim, J.-H., Yoon, M.-S., and Chen, J. (2009) Signal Transducer and Activator of Transcription 3 (STAT3) Mediates Amino Acid Inhibition of Insulin Signaling through Serine 727 Phosphorylation. *Journal of Biological Chemistry* **284**, 35425-35432
125. Paulson, M., Pisharody, S., Pan, L., Guadagno, S., Mui, A. L., and Levy, D. E. (1999) Stat Protein Transactivation Domains Recruit p300/CBP through Widely Divergent Sequences. *Journal of Biological Chemistry* **274**, 25343-25349
126. Giese, B., Au-Yeung, C.-K., Herrmann, A., Diefenbach, S., Haan, C., Küster, A., Wortmann, S. B., Roderburg, C., Heinrich, P. C., Behrmann, I., and Müller-Newen, G. (2003) Long Term Association of the Cytokine Receptor gp130 and the Janus Kinase Jak1 Revealed by FRAP Analysis. *Journal of Biological Chemistry* **278**, 39205-39213
127. O'Sullivan, L. A., Liongue, C., Lewis, R. S., Stephenson, S. E., and Ward, A. C. (2007) Cytokine receptor signaling through the Jak-Stat-Socs pathway in disease. *Molecular immunology* **44**, 2497-2506
128. Ehret, G. B., Reichenbach, P., Schindler, U., Horvath, C. M., Fritz, S., Nabholz, M., and Bucher, P. (2001) DNA Binding Specificity of Different STAT Proteins: COMPARISON OF IN VITRO SPECIFICITY WITH NATURAL TARGET SITES. *Journal of Biological Chemistry* **276**, 6675-6688
129. O'Shea, J. J., Pesu, M., Borie, D. C., and Changelian, P. S. (2004) A new modality for immunosuppression: targeting the JAK/STAT pathway. *Nature Reviews Drug Discovery* **3**, 555
130. Shuai, K., and Liu, B. (2003) Regulation of JAK–STAT signalling in the immune system. *Nature Reviews Immunology* **3**, 900
131. Deng, J., Hua, K., Lesser, S. S., and Harp, J. B. (2000) Activation of signal transducer and activator of transcription-3 during proliferative phases of 3T3-L1 adipogenesis. *Endocrinology* **141**, 2370-2376
132. Deng, J., Hua, K., Caveney, E. J., Takahashi, N., and Harp, J. B. (2006) Protein inhibitor of activated STAT3 inhibits adipogenic gene expression. *Biochemical and biophysical research communications* **339**, 923-931
133. Machinal-Quelin, F., Dieudonne, M. N., Leneveu, M. C., Pecquery, R., and Giudicelli, Y. (2002) Proadipogenic effect of leptin on rat preadipocytes in vitro: activation of MAPK and STAT3 signaling pathways. *American journal of physiology. Cell physiology* **282**, C853-863
134. Hogan, J. C., and Stephens, J. M. (2005) Effects of leukemia inhibitory factor on 3T3-L1 adipocytes. *The Journal of endocrinology* **185**, 485-496
135. Cernkovich, E. R., Deng, J., Hua, K., and Harp, J. B. (2007) Midkine is an autocrine activator of signal transducer and activator of transcription 3 in 3T3-L1 cells. *Endocrinology* **148**, 1598-1604

136. Muramatsu, T. (2002) Midkine and Pleiotrophin: Two Related Proteins Involved in Development, Survival, Inflammation and Tumorigenesis. *The Journal of Biochemistry* **132**, 359-371
137. Zhang, K., Guo, W., Yang, Y., and Wu, J. (2011) JAK2/STAT3 pathway is involved in the early stage of adipogenesis through regulating C/EBPbeta transcription. *J Cell Biochem* **112**, 488-497
138. Wang, D., Zhou, Y., Lei, W., Zhang, K., Shi, J., Hu, Y., Shu, G., and Song, J. (2009) Signal transducer and activator of transcription 3 (STAT3) regulates adipocyte differentiation via peroxisome-proliferator-activated receptor gamma (PPARgamma). *Biol Cell* **102**, 1-12
139. Derecka, M., Gornicka, A., Koralov, S. B., Szczepanek, K., Morgan, M., Raje, V., Sisler, J., Zhang, Q., Otero, D., Cichy, J., Rajewsky, K., Shimoda, K., Poli, V., Strobl, B., Pellegrini, S., Harris, T. E., Seale, P., Russell, A. P., McAinch, A. J., O'Brien, P. E., Keller, S. R., Croniger, C. M., Kordula, T., and Larner, A. C. (2012) Tyk2 and Stat3 regulate brown adipose tissue differentiation and obesity. *Cell Metab* **16**, 814-824
140. Cernkovich, E. R., Deng, J., Bond, M. C., Combs, T. P., and Harp, J. B. (2008) Adipose-specific disruption of signal transducer and activator of transcription 3 increases body weight and adiposity. *Endocrinology* **149**, 1581-1590
141. Richard, A. J., and Stephens, J. M. (2014) The role of JAK-STAT signaling in adipose tissue function. *Biochimica et biophysica acta* **1842**, 431-439
142. Logan, C. Y., and Nusse, R. (2004) The Wnt signaling pathway in development and disease. *Annual review of cell and developmental biology* **20**, 781-810
143. Sokol, S. Y. (2011) Maintaining embryonic stem cell pluripotency with Wnt signaling. *Development (Cambridge, England)* **138**, 4341-4350
144. Willert, K., and Nusse, R. (2012) Wnt Proteins. *Cold Spring Harbor Perspectives in Biology* **4**
145. Mikels, A. J., and Nusse, R. (2006) Wnts as ligands: processing, secretion and reception. *Oncogene* **25**, 7461-7468
146. Lorenowicz, M. J., and Korswagen, H. C. (2009) Sailing with the Wnt: charting the Wnt processing and secretion route. *Experimental cell research* **315**, 2683-2689
147. Das, S., Yu, S., Sakamori, R., Stypulkowski, E., and Gao, N. (2012) Wntless in Wnt secretion: molecular, cellular and genetic aspects. *Frontiers in biology* **7**, 587-593
148. Gordon, M. D., and Nusse, R. (2006) Wnt Signaling: Multiple Pathways, Multiple Receptors, and Multiple Transcription Factors. *Journal of Biological Chemistry* **281**, 22429-22433
149. Valenta, T., Hausmann, G., and Basler, K. (2012) The many faces and functions of beta-catenin. *The EMBO journal* **31**, 2714-2736
150. Verheyen, E. M., and Gottardi, C. J. (2010) Regulation of Wnt/ β -Catenin Signaling by Protein Kinases. *Developmental dynamics : an official publication of the American Association of Anatomists* **239**, 34-44
151. Zeng, X., Tamai, K., Doble, B., Li, S., Huang, H., Habas, R., Okamura, H., Woodgett, J., and He, X. (2005) A dual-kinase mechanism for Wnt co-receptor phosphorylation and activation. *Nature* **438**, 873-877
152. MacDonald, B. T., Tamai, K., and He, X. (2009) Wnt/beta-catenin signaling: components, mechanisms, and diseases. *Developmental cell* **17**, 9-26

153. Huang, S. M., Mishina, Y. M., Liu, S., Cheung, A., Stegmeier, F., Michaud, G. A., Charlat, O., Wiellette, E., Zhang, Y., Wiessner, S., Hild, M., Shi, X., Wilson, C. J., Mickanin, C., Myer, V., Fazal, A., Tomlinson, R., Serluca, F., Shao, W., Cheng, H., Shultz, M., Rau, C., Schirle, M., Schlegl, J., Ghidelli, S., Fawell, S., Lu, C., Curtis, D., Kirschner, M. W., Lengauer, C., Finan, P. M., Tallarico, J. A., Bouwmeester, T., Porter, J. A., Bauer, A., and Cong, F. (2009) Tankyrase inhibition stabilizes axin and antagonizes Wnt signalling. *Nature* **461**, 614-620
154. Ross, S. E., Hemati, N., Longo, K. A., Bennett, C. N., Lucas, P. C., Erickson, R. L., and MacDougald, O. A. (2000) Inhibition of Adipogenesis by Wnt Signaling. *Science* **289**, 950
155. Bennett, C. N., Ross, S. E., Longo, K. A., Bajnok, L., Hemati, N., Johnson, K. W., Harrison, S. D., and MacDougald, O. A. (2002) Regulation of Wnt signaling during adipogenesis. *J Biol Chem* **277**, 30998-31004
156. Kang, S., Bajnok, L., Longo, K. A., Petersen, R. K., Hansen, J. B., Kristiansen, K., and MacDougald, O. A. (2005) Effects of Wnt Signaling on Brown Adipocyte Differentiation and Metabolism Mediated by PGC-1 α . *Molecular and Cellular Biology* **25**, 1272-1282
157. Tseng, Y. H., Butte, A. J., Kokkotou, E., Yechoor, V. K., Taniguchi, C. M., Kriauciuinas, K. M., Cypess, A. M., Niinobe, M., Yoshikawa, K., Patti, M. E., and Kahn, C. R. (2005) Prediction of preadipocyte differentiation by gene expression reveals role of insulin receptor substrates and necdin. *Nat Cell Biol* **7**, 601-611
158. Kanazawa, A., Tsukada, S., Kamiyama, M., Yanagimoto, T., Nakajima, M., and Maeda, S. (2005) Wnt5b partially inhibits canonical Wnt/beta-catenin signaling pathway and promotes adipogenesis in 3T3-L1 preadipocytes. *Biochemical and biophysical research communications* **330**, 505-510
159. Kennell, J. A., and MacDougald, O. A. (2005) Wnt signaling inhibits adipogenesis through beta-catenin-dependent and -independent mechanisms. *J Biol Chem* **280**, 24004-24010
160. Wang, L., Jin, Q., Lee, J. E., Su, I. H., and Ge, K. (2010) Histone H3K27 methyltransferase Ezh2 represses Wnt genes to facilitate adipogenesis. *Proc Natl Acad Sci U S A* **107**, 7317-7322
161. Liu, J., and Farmer, S. R. (2004) Regulating the balance between peroxisome proliferator-activated receptor gamma and beta-catenin signaling during adipogenesis. A glycogen synthase kinase 3beta phosphorylation-defective mutant of beta-catenin inhibits expression of a subset of adipogenic genes. *J Biol Chem* **279**, 45020-45027
162. Liu, J., Wang, H., Zuo, Y., and Farmer, S. R. (2006) Functional interaction between peroxisome proliferator-activated receptor gamma and beta-catenin. *Mol Cell Biol* **26**, 5827-5837
163. Staal, F. J. T., and Clevers, H. C. (2005) WNT signalling and haematopoiesis: a WNT-WNT situation. *Nature Reviews Immunology* **5**, 21
164. Yuan, Y., Xi, Y., Chen, J., Zhu, P., Kang, J., Zou, Z., Wang, F., and Bu, S. (2017) STAT3 stimulates adipogenic stem cell proliferation and cooperates with HMGA2 during the early stage of differentiation to promote adipogenesis. *Biochemical and biophysical research communications* **482**, 1360-1366
165. Shin, D. S., Kim, H. N., Shin, K. D., Yoon, Y. J., Kim, S. J., Han, D. C., and Kwon, B. M. (2009) Cryptotanshinone inhibits constitutive signal transducer and activator of

- transcription 3 function through blocking the dimerization in DU145 prostate cancer cells. *Cancer Res* **69**, 193-202
166. Nanbu-Wakao, R., Morikawa, Y., Matsumura, I., Masuho, Y., Muramatsu, M. A., Senba, E., and Wakao, H. (2002) Stimulation of 3T3-L1 adipogenesis by signal transducer and activator of transcription 5. *Molecular endocrinology (Baltimore, Md.)* **16**, 1565-1576
167. Tang, Q.-Q., Otto, T. C., and Lane, M. D. (2003) Mitotic clonal expansion: A synchronous process required for adipogenesis. *Proceedings of the National Academy of Sciences* **100**, 44
168. Ye, R., Wang, Q. A., Tao, C., Vishvanath, L., Shao, M., McDonald, J. G., Gupta, R. K., and Scherer, P. E. (2015) Impact of tamoxifen on adipocyte lineage tracing: Inducer of adipogenesis and prolonged nuclear translocation of Cre recombinase. *Molecular metabolism* **4**, 771-778
169. Floyd, Z. E., and Stephens, J. M. (2002) Interferon- γ -mediated Activation and Ubiquitin-Proteasome-dependent Degradation of PPAR γ in Adipocytes. *Journal of Biological Chemistry* **277**, 4062-4068
170. Taylor, J. L., D'Cunha, J., Tom, P., O'Brien, W. J., and Borden, E. C. (1996) Production of ISG-15, an interferon-inducible protein, in human corneal cells. *J Interferon Cytokine Res* **16**, 937-940
171. Raje, V., Derecka, M., Cantwell, M., Meier, J., Szczepanek, K., Sisler, J. D., Strobl, B., Gamero, A., Harris, T. E., and Larner, A. C. (2017) Kinase Inactive Tyrosine Kinase (Tyk2) Supports Differentiation of Brown Fat Cells. *Endocrinology* **158**, 148-157
172. Christodoulides, C., Lagathu, C., Sethi, J. K., and Vidal-Puig, A. (2009) Adipogenesis and WNT signalling. *Trends in endocrinology and metabolism: TEM* **20**, 16-24
173. Prestwich, T. C., and Macdougald, O. A. (2007) Wnt/beta-catenin signaling in adipogenesis and metabolism. *Current opinion in cell biology* **19**, 612-617
174. Song, B. Q., Chi, Y., Li, X., Du, W. J., Han, Z. B., Tian, J. J., Li, J. J., Chen, F., Wu, H. H., Han, L. X., Lu, S. H., Zheng, Y. Z., and Han, Z. C. (2015) Inhibition of Notch Signaling Promotes the Adipogenic Differentiation of Mesenchymal Stem Cells Through Autophagy Activation and PTEN-PI3K/AKT/mTOR Pathway. *Cellular physiology and biochemistry : international journal of experimental cellular physiology, biochemistry, and pharmacology* **36**, 1991-2002
175. Moisan, A., Lee, Y. K., Zhang, J. D., Hudak, C. S., Meyer, C. A., Prummer, M., Zoffmann, S., Truong, H. H., Ebeling, M., Kjialainen, A., Gerard, R., Xia, F., Schinzel, R. T., Amrein, K. E., and Cowan, C. A. (2015) White-to-brown metabolic conversion of human adipocytes by JAK inhibition. *Nat Cell Biol* **17**, 57-67
176. Kamakura, S., Oishi, K., Yoshimatsu, T., Nakafuku, M., Masuyama, N., and Gotoh, Y. (2004) Hes binding to STAT3 mediates crosstalk between Notch and JAK-STAT signalling. *Nat Cell Biol* **6**, 547-554
177. Gu, D., Fan, Q., Zhang, X., and Xie, J. (2012) A Role for Transcription Factor STAT3 Signaling in Oncogene Smoothened-driven Carcinogenesis. *The Journal of Biological Chemistry* **287**, 38356-38366
178. Fragoso, M. A., Patel, A. K., Nakamura, R. E., Yi, H., Surapaneni, K., and Hackam, A. S. (2012) The Wnt/beta-catenin pathway cross-talks with STAT3 signaling to regulate survival of retinal pigment epithelium cells. *PloS one* **7**, e46892

179. Masumoto, N., Lanyon-Hogg, T., Rodgers, U. R., Konitsiotis, A. D., Magee, A. I., and Tate, E. W. (2015) Membrane bound O-acyltransferases and their inhibitors. *Biochemical Society transactions* **43**, 246-252
180. Inagaki, T., Sakai, J., and Kajimura, S. (2016) Transcriptional and epigenetic control of brown and beige adipose cell fate and function. *Nature reviews. Molecular cell biology* **17**, 480-495
181. Creyghton, M. P., Cheng, A. W., Welstead, G. G., Kooistra, T., Carey, B. W., Steine, E. J., Hanna, J., Lodato, M. A., Frampton, G. M., Sharp, P. A., Boyer, L. A., Young, R. A., and Jaenisch, R. (2010) Histone H3K27ac separates active from poised enhancers and predicts developmental state. *Proc Natl Acad Sci U S A* **107**, 21931-21936
182. Lo, K. A., Ng, P. Y., Kabiri, Z., Virshup, D., and Sun, L. (2016) Wnt inhibition enhances browning of mouse primary white adipocytes. *Adipocyte* **5**, 224-231
183. Niida, A., Hiroko, T., Kasai, M., Furukawa, Y., Nakamura, Y., Suzuki, Y., Sugano, S., and Akiyama, T. (2004) DKK1, a negative regulator of Wnt signaling, is a target of the beta-catenin/TCF pathway. *Oncogene* **23**, 8520-8526
184. Jho, E. H., Zhang, T., Domon, C., Joo, C. K., Freund, J. N., and Costantini, F. (2002) Wnt/beta-catenin/Tcf signaling induces the transcription of Axin2, a negative regulator of the signaling pathway. *Mol Cell Biol* **22**, 1172-1183
185. Chen, B., Dodge, M. E., Tang, W., Lu, J., Ma, Z., Fan, C.-W., Wei, S., Hao, W., Kilgore, J., Williams, N. S., Roth, M. G., Amatruda, J. F., Chen, C., and Lum, L. (2009) Small molecule-mediated disruption of Wnt-dependent signaling in tissue regeneration and cancer. *Nature chemical biology* **5**, 100-107
186. Thomson, A. W., Bonham, C. A., and Zeevi, A. (1995) Mode of action of tacrolimus (FK506): molecular and cellular mechanisms. *Therapeutic drug monitoring* **17**, 584-591
187. Zaragozi, L.-E., Wdziekonski, B., Fontaine, C., Villageois, P., Peraldi, P., and Dani, C. (2008) Effects of GSK3 inhibitors on in vitro expansion and differentiation of human adipose-derived stem cells into adipocytes. *BMC Cell Biology* **9**, 11-11
188. Szczepanek, K., Chen, Q., Derecka, M., Salloum, F. N., Zhang, Q., Szelag, M., Cichy, J., Kukreja, R. C., Dulak, J., Lesnefsky, E. J., and Larner, A. C. (2011) Mitochondrial-targeted Signal transducer and activator of transcription 3 (STAT3) protects against ischemia-induced changes in the electron transport chain and the generation of reactive oxygen species. *J Biol Chem* **286**, 29610-29620
189. Meier, J. A., and Larner, A. C. (2014) Toward a new STATe: the role of STATs in mitochondrial function. *Semin Immunol* **26**, 20-28
190. Meier, J. A., Hyun, M., Cantwell, M., Raza, A., Mertens, C., Raje, V., Sisler, J., Tracy, E., Torres-Odio, S., Gispert, S., Shaw, P. E., Baumann, H., Bandyopadhyay, D., Takabe, K., and Larner, A. C. (2017) Stress-induced dynamic regulation of mitochondrial STAT3 and its association with cyclophilin D reduce mitochondrial ROS production. *Science signaling* **10**
191. Buzelle, S. L., MacPherson, R. E. K., Peppler, W. T., Castellani, L., and Wright, D. C. (2015) The contribution of IL-6 to beta 3 adrenergic receptor mediated adipose tissue remodeling. *Physiological Reports* **3**, e12312
192. Fragoso, M. A., Patel, A. K., Nakamura, R. E. I., Yi, H., Surapaneni, K., and Hackam, A. S. (2012) The Wnt/β-Catenin Pathway Cross-Talks with STAT3 Signaling to Regulate Survival of Retinal Pigment Epithelium Cells. *PloS one* **7**, e46892

193. Hao, J., Li, T. G., Qi, X., Zhao, D. F., and Zhao, G. Q. (2006) WNT/beta-catenin pathway up-regulates Stat3 and converges on LIF to prevent differentiation of mouse embryonic stem cells. *Developmental biology* **290**, 81-91
194. Katoh, M., and Katoh, M. (2007) STAT3-induced WNT5A signaling loop in embryonic stem cells, adult normal tissues, chronic persistent inflammation, rheumatoid arthritis and cancer (Review). *International journal of molecular medicine* **19**, 273-278
195. Ogawa, K., Nishinakamura, R., Iwamatsu, Y., Shimosato, D., and Niwa, H. (2006) Synergistic action of Wnt and LIF in maintaining pluripotency of mouse ES cells. *Biochemical and biophysical research communications* **343**, 159-166
196. Hemming, S., Cakouros, D., Isenmann, S., Cooper, L., Menicanin, D., Zannettino, A., and Gronthos, S. (2014) EZH2 and KDM6A act as an epigenetic switch to regulate mesenchymal stem cell lineage specification. *Stem cells (Dayton, Ohio)* **32**, 802-815
197. Beurel, E., and Jope, R. S. (2008) Differential Regulation of STAT Family Members by Glycogen Synthase Kinase-3. *Journal of Biological Chemistry* **283**, 21934-21944
198. Moh, A., Zhang, W., Yu, S., Wang, J., Xu, X., Li, J., and Fu, X. Y. (2008) STAT3 sensitizes insulin signaling by negatively regulating glycogen synthase kinase-3 beta. *Diabetes* **57**, 1227-1235
199. Shin, M., Yi, E. H., Kim, B. H., Shin, J. C., Park, J. Y., Cho, C. H., Park, J. W., Choi, K. Y., and Ye, S. K. (2016) STAT3 Potentiates SIAH-1 Mediated Proteasomal Degradation of beta-Catenin in Human Embryonic Kidney Cells. *Molecules and cells* **39**, 821-826
200. Li, B., Shin, J., and Lee, K. (2009) Interferon-stimulated gene ISG12b1 inhibits adipogenic differentiation and mitochondrial biogenesis in 3T3-L1 cells. *Endocrinology* **150**, 1217-1224
201. Vidal, C., Bermeo, S., Li, W., Huang, D., Kremer, R., and Duque, G. (2012) Interferon gamma inhibits adipogenesis in vitro and prevents marrow fat infiltration in oophorectomized mice. *Stem cells (Dayton, Ohio)* **30**, 1042-1048
202. Kissig, M., Ishibashi, J., Harms, M. J., Lim, H. W., Stine, R. R., Won, K. J., and Seale, P. (2017) PRDM16 represses the type I interferon response in adipocytes to promote mitochondrial and thermogenic programming. *The EMBO journal* **36**, 1528-1542

VITA

Marc Taylor Cantwell
Cancer and Molecular Medicine Program
Center for Clinical and Translational Research
Virginia Commonwealth University School of Medicine
1220 East Broad Street, MMRB Room 2-055
Richmond, VA 23298
Phone: 804-828-2772
Email: cantwellmt@vcu.edu

PERSONAL INFORMATION

Date of Birth: May 30, 1985

Place of Birth: Alexandria, VA

Citizenship: United States

EDUCATION

B.S. Biology, Virginia Commonwealth University, 2008
B.S. Chemistry, Virginia Commonwealth University, 2008

AWARDS

2014 M2 (Medical Year 2) Award for Highest Score in Pathogenesis Course
2014 Selected to Alpha Omega Alpha Medical Honor Society
2007 Herbert John Evans Award for Excellence in Biochemistry

FUNDING

1F30DK109633, "Role of STAT3 in Brown Adipose Tissue Development", August 2016-August 2020.

PUBLICATIONS

Cantwell MT, Farrar JS, Lownik JC, Meier JA, Hyun M, Raje V, Waters MR, Celi FS, Conrad DH, Harris TE, Larner AC. STAT3 Suppresses Wnt/β-Catenin Signaling During the Induction Phase of Primary Myf5+ Brown Adipogenesis. *FASEBJ*. Under Review.

Meier JA, Hyun M, **Cantwell M**, Raza A, Mertens C, Raje V, Sisler J, Tracy E, Torres-Odio S, Gispert S, Shaw PE, Baumann H, Bandyopadhyay D, Takabe K, Larner AC (2017). Stress-induced dynamic regulation of mitochondrial STAT3 and its association with cyclophilin D reduce mitochondrial ROS production. *Sci Signal* 10(472)

Raje V, Derecka M, **Cantwell M**, Meier J, Szczepanek K, Sisler JD, Strobl B, Gamero A, Harris TE, Larner AC (2017). Kinase Inactive Tyrosine Kinase (Tyk2) Supports Differentiation of Brown Fat Cells. *Endocrinology* 158(1):148-157

Sisler, JD, Magdalena Morgan, Vidisha Raje, Rebecca C. Grande, Marta Derecka, Jeremy Meier, **Marc Cantwell**, Karol Szczepanek, William J. Korzun, Edward J. Lesnfsky, Thurl E. Harris, Colleen M. Croniger, and Andrew C. Larner (2015). The Signal Transducer and Activator of Transcription 1 (STAT1) Inhibits Mitochondrial Biogenesis in liver and fatty acid oxidation in adipocytes. *PLoS ONE* 10(12): e0144444

Marc T. Cantwell, Sarah E. G. Porter, Sarah C. Rutan (2007). Evaluation of the multivariate selectivity of multi-way liquid chromatography methods. *J. Chemometrics* 21:335-345